Microscopic, chemical and spectroscopic investigations on emeralds of various origins

Le Thi Thu Huong
geb. in Thanh Hoa, Vietnam

Mainz, 2008

Dekan:

1. Berichterstatter:

2. Berichterstatter:

Tag der mündlichen Prüfung:

Hereby I declare that I have written the present doctoral thesis on my own and without any illegal help. All literature sources are indicated.

Mainz, April 2008

CONTENTS

INDEX OF FIGURES

INDEX OF TABLES

ABBREVIATIONS

Cap	Capoeirana
CCD	Charge-Coupled Device
Ch	Chivor
Cnb	Carnaiba
EMS	Elektronennenstrahl- Mikrosonde
EMPA	Electron Microprobe Analysis
FWHM	Full Width at Half Maximum
Gw	Gwantu
Hyd.	Hydrothermal
Hbt	Habachtal
LA-ICP-MS	Laser Ablation - Inductively Coupled Plasma - Mass Spectrometer
IR	Infra-Red
Ita	Itabira
Kfb	Kafubu
Ma	Malipo
Man	Mananjary
ppm	parts per milion
ppb	parts per bilion
So	Socoto
ST	Santa Terezinha
Tr	Transvaal
Ur	Ural
wt	weight

ACKNOWLEDGEMENTS

Sometime you just keep still in front of someone you love or of someone you appreciate just because there is not sufficient word for you to express how you feel. It is also my case when I stand in front of my advisor Prof. Dr. Wolfgang Hofmeister without whose helps and supports I would have never got the great chance in my life to study in Mainz and this thesis would never have been completed. When I met him at the first time in one Conference in Hanoi on October 2003, with his profound scientific knowledge I wished I can follow him to learn from him and to achieve my scientific career. Four years after that, now, I finished my work with some successes I wish I can express my deep thankfulness to him and I wish him everything best in his life. Another person of great importance is my other advisor Dr. Tobias Häger without whose help my work could hardly be finished. I would like to acknowledge the enormous debt to him for his wise scientific advices and his careful inspection throughout my work. It is always my big luckiness to be his student.

I would like to express my appreciation to Dr. Mathias Barth for his patient help in difficulties in LA-ICP-MS measurements, to Dr. Schulz-Dobrick for the EMPA measurements, to Dr. Quan Han Khang, Dr. Arun Banejee for the documents and to all staffs of the Institute of Geosciences/Gemstone Research for their kind scientific helps.

My best regards I would like to give to Ms. Ursula Wehrmeister, Ms. Giovanna Bortolaso and Ms. Eveline Fuchs for their thoughtful cares during my studying time in Germany. I owed my friends and colleagues in the Institute of Geosciences/Gemstone Research my appreciation for the friendly atmosphere and the helpfulness: James, Daniel, Kathrin, Toey, Wenxing. I thank my best friend - Mai Huong who helped me resolve small and big difficulties in my daily life in Germany during my study. I thank her and her family for the accommodation and kindly taking care for my little daughter while I was writing my thesis. I am also grateful to all my former professors, my friends, my colleagues from Honour Program (HUS) as well as from the Faculty of Geology (HUS) for their encouragement during my study in Germany. I thank Vietnamese government, DAAD, and the Institute of Geosciences/Gemstone Research (Johannes Gutenberg University) for the financial supports.

Last but not least, I give my special thanks to my family, my parents, my husband and my little daughter for giving me motivation to finish my thesis.

*Microscopic, chemical and spectroscopic
Investigations on emeralds of various origins*

Doctoral Thesis
Le Thi Thu Huong

Abstract

In this work a total of 260 natural emeralds and 66 synthetic "emeralds" were thoroughly studied in microscopic, chemical and spectroscopic features by means of LA-ICP-MS, EMP, Raman and IR spectroscopy. The microscopic, spectroscopic features and the concentrations of chemical elements were quite different between natural and synthetic "emeralds", and also among natural emeralds of different deposits. Using these features, criteria were deduced for differentiating between natural and synthetic emeralds and among different localities of natural emeralds.

The use of ICP-MS and EMPA allowed us to identify the concentrations of elements in emeralds. Basing on Si, Al, Be amounts we are able to separate synthetic "emeralds" from natural emeralds since the concentration of these elements approximates the ideal amounts, while in natural ones these amounts are very variable. The concentrations of chromophoric elements, like Cr and V and Fe, helped to attribute Malipo, Chivor and synthetic emeralds. The uses of concentrations of Mg, Na, K allowed us to identify whether an unknown emerald belongs to "schist type" or to "non-schist type", where these two antipodes are only the endmembers of an obviously continuously running solid solution between emeralds of a relatively wide spread crystal chemistry. The crystal structure of beryl, esp. emerald, is able to react constructively on different chemical environments, which may be paralled by a somewhat distinct petrological background of more "schistoid" or "non-schistoid" (pegmatitic, hydrothermal etc.) character. Microscopic investigation allowed to see a variety of inclusions in emeralds of various deposits and producers and therefore is an effective method for separating emeralds of different origins. Pyrite inclusions for example can be used as a criterion to separate Santa Terezinha, Chivor, Kafubu emeralds from all others. The combination of this method with spectroscopic ones makes the separation even much more precise. Features of FWHM and position of Raman band at about 1068 cm^{-1} and IR band at about 1200 cm^{-1} can be used to distinguish between synthetic and natural emeralds. The Raman and IR bands in the range of water vibrations and an IR band at 1140 cm^{-1} lead to separate flux-grown synthetic "emeralds", hydrothermally-grown "emeralds" and natural ones. On the basis of chemical data, the Raman peak at 1068 cm^{-1} and the IR peak at 1200 cm^{-1} were assigned to Si-O vibrations.

Mikroskopische, chemische und spektroskopische
Untersuchungen von Smaragden verschiedener Herkunft

Dissertation
Le Thi Thu Huong

Zusammenfassung

In dieser Arbeit werden die mikroskopischen, chemischen und spektroskopischen Charakteristika von 260 natürlichen Smaragden und 66 synthetischen „Smaragden" untersucht. Die Konzentrationen der chemischen Elemente von Smaragden wurden mit Hilfe der LA-ICP-MS und EMS bestimmt. Ergänzende Raman- und IR spektroskopische Methoden ermöglichen es, die Herkunft der verschiedenen Smaragde und ihrer synthetischen Analoga zu bestimmen.

Auf Grund der verschiedenen Gehalte von Si, Al und Be können synthetische „Smaragde" von natürlichen getrennt werden. Die Smaragde von Malipo, Chivor und auch synthetische „Smaragde" können von allen anderen natürlichen Smaragden wegen der unterschiedlichen Cr-, V-, und Fe-Gehalte von einander getrennt werden. Wegen der unterschiedlichen Mg-, Na-, K-Gehalte lassen sich eher „schiefer-gebundene" Smaragde identifizieren. Dabei wird festgestellt, dass die Unterscheidung in „schiefer-„ und „nichtschiefer-gebundene" Smaragd-Vorkommen im Wesentlichen nur die Endglieder einer offensichtlich kristallchemisch sehr variablen Mineralchemie der Berylle, bzw. Smaragde beschreibt, dass damit aber keinesfalls eine petrologisch vertretbare Trennung belegbar ist, sondern dass Smaragde nur das jeweils regierende chemische Regime unter geeigneten Druck-Temperatur-Bedingungen widerspiegeln. Einschlussmerkmale spielen eine große Rolle bei der Unterscheidung verschiedener Lagerstätten und Herstellungsmethoden. Zum Beispiel können die Smaragde der drei Lagerstätten Santa Terezinha, Chivor, und Kafubu mit Hilfe ihrer charakteristischen Pyriteinschlüsse identifiziert werden. Die Band-Positionen und FWHM -Werte der Raman-Bande bei 1068 cm^{-1} und der IR-Bande bei 1200 cm^{-1} ermöglichen eine Differenzierung zwischen synthetischen und natürlichen Smaragden, und können darüber hinaus auch Auskunft geben über die Lagerstätte. Zusammen mit chemischen Messwerten kann bewiesen werden, dass diese Banden von Si-O Schwingungen verursacht werden. Die Raman- und IR-Banden im Bereich der Wasserschwingungen und insbesondere das IR-Band um 1140 cm^{-1} führen zur Trennung von Flux-Synthesen, Hydrothermal-Synthesen und natürlichen Smaragden.

1. INTRODUCTION AND OBJECTIVES

The main purpose of this thesis is to find out the possibilities and limitation of origin determination of emeralds (the most important gemstone of the beryl group) as well as the separation of natural emeralds from their synthetic counterparts. Methods used to achieve these objectives are inclusion identification with the help of phase discriminating micro-Raman spectroscopy and chemical component identification (Electron Microprobe and Laser Ablation - Inductively Coupled Plasma - Mass Spectrometer) as well as spectroscopic methods (vibrational Raman- and Infrared spectroscopy). The thesis brought out also results concerning types of water in the channel structure of the beryl topology which are at first time investigated by means of Raman spectroscopy. Last but not least, some controversial Raman and IR bands which have been assigned to Si-O or Be-O vibrations are elucidated and assigned by this study to stem from Si-O vibrations.

1.1. The crystal structure of Beryl

Beryl, $Al_2Be_3Si_6O_{18}$, belongs to space group P6/mcc (D^2_{6h}) and is typical for ring silicate minerals; it has two units of the general formula per unit cell. Small amounts of Cr^{3+} and/or V^{3+} substituting in the Al^{3+} position causes the typical green colour of emerald by crystal field energy reaction. The amounts of the main elements ideally are: SiO_2-67 wt%, Al_2O_3-18,9 wt%, BeO-14,1 wt%. The structure of beryl was first determined by Bragg & West (1926) and later refined by Below & Matveeva (1951), Gibbs et al. (1968) and Morosin (1972).

The lattice parameters at room temperature are: a_o = 9,2088 Å, c_o = 9,1896 Å. Figure 1 (left side) shows a sketch of the structure of beryl in the projection perpendicular to the c axis. It illustrates that the structure is composed of six-membered rings of $[SiO_4]^{4-}$ - tetrahedrons, where each tetrahedron has two bridging oxygen atoms O(1) that are shared with two neighbouring tetrahedral and two nonbridging oxygen atoms O(2). Each ring is horizontally and vertically bonded by octahedrally (oxygen-) coordinated Al^{3+} and tetrahedrally (oxygen-) coordinated Be^{2+} with others. Each of these atoms lies on the plane between the rings, in which each aluminium atom is

1

surrounded by six rings and bonded by six oxygen atoms while each beryllium atom is surrounded by four rings and bonded by four oxygen atoms.

In fact, the chemical compositions of natural beryls substantially deviate from the ideal formula $Al_2Be_3Si_6O_{18}$, owing to straight forward but even complex cationic substitutions. The most common replacements are the anisomorphous substitutions of Si^{4+} by Al^{3+} in tetrahedral sites, or of Al^{3+} by divalent, trivalent ions (Mg^{2+}, Mn^{2+}, Fe^{2+}, Fe^{3+}, Cr^{3+}, V^{3+}) as well as Ti^{4+} in octahedral sites (Aurisicchio et al., 1994; De Almeida Sampaio Filho & Sighinolfi, 1973; Khaibullin et al., 2003). The replacements of Li^+ and, sometimes argued - Na^+ for Be^{2+} in tetrahedral sites could also occur. Anisomophous substitutions giving rise to charge imbalance require the incorporation of alkali ions into the channel.
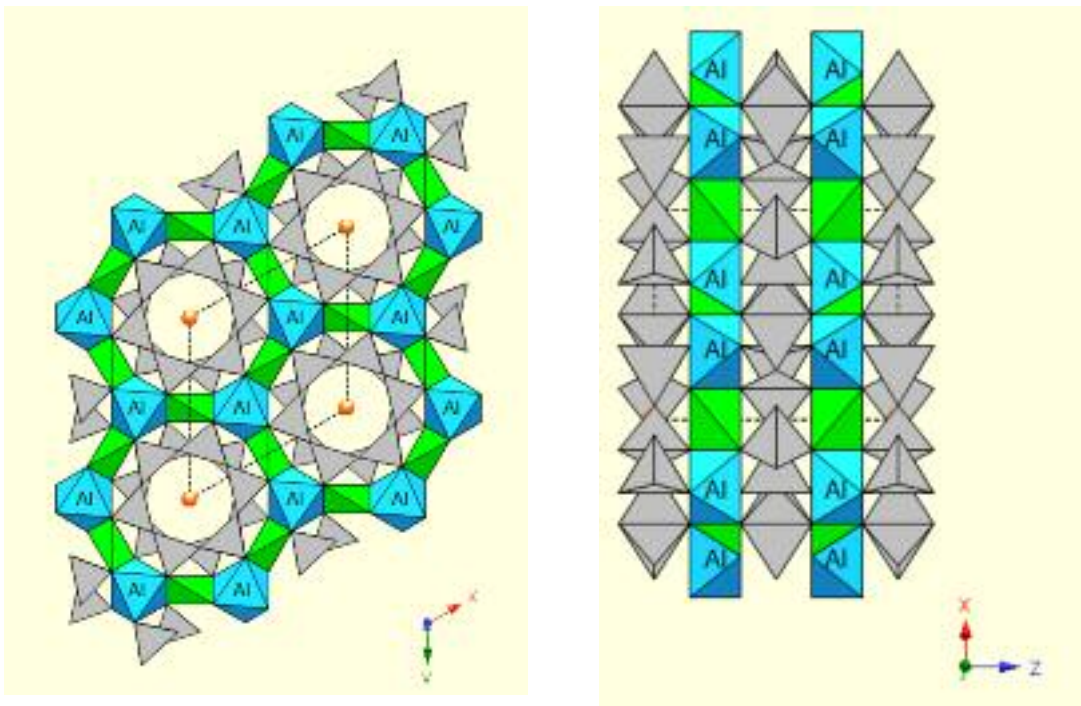
Figure 1: View of the emerald structure with the c-axis perpendicular (left); view of the emerald structure with the c-axis parallel (right).

In the direction of the hexagonal axis, the Si_6O_{18}-rings are aligned precisely over each other; therefore, they form continuous and open channels parallel to the c-axis of the crystal in the same direction. The effective diameter of the channels varies from 2.8 Å in the plane of the silicate rings to 5.1 Å midway between adjacent rings. The diameter of the channels, therefore, is large enough, so that they may host big ions or molecules such as alkalis, earth alkalis, OH^-, H_2O, F^-, He, CO_2, CH_4, N, NO_3… and

even the main elements of beryl may also at least partially occupy positions in the channel (Aines and Rossman, 1984; Goldman et al., 1978; Bershov 1970). It has been shown that the most common alkali ions entering channel positions are Na, Cs, and K, and in most cases these alkalis were found to be related to water within the crystal structure. The location of Na in the channel is said to be in the 2a positions (0 0 ¼) and (0 0 ¾), i.e., the positions between 2 rings in the central topology of the channel in the level of Al and Be atoms, whereas 2b positions are positioned in the same height (relative to c) , in the level of the Si atoms (0 0 0) and (0 0 ½) being occupied preferentially by Cs, K, and water molecules (Aurisicchio et al., 1988; Andersson, 2006).

The first who seriously considered water as a component of beryl is Penfield (1884) and according to his interpretation water can reach 1.50 to 2.50 weight percent. By heating experiments, it was found that water could be expelled totally at 800 to 900^0C and this removal did not affect the crystal structure (Ginzburg, 1955; Polupanova et al., 1985; Kolesov and Geiger, 2000; Pankrath and Langer, 2002). In the study of Wickersheim and Buchanan (1959) it is reported that in many cases water molecules can be found to be related with the incorporation of alkali ions. Nevertheless, until that time, the real configuration showing the presence of water in channels of beryl has not been known yet.

As one of the components existing in the structural channels of beryl, water (and also carbon dioxide) has been investigated by Wood and Nassau (1967) by using infrared spectroscopy. And it has been Wood and Nassau, who firstly improved the study of Wickersheim and Buchanan (1959), that beside water molecules which were found alone in the channel, in many cases there were water molecules existing with alkali ions nearby. The presence of alkali ions nearby the water molecules influence the orientation of water molecules. Accordingly, water could be classified in to two types: Type I is that which occur alone and with a typical orientation in the way that the symmetry axis of the water molecules is perpendicular to the c axis of the emerald crystal; type II is water molecules which are associated with nearby alkalis and the water molecule symmetry axis is parallel to c-axis of the host crystal as a result of interaction with alkali ions. The first schematic drawing showing types of water in channel has been then published by Wood and Nassau (1967).

Later, Schmetzer (1989), Schmetzer and Kiefert (1990) in their studies concerning the distinction of natural and synthetic emeralds supplemented that water molecules can either exist alone or with alkalis nearby (mainly sodium). In the case, that there is an alkali ion nearby, water type II may be associated with this ion in two sequences, H_2O-Na-OH_2 or H_2O-Na- in which   represents a vacancy of water (no water) in the channel sites. Therefore, they divided water type II into two subtypes: type IIa is water molecules like H_2O-Na-OH_2 and type IIb is water molecules like H_2O-Na- . Furthermore, they found that also hydroxyl ions (OH^-) can be associated with alkali ions in a sequence like HO-Na- . The study of Aurisicchio et al. (1994) confirmed the existence of two types of water and also suggested the presence of OH groups associated with alkali ions in the channels (Figure 2). According to Aurisicchio et al. (1994) and Brown and Milis (1986) Na^+ together with other alkali ions such as Cs^+, Rb^+ and K^+ can occupy the channel positions of the beryl structure.
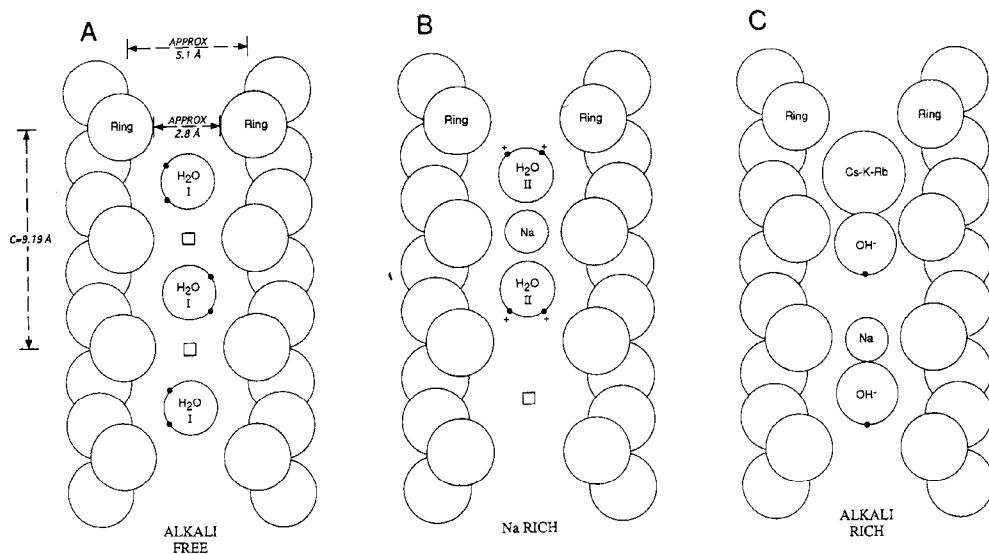
Figure 2: Possibilities of water and hydroxyl occurring in channel of beryl: A. Water type I without alkali nearby. B. Water type II with alkali nearby. C. Hydroxyl with alkali nearby.
After Aurisicchio et al. (1994).

1.2. Possibilities to determine origins of emeralds and separation between natural emeralds from synthetic ones - State of the art study and results of the present thesis.

To bring out the possibilities of discrimination, determination of the origins of emeralds as well as the growth routines of synthetically manufactured counterparts is the objective of mineralogists and gemmologists. The methods which have been

4

applied to obtain these objectives include spectroscopic methods, microscopic methods, chemical analyses and recently method of oxygen isotope investigation (Zwaan et al., 2004, Giuliani et al., 2000, 1998). Nevertheless, the most common methods are based on microscopic techniques which are used to identify inclusions or other microscopic features in emeralds (Moroz and Eliezri, 1999). The theory that one can distinguish synthetic and natural gem materials is based on the premise that natural gems incorporate a variety of inclusions from natural environments in which they are formed that are not present in the manufactured synthetic counterparts. Between natural gem materials from different environments there should be a observable content of different ingredients either in amount or in type of components that intruded in the emerald structure during the forming processes (Schrader, 1987).

With the same premise, many studies based on the chemical composition, especially on the amount of minor and trace elements of emeralds, have shown some special composition of certain localities with extreme differences, e.g. Staatz et al. (1965), Hänni (1982), Schrader (1983) and Stockton (1984). The study of Hänni (1982) could show the differences in the concentration of Cr_2O_3, FeO, MgO and Na_2O between natural emeralds and synthetic ones, that is, the concentrations of these elements in synthetic "emeralds" are found to be much lower than those in natural emeralds. Nevertheless, the separation could not be transferred and established among different natural stones. And, in the actual study it is found that there is an overlap in the concentration of Na between synthetic "emeralds" and some emeralds from Nigeria. The study of Schrader (1983) claimed to separate not only natural stones from synthetic ones but also presented additional criteria that could be used to distinguish between natural emeralds from some localities due to different amounts of minor elements. Stockton (1984) supposed the idea that Al_2O_3 and SiO_2 could supply additional information about origin. We found that, these two main elements show to have higher amounts in "non-schist-type" emeralds than in "schist-type" emeralds, and in synthetic stones these contents attain almost the ideal amounts. It should be noted that a phenomenological differentiation of localities with schist- and non-schist-background is sometimes used, being transferred to the inclusion archive or chemical content of emeralds. During this study, it becomes obvious that schist (mica-schist, gneissic etc.) or non-schist (e.g. pegmatitic - hydrothermal etc.) are only antipodes of a great variability of the crystal chemistry of the crystal structure of beryl and should

not be used as a reliable discriminating argument. Beryls are able to incorporate a great number of anions, cations, or molecules, and they react on chemical supply during growth, as long as the physico-chemical parameters allow the growth of crystals. Nevertheless, the terms "schist-" and "non-schist-type", which are widespread in gemmology, are used in this thesis in the sense of end-member representatives. With 36 stones from 13 localities and 5 manufactures, the chemical analyses section of this study fulfilled the large range contributing the abilities to compare chemical characteristics among emeralds. Furthermore, this section provided the basement to other spectroscopic sections, namely Raman and Infrared spectroscopy, to assign the respective bands.

There are some studies that used Raman spectroscopy to identify the locality of emeralds (Moroz et al, 2000; Hagemann et al, 1990). These authors compared the single-crystal Raman spectra between synthetic emeralds and emeralds from different deposits. Moroz et al. (2000) were able to differentiate between several emerald deposits based on peculiar Raman bands. In our study, we focused on the main Raman peak which shifts from about 1067 cm^{-1} to about 1072 cm^{-1}. This peak shifts to longer wavenumbers (about 1069-1072 cm^{-1}) in emeralds of "schist type" while in emeralds of "non schist type" this peak is around 1068-1070 cm^{-1}, and in synthetic emeralds, this peak is around 1067-1068 cm^{-1}. The values for the Full Width at Haft Maximum (FWHM) change from about 19 cm^{-1} to 26 cm^{-1} in "schist-type" emeralds, from about 11 cm^{-1} to 14 cm^{-1} in synthetic and from about 12 cm^{-1} to 15 cm^{-1} in "non-schist type" emeralds, respectively. Therefore, basing on the position and FWHM of the Raman peaks at 1067-1072 cm^{-1} one may in some cases identify natural emeralds from synthetic ones, or identify emeralds of "non schist type" from emeralds of "schist type". Special cases are emeralds from Malipo (China), these emeralds in the usually applied phenomenological nomenclature "non-schist-type" emeralds but the peak position is at about 1700 cm^{-1} and FWHM is about 17 to 21 cm^{-1}. It will be obvious during this investigation that Malipo emeralds are typical representatives of the so-called "solid-solution" between "schist-" and "non-schist-type" emeralds. Some published papers assigned this Raman band to a Be-O vibration (Moroz et al., 2000; Kim et al., 1995) or to a Si-O vibration (Charoy et al., 1996; Adams and Gardner, 1974). Prior to now, a reliable assignment of observed bands to certain vibrations in the samples is always one of the most challenging tasks in vibrational spectroscopy

(both Raman and IR spectroscopy). In this study, correlating spectroscopic with chemical data, it is proved that the band is generated by Si-O vibrations, since both band position and band width are effected by the concentration of Si but not of Be.

Other Raman bands which are also of particular interest are those stemming from water vibrations which range from 3300 cm^{-1} to 3800 cm^{-1}. In flux-grown synthetic "emeralds" no band of water is observed. In alkali-free hydrothermal synthetic "emeralds" (Tairus, Biron) only one Raman peak at 3068 cm^{-1} may be seen. "Non-schist type" emeralds and "schist type" emeralds show two peaks at 3598 cm^{-1} and at 3608 cm^{-1} at room temperature. Emeralds from these two types of origins could be separated from each other by the intensity ratios of these two peaks, since the intensity of band 3608 cm^{-1} is lower than that of band 3598 cm^{-1} in "schist-type" emeralds; conversely, intensity of band 3608 cm^{-1} is higher than that of band 3598 cm^{-1} in "non-schist-type" emeralds. Bands at 3608 cm^{-1} and at 3598 cm^{-1} are therefore assigned to water type I (without alkali nearby) and water type II (with alkali nearby), respectively. The Raman spectra obtained under different temperatures between 300 K and 78 K show different behaviours of water types and only below 198 K a peak splitting could be observed.

Assigning Infrared bands for vibration in the range of the Si-O and the Be-O vibrations is also still controversially discussed in literature. Many authors assigned the IR band around 1200 cm^{-1} to vibrations of Si-O (Gervais and Pirou, 1972; Adams and Gardner, 1974; Hofmeister et al., 1987; Aurisicchio et al., 1994) but some others assigned this band to Be-O vibrations (Plyusnina, 1964; Plyusnina & Surzhanskaya, 1967). Also this band has been confirmed to belong to Si-O vibrations in this study. The shoulder at around 1140 cm^{-1} was found to be a good signal to separate between natural and alkali-free synthetic "emerald", since this shoulder is not to be observed in all synthetic "emerald" which are flux or hydrothermally grown in alkali-free medium. The plots of the intensity ratios of the band around 1200 cm^{-1} and the shoulder versus the alkali amount in emeralds show to behave with negative linearity. Besides, the plots of the intensity ratios of the band around 1200 cm^{-1} and the shoulder versus the Si concentration showed to behave with positive linearity. These observations support the interpretation of the presence of the shoulder as being concerned with the Si and Na "density" in Beryl.

Features of water and/or hydroxyl bands in the Infrared spectra could also be used as good criteria to separate synthetic and natural emeralds. Separation between synthetic (flux and hydrothermal) and natural emeralds by means of IR spectroscopy was firstly published by Flanigen et al. (1967). These authors reported that in Infrared spectra of flux synthetic emeralds no bands in the regions 3500-3800 cm^{-1} and 1500-1700 cm^{-1} (IR vibration ranges of water and hydroxyl) were seen, while emeralds of natural origins and of hydrothermal synthesis showed one or more absorption bands. The hydrothermally grown emeralds could be distinguished from natural ones by the absence of bands near 3600 cm^{-1}. However, calculating the ratios of band intensity of water type I, water type II and hydroxyl, one can estimate qualitatively the concentration of alkalis in the host emerald for each deposit, since the type of water depends directly on the alkali concentration and therefore, more or less, it enables the determination of origins of some natural emeralds.

		Locality	Inclusion investigation	LA-ICP-MS, EMPA	Raman	IR
natural emerald	„schist type"	Carnaiba	15	1	2	1
		Socoto	15	1	2	1
		Brazil / Itabira	15	1	2	1
		Capoeirana	15	1	2	1
		Santa-Terezinha	20	1	2	1
		Russia / Ural	10	2	5	1
		Austria / Habachtal	10	2	5	1
		Madagascar / Mananjary	30	2	5	1
		South Africa / Transvaal	30	2	5	1
		Zambia / Kafubu	30	2	5	1
	"non- schist type"	Colombia / Chivor	30	5	10	1
		Nigeria / Gwantu	30	5	10	1
		China / Malipo	10	2	4	1
synthetic „emerald"		Hyd. Biron	10	2	5	1
		Hyd. Tairus	15	2	5	1
		Flux Chatham	20	2	5	1
		Flux Gilson	20	2	5	1
		Flux Lennix	1	1	1	1

Table 1: Origin or growth technique, measuring methods and individual numbers of emeralds investigated in this study.

2. SHORT DESCRIPTION OF SAMPLES AND ORIGINS

Over 300 natural and synthetic emeralds samples have been investigated in this study. Natural emeralds were collected from 9 different countries including 13 occurrences: Colombia (Chivor), Brazil (Carnaiba, Capoeirana, Itabira, Santa Terezinha, Socoto), Madagascar (Mananjary), China (Malipo), Nigeria (Gwantu), Austria (Habachtal), Russia (Ural), Zambia (Kafubu), and South Africa (Transvaal). Natural emeralds can be separated into two types of geological occurrence based on their relation to the host rocks: Type I deposits: Non-schist-related emerald mineralization, type II deposits: Schist related emerald mineralization. In short term, emeralds may be separated roughly and only by their known geological setting as "non-schist-type" emerald and "schist type" emerald. Investigated synthetic "emeralds" were from five producers: Biron, Tairus (hydrothermal synthesis), Lennix, Gilson and Chatham (flux synthesis). This section gives the short overview about localities, host rocks, associated rocks of natural emeralds as well as manufacture technique of synthetic ones.

2.1. Natural emeralds.

Colombia:

Chivor

Figure 3: Emerald in host rock (quartz), sample from Chivor, sample size 2.5 x 2.4 x 1.8 cm^3.
Source: http://www.mineralatlas.com

The Chivor mine is one of the two important mining areas in Colombia, which is also known as Somondoco, a word which means ''God of the green stones'' (Webster,

1955). Together with the Muzo mine, Chivor has placed Colombia in the first position of emerald contributors to the world. The Chivor mine is situated in the Cordillera Oriental, the eastern range of the Andes, about 200 km north-east-ward of Bogota - the capital of Colombia. Emeralds in Chivor are found in dark, carboneus shale and thin, inter-layered limestones which spread widely as vein systems. The veins are known to be rich in albite, pyrite and found between or underneath nearly horizontal limonite beds. Limonite (mainly goethite) on one side as well as micas plus clay minerals on the other side are encountered as dissociation products of pyrite and albite (Johnson, 1961).

Brazil:

Brazil is another important source of emerald in the world. Emerald itself is also one of its most economical gemstones. According to Schwarz (1987) emerald occurs in four states of Brazil: Minas Gerais, Goias, Bahia and Ceara. All four states are situated in the eastern part of Brazil. The samples collected for this study are from the mines of Itabira, Capoeirana (Minas Gerais), Santa Terezinha (Goias), Carnaiba, Socoto (Bahia).

Capoeirana

Petrographic investigations of Souza et al. (1991) in the area of the Capoeirana emerald deposit, Minas Gerais State, revealed two main lithostructural units. The first unit is comprised of gneissic rocks of granitic composition belonging to the basement complex, and the second is composed of a highly weathered metasedimentary-metavolcanic sequence represented by metapelitic schists, amphibolites, schists derived from ultramafic rocks, and quartzites. Quartz and pegmatoid veins appear near the contacts between the gneissic rocks and the mineralization of the metasedimentary-metavolcanic sequence. The emeralds of the Capoeirana mine generally occur in association with a biotite-phlogopite mica schist sequence. The emeralds apparently formed along with their associated schist minerals during a hydrothermal episode following the metamorphism of the original rocks (Schwarz et al., 1988; Epstein, 1989).

Itabira

The whole Itabira region from the lowest to the uppermost is composed of paragneisses, green schist and other groups which are separated from the basement by a structural and metamorphic discontinuity, namely Caraca group, Itabira group and Piracicaba group. The paragneisses were formed through the metamorphism of greywackes and other sandstones. The Caraca group is composed of micaceous quartzite and phyllite. The Itabira group is the economically most important unit due to its itabirite and hematite iron ore contents. Quartzite, sericite and phyllite dominate in the Piracicaba group. This region was subjected to a regional metamorphism and folded. In the area of the emerald occurrence, a belt of schist dominates, stretching in a north to northeast direction. The width of the belt varies between 750 and 1200 metres. The schist belt, together with the mafic rocks is strongly folded, with axes trending north to northeast. The gneiss and the schist are riddled with small pegmatite bodies which are concentrated between the gneiss and the schist belt. Emeralds occur in biotite-phlogopite schist, in green chlorite schist or in kaolinitic masses (altered pegmatite). Crystals of lower quality are also found in quartzitic masses (Mulller-Bastos, 1981; Hänni et al., 1987).

Carnaiba and Socoto

Figure 4: A large green opaque emerald crystal from Carnaiba (Bahia, Brazil) embedded in a schist matrix. There are silvery flakes of molybdenite scattered all about. Sample size: 15 x 13 x 25 cm^3.
Source: http://www.mineralatlas.com

The mining region of Carnaiba and Socoto in the state of Bahia are located at a distance of about 40 km from each other. The first one belongs to the county of Pindobacu, the latter to the county of Campo Formoso. The regional geological

12

conditions are practically identical for the emerald deposits of Carnaiba and Socoto. They are characterized by the occurrence of granite batholiths whose pegmatite penetrated rock units and in contact with its chromium bearing rocks caused the formation of emerald mineralization. Metasomatic processes accompanying the intrusion of pegmatite bodies into the surrounding ultrabasic rocks are responsible for the formation of Carnaiba emeralds. Schwarz and Eidt, (1989) differentiated three zones in Carnaiba mining area: 1. The schistified ultramafic intercalation in the quartzites. 2. The less schistified ultramafic belt in the contact region between Carnaiba granite and the quartzites at the base. 3. The ultrabasic, somewhat granitized rock body intercalated into the Carnaiba granites. In the Carnaiba mine, emeralds are found mainly in phlogopite-biotite schist associated with quartz veins.

The ultramafite body which host the emerald mineralization of Socoto has a length of 3650m with an average width 200m. In the centre of the body occur serpentinites, talcites, amphibolitic rocks, biotite schist, gabbros, metadiabasites and cataclastic rocks. The following petrographic types predominate: actinolite-talc, biotite-phlogopite schist, and amphibolite. Although the regional geological features are practically identical in Carnaiba and Socoto, some peculiarities of the later deposit should be emphasized, that is the area of Socoto shows a larger variety of tectonic structures and rock types. These factors result in a larger range of variation in the mechanism of formation of the Socoto emeralds (Schwarz et al., 1990).

Santa Terezinha

Figure 5: Santa Terezinha emeralds in schist.
Source: http://www.coloradogem.com

The Santa Terezinha emerald deposit is about 275 km north of Goiania, the capital of Goias state. Emeralds in this deposit are exploited in two main workings, namely Garimpo de Cima and Garimpo de Baixo. In Garimpo de Cima, there are two distinct continuously mineralized beds of emeraldiferous rock. Each is presently worked and exploited. Mineralized lenses are relatively poor in emeralds and are no longer exploited. The emerald-bearing rock consists of partially weathered talc schist, pale brownish grey in colour and stained by iron oxide. In the other mine, Garimpo de Baixo, there is only one mineralized bed. The emerald-bearing talc schist is similar to that of Garimpo de Cima. Nevertheless, there are pegmatite veins intersecting the schist. They are essentially composed of pearly white sericitized and kaolinized feldspar, associated with quartz. Near the contact with pegmatite the emeraldiferous talc schist includes irregular bands of greyish mica (Cassedane and Sauer, 1984).

Austria:

Habachtal

Figure 6: Emerald in host rock from Habachtal. Crystal size ca. 4 cm.
Source: http://www.snapmania.com

The emerald deposit of Habachtal, in Austria, is one of the few sources of emeralds on the continent of Europe and one of the oldest known to man. The regional geology is described by Grundmann and Morteani (1989) who describe the emerald deposit situated near the tectonic contact between ortho-augengneisses of the central gneiss and a series of amphibolites, mica schists, and black phyllite with interlayered serpintinites which is called the Habach formation. Both the central gneisses and the Habach formation belong to the lowest tectonic unit of the eastern Alps. The Habach formation is part of the lower schist cover which is interpreted as an alpine nappe

above the central gneisses. The emerald mineralization itself occurs in a sequence of metasomatic blackwall zones developed between a series of metamorphosed pelites, mafic volcanics and ultramafics, including serpentinites. The emerald occurs predominantly in (tourmaline-bearing) biotite, chlorite, actinolite, and talc schist.

Russia:

Ural

Figure 7: Emerald in host rock with cassiterite from Ural mountain.
Sample size: 8 x 6 x 3 cm.
Source: http://www.mineralatlas.com

The main mine is on the Asiatic side of the Ural mountains and near the Tokovaya river, about 60 km north-east-ward of Ekatharinburg. In general, the mining area consists of two emerald-bearing belts. The main belt runs approximately north-south more than 20 km, at its southern end it intersects with the second belt, about 8 km long, that run northeast-southwest. The emeralds occur in metamorphic rocks trapped between the acidic rocks of a granite massif to the west and ultrabasic rocks to the east. The metamorphic rocks of the emerald-bearing central contact zone include talc, mica, chlorite and actinolite schists. The emerald deposits consist of four dominant rock types: Pegmatite or pegmatitic rocks, including albitite and kaolinite; tourmaline-bearing biotite schist; chlorite-actinolite biotite schists; talc schists (Fersmann, 1929 and Schmetzer et al., 1997).

Zambia:

Kafubu

The main emerald-producing area in Zambia is the Kafubu area. Famous mines are Miku, Kagem, Grizzly and Kafubu, which lie a few kilometres from each other. This emerald field is located in the Kitwe district of northern Zambia, about 30 km south-west of Kitwe and 40 km west-northwest of Luanshya. The investigated emeralds are collected in Kafubu mine and are found in biotite-phlogopite schists in which dark brown to black tourmaline also occurs. Other rocks intimately associated with the emerald-and tourmaline-bearing mica schists are talc-magnetite schists and quartz-amphibolite-chlorite schists with secondary quartz veining (Zwaan et al., 2005; Graziani et al., 1983).

South Africa:

Transvaal

Since 1890 emerald from Transvaal has been known and exploited. According to Robb and Robb (1986) the emerald mines in Transvaal are situated at the contact of Archean tonalitic gneisses with talc-chlorite, actinolite and biotite schist. Several gneissic metatonalitic to metagranodioritic bodies are associated with an albitite-pegmatoid which shows a tectonometamorphic overprint within a sequence of biotite, actinolite, chlorite, and talc chlorite schist. It should be emphasized that the magmatic bodies including the pegmatoid rocks show clear gneissic textures, indicating that the whole series has been affected by deformation and green schist facies metamorphism.

China:

Malipo

Malipo County (Yunnan) locates near the Vietnam-Chinese border and has been investigated to have emerald mines with important potential since the beginning of the 1980s. So far, here is the only emerald deposit found in China and formation characteristics of these emeralds have not been known yet. However, Malipo emeralds have been thought to belong to "non-schist type" since big emerald crystals are found in pegmatite bodies lying NW-SE through the border to the Vietnamese vicinity (Ha

Giang province). This opens the ambition for many geologists and mineralogists to study in regional geology for this area and to find emerald in the next Vietnamese vicinity which has not yet been thoroughly investigated mineralogically on emerald occurrences. Emerald bearing pegmatite bodies can be separated into two types, the one is big-grain-metapegmatite in association with fibrous shaped tourmaline crystals, and the other is an albitized fluorite bearing pegmatite with quartz- and calcite lenses.

Figure 8: Emerald crystals in host rock from Malipo.

<u>Nigeria:</u>

Gwantu

The source of emeralds from Nigeria is situated in Gwantu, south east Kaduna State. Emeralds are found in two types of occurrence, one is usually pegmatite, whereas the other is in the roof zones of granites. In addition to quartz and microcline, pegmatites contain both biotite and muscovite and in many cases considerable amounts of albite with beryl and tourmaline. Especially, there are albitized pegmatites with important gem potential. Besides the typical minerals, these pegmatites contain beryl, tourmaline, apatite, spinel, chrysoberyl, and cassiterite. Furthermore, emeralds may occur in small pegmatite pockets in association with quartz, feldspar and topaz or in soft decomposed granites, in which emerald crystals have grown in small miarolitic cavities formed by gas loss in the roof of the granite (Schwarz et al. 1996).

<u>Madagascar:</u>

Mananjary

The emerald occurrence is in the vicinity of the coastal town of Mananjary, about 250 km southeast of Antananarivo, the capital of Madagascar. The region represents a mining area of considerable potential and size. In general, the emerald crystals are found embedded in host mica or amphibole schists. (Schwarz, 1994)

Classification of the emerald deposits

Depending on the host rock of emerald relating or not relating to schist formation, in gemmology emeralds may be separated into two types. The one is "schist-type" emerald and the other is "non-schist-type" emerald. For the samples in this work, emeralds may be separated as follows:

"Schist-type emerald"	"Non-schist-type emerald"
- Itabira (Brazil)	- Chivor (Colombia)
- Capoeirana (Brazil)	- Malipo (China)
- Socoto (Brazil)	- Gwantu (Nigeria)
- Carnaiba (Brazil)	
- Santa Terezinha (Brazil)	
- Mananjary (Madagascar)	
- Ural (Russia)	
- Habachtal (Austria)	
- Transvaal (South Africa)	
- Kafubu (Zambia)	

Table 2: Localities grouped due to host rock of emerald into "schist type" and "non-schist type".

2.2. Synthetic "emeralds".

Emerald is a rare and valuable gemstone and, as such, it has provided the incentive for developing synthetic emerald-like products ("emeralds"). Both hydrothermal and flux syntheses have been produced, and a method has been developed for producing an "emerald" overgrowth on colourless beryl (Gübelin, 1961). The flux-grown

"emeralds" are first commercially successful accomplished by Carroll Chatham at about 1940. The other large producers of flux "emeralds" are Pierre Gilson Sr., and M. Lens. Gilson's "emeralds" have been on the market since 1964 and are usually grown on natural colourless beryl seeds which become coated on all sides (Webster, 1964). Lens's "emeralds" (normally called Lennix "emeralds") have been later on the market and are unusual in that their habit is four-sided rather than hexagonal. Other "emerald" crystals produced by IG-Farben and Nacken, long claimed to be hydrothermal, have been shown to be flux-grown (Nassau, 1976). The really first satisfactory commercial hydrothermal product was that of Johann Lechleitner of Innsbruck, Austria, which appeared on the market in the 1960s. These stones were initially sold under the names "Emerita" and "Symeralds", and they were grown as a thin layer of "emerald" on top of natural colourless beryl stones. Although not much is known about the original process, it is assumed that Lechleitner "emeralds" were grown in acidic conditions. Later, from 1965 to 1970, the Linde Division of Union Carbide produced completely synthetic "emeralds" by hydrothermal synthesis. At the end of the 1970s, Biron hydrothermally grown "emeralds" were announced by a mineral company of Australia and they became commercially available as faceted stones in substantial quantities around the end of 1985 (Kane & Liddicoat, 1985). In 2001, the know-how and apparatus of this company was sold for another joint venture company from Thailand and Russia, Tairus, thus, a new "emerald" producer is known to the market.

Synthetic samples collected for this study are those of Chatham, Gilson, Lennix, Biron and Tairus producers.

2.2.1. Flux-grown synthesis

The flux method for emerald-like crystals is based on the chemical interaction between beryllium, aluminium and silicon oxides as well as the colouring substances in a molten flux (e.g. lithium molybdate). The material used as crucible is platinum which is stable under the temperature of $900^{\circ}C$ with the flux. Theoretically, the process can be described as follows: The platinum crucible containing molten flux is supplied with beryllium and aluminium oxides, which, being heavier than the flux,

sink to the bottom. Pieces of silicon oxide in the form of SiO_2-glass are floating on the top of the melt and slowly diffuse silicon oxide into the flux.
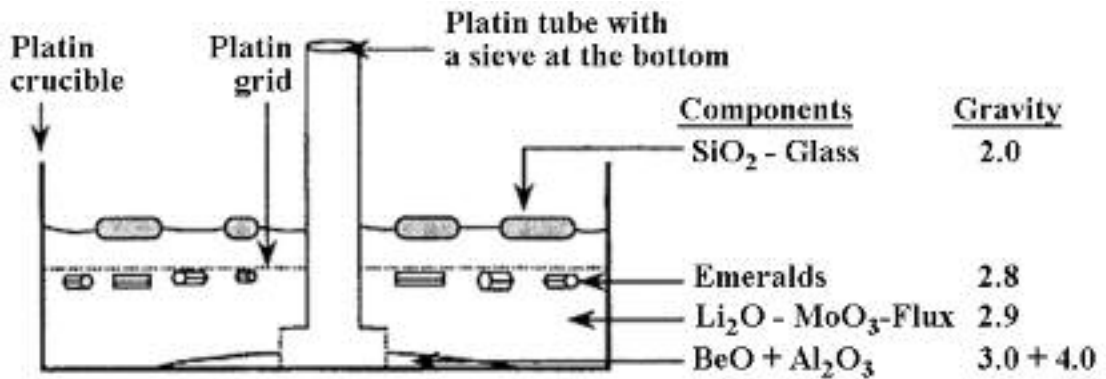
Figure 9: Schematic sketch illustrating the apparatus to grow emerald-like crystals using a flux of lithium and molybdenum oxides. *After Greiff & Häger (1992).*

Simultaneously, the beryllium and aluminium oxides also dissolve and react with the flux to form complex oxides which through diffusion and convection pass toward the top of the melt. In between they meet and react with silicon oxide. As long as the oxides interact, "emerald" crystals form. V_2O_5 as well as lithium tungstate or molybdate were utilized as a flux, however, preference was given to lithium molybdate (Barilo et al., 1999). The lithium molybdate flux is normally chosen, because of basing on the fact that beryl-like solids are less soluble in lithium molybdate than the ingredient oxides. Thus emerald-like crystals can grow while the oxides slowly dissolve to provide the necessary nourishment within a weak but constantly saturated environment (Nassau, 1980).

2.2.2. Hydrothermally-grown synthesis

The actual hydrothermal growth method relies on the fact that many mineral solids dissolve in hot "water" at a certain quantity under high pressure (above the critical point of pure water). The solution of dissolved beryllium, aluminium and silicon oxides as well as the colouring substances is heated to a temperature between 300°C and 400°C with an internal pressure of 1000 bars. Slight differences in temperature are maintained at opposite ends of the growth chamber, the hotter end dissolving the nutrient and the cooler end causing seeds to take on additional growth (Sinkankas and Read, 1986).
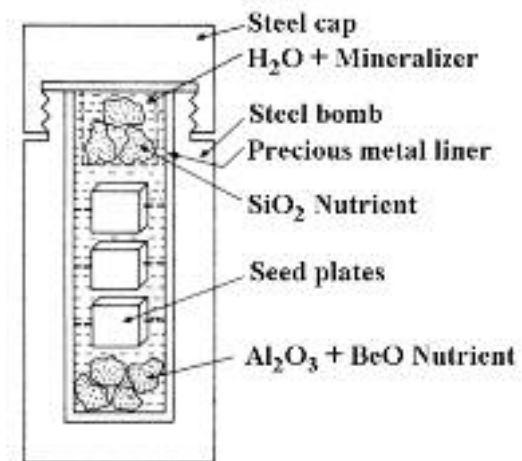
Figure 10: Schematic sketch illustrating the autoclave growing hydrothermally emerald-like crystals. *After Nassau (1980).*

3. INCLUSIONS

Inclusion examination is the most conclusive method in traditional gemmology to differentiate between natural and synthetic "emeralds", and to differentiate between different localities of natural emeralds. "Schist-type" emeralds could be specified by the association of quartz, mica, amphibole, and fluid inclusions while other inclusions such as carbonate minerals, apatite, fluorite, feldspars, etc., are responsive for the "non-schist-type" ones. Phenakite crystals and typical growth features which originated during manufacturing processes are the criteria for the technical origin of synthetic "emeralds".

For this research, the inclusions were firstly observed, described, and classified using a gemmological microscope with Zeiss optics. Then all of the different types of inclusions were photographed and determined using confocal-Raman spectroscopy. All host emerald samples were polished at two parallel sides with the thickness varying from 1 mm to 4 mm. The experiments determining inclusions of emeralds were carried out on a LabRam confocal micro-Raman-system HR-800 equipped with an Olympus-BX41 by JOBIN YVON HORIBA. For searching inclusions as well as measuring a certain point, an objective with a 50 times magnifying power and green laser light (514.532 nm) were used. Raman spectroscopy is a non-destructive technique to identify not only solid but also fluid inclusions in gemstones. LA-ICP-MS was used to determine metal inclusions found in synthetic samples.

3.1. Chivor (Colombia)

Observations in emeralds from Chivor lead to conclude that the main internal characteristic is the appearance of fluid inclusions in very peculiar forms (see figure 11), pyrite crystals as well as inhomogeneous growth features. Other frequently observed inclusions are carbonate crystals (calcite, dolomite) and albite. The fluid inclusions appear in a variety of forms, in which the peculiar one shown in figure 11 is the unique feature that can be seen – up till now - only in emeralds from this locality. Normally, they were more or less shallow primary cavities and then healed with liquid and one or two solid substances.
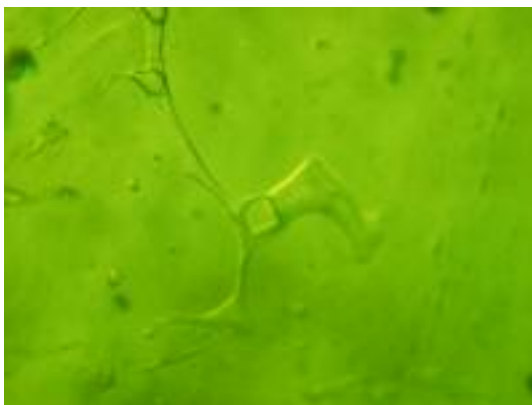
Figure 11: The peculiar form of fluid-solid-gaseous inclusions which make Chivor emeralds easy to be distinguished. x50
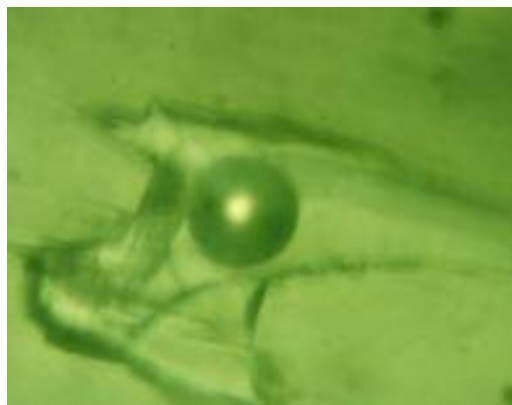
Figure 12: A large amount of fluid inclusion presented with angular or jagged contours. This feature can be seen also in Nigerian emeralds. x50

With the crystallographic orientation (parallel to the main growth axis c) they are considered as primary fluid inclusions. The secondary fluid inclusions are usually smaller than the primary ones and are not orientated in the host crystals. Not only occurring in crotch-looked-like forms, fluid inclusions show slightly to strongly vaulted shapes. A large amount of fluid inclusions presented angular or jagged contouring (figure 12). Two-phase fluid inclusions were found less frequent than three-phase ones. Three-phase inclusions can be made up of a liquid carbon dioxide, gas bubbles (carbon dioxide) and halite crystals, in which halite crystals show very clearly rectangular (cubic) forms. The volume of gas in fluid inclusions was estimated to be less than that of the solids.
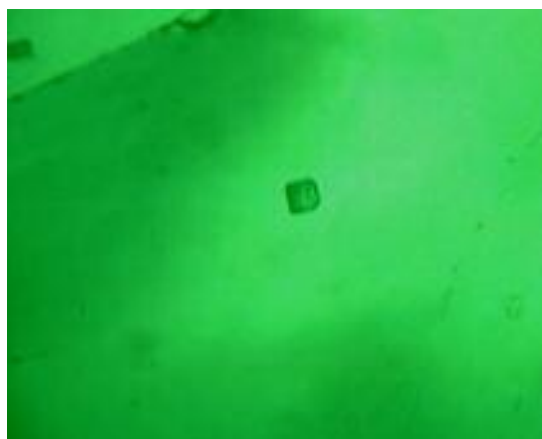
Figure 13a: Pyrite (FeS_2) as well-formed cube in Chivor emerald. x50
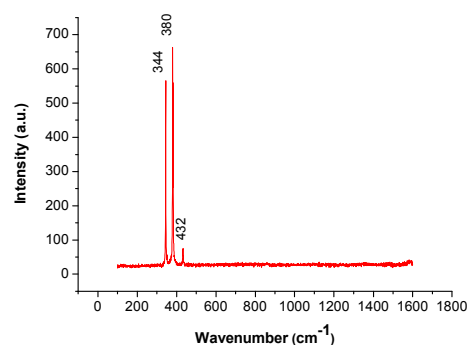
Figure 13b: Raman-spectrum obtained from pyrite inclusion in one Chivor emerald sample.

Mineral inclusions do not appear as frequently as fluid inclusions do in Chivor emeralds. Nevertheless, the appearance of pyrite crystals is the very characteristic feature of these emeralds, because, firstly, pyrite itself is not a frequent inclusion in emerald; secondly, only in Chivor and in two other localities (see *Santa Terezinha (Brazil)* and *Kafubu (Zambia)*) it can be found, and pyrite is found to be more frequent in Chivor emeralds. Another study (Eppler, 1973) stated that the well-formed crystals of pyrite are the most typical mineral inclusion in this locality. Under the microscope these well-formed pyrites were observed with a very typical metallic lustre (figure 13a). Not only well-formed crystals but also rounded grains of pyrite were found.

Carbonate inclusions (calcite, dolomite, etc) are transparent, colourless to brown, forming either rhombohedral crystals or irregular bordered grains, and in general, they are small. Albite crystals show yellowish-brown colour in triclinic crystal form.
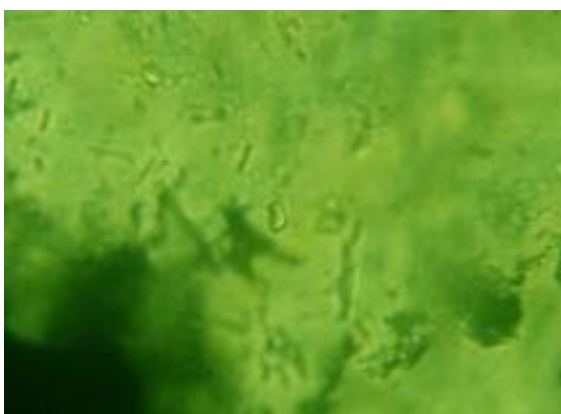
Figure 14a: Transparent, colourless dolomite ($CaMg(CO_3)_2$) crystal in Chivor emerald. x10
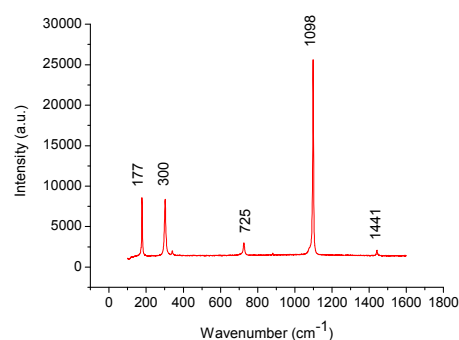
Figure 14b: Raman-spectrum obtained from dolomite inclusion in Chivor emerald.

Other mineral inclusions are sometimes found, including clinochlore and quartz which are considered as atypical inclusions of Chivor emeralds. According to Webster (1975), pargasite, muscovite and hematite can also be found. Furthermore, another frequent feature of Chivor emeralds is aggregates of tiny, dark grains which are thought to be particles of the wall rocks that may be carbonaceous shale.
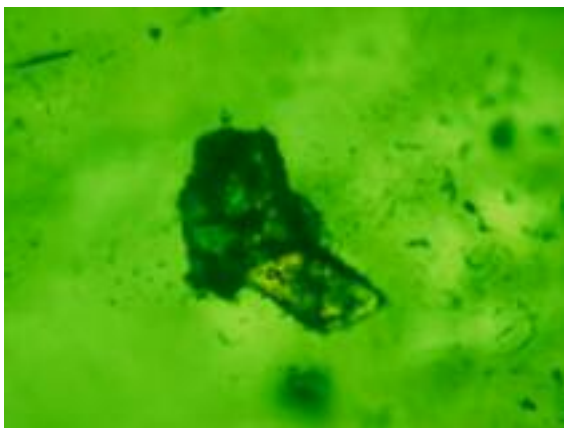
Figure 15a: Feldspar inclusions in Chivor emerald, both the well-shaped crystal and the adhered dark part were determined as albite (NaAlSi$_3$O$_8$). x50
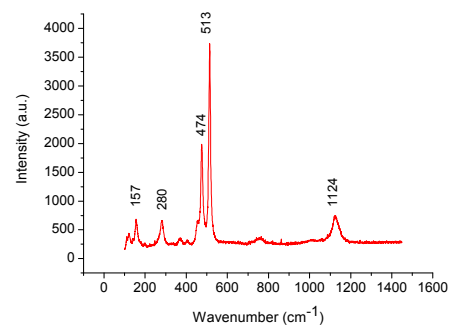
Figure 15b: Raman-spectrum obtained from albite inclusion.

Other features known as main internal characteristics of Chivor emeralds are colour zoning and growth zoning. Colour zoning can be described as follows: Pyramidal colour zoning and basal colour zoning. The basal colour zoning can be a sequence of colourless and green, flat and well defined lamellae. The pyramidal colour zoning normally starts on the basal planes. These pyramids may show a very strong green colour saturation, taper in the growth direction and may present the well-defined zigzag form. This conclusion corresponds to the observation of another study by Kiefert and Schmetzer (1991) in which it is indicated that the most significant growth planes in all Colombian emeralds are the first-order hexagonal prism m (10$\bar{1}$0) and the basal pinacoid c (0001).

3.2. Santa Terezinha (Brazil)

Mineral inclusions are found to be abundant in emeralds from the Santa Terezinha deposit. The Santa Terezinha emerald has been comprehensively reported by Hänni and Schwarz (1986), Schwarz (1990), Cassedanne and Sauer (1984) and Miyata et al. (1987). Inclusions were listed including chromite, pyrite, calcite and two-phase inclusions. For pyrite and chromite these authors paid special regard and concluded these as the typical inclusions in emerald of this region. Furthermore, Miyata et al. (1987) stated that Santa Terezinha was the only region except Colombia with emerald including pyrite inclusions. (Nevertheless, according to our study, Kafubu (Zambia) is the third region that emerald with pyrite inclusion can be seen). And the inclusions of most significance which are found out by this study are not only pyrite and chromite

but also members of the carbonate group, talc and mica (biotite). Other minerals that we considered as atypical inclusions are hematite, goethite, amphibole, feldspar, quartz, and magnetite. Pyrite inclusions normally occur as sharp or slightly rounded cubes. They can occur solitaire or in groups. Numerous minute crystals may form tiny clouds. It is difficult to say in which deposit, Chivor or Santa Terezinha, emeralds contain more pyrite.
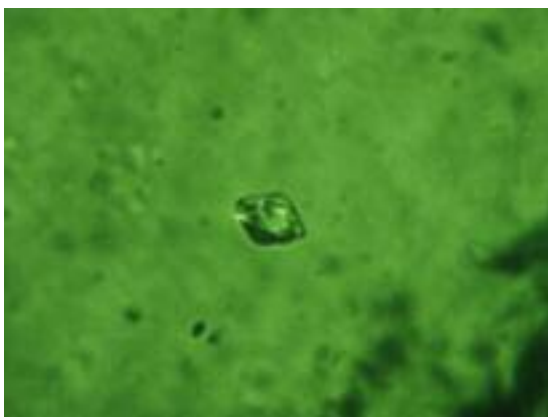
Figure 16a: Chromite inclusion ($FeCr_2O_4$) in Santa Terezinha emerald as a well shaped octahedron. x50
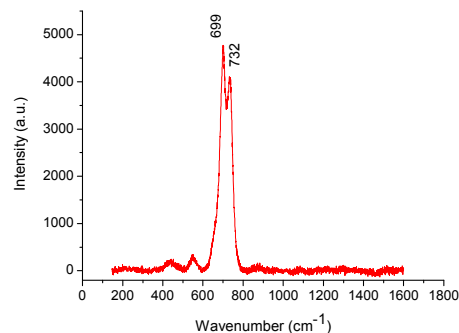
Figure 16b: Raman-spectrum obtained from chromite inclusion in Santa Terezinha emerald.

Chromite is present as black rounded crystals or in octahedrons (figure 16a). The big individual crystals are isolated, and the small ones form irregular clouds or trails parallel to the basal faces. Carbonate minerals are colourless to brown, irregularly bordered grains, found either singly or in groups. They were determined by Raman microscopy to be calcite, dolomite, hydrozincite and magnesite (figure 17a).
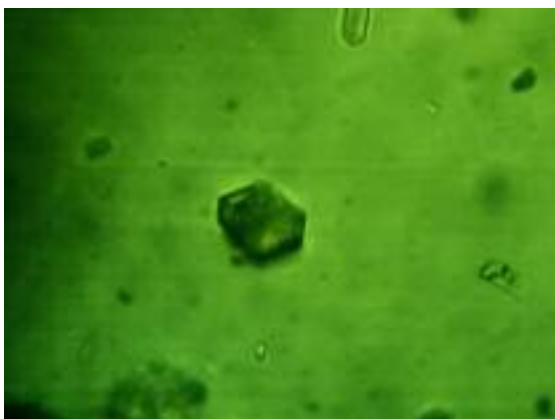
Figure 17a: Magnesite ($MgCO_3$) in Santa Terezinha emerald. x50
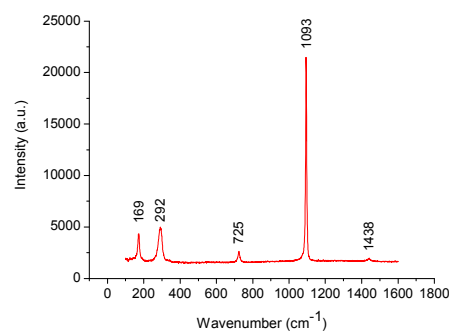
Figure 17b: Raman-spectrum obtained from magnesite in Santa Terezinha emerald.

Talc minerals are colourless, transparent to white or silky, in flake-like shapes (figure 18a). They are sometimes gathered in agglomerations that make the crystals appear cloudy. Mica inclusions were determined to be biotite as brown flakes. Two-phase inclusions are so tiny that they rarely appear solitaire but often gather in form of "fingerprints". Colour zoning is another feature of emeralds from Santa Terezinha. In many samples, this feature can be observed with the naked eyes.

Figure 18a: Talc flakes usually are very small aggregates in Santa Terezinha emerald, the big one as shown in photo is very infrequent. x50
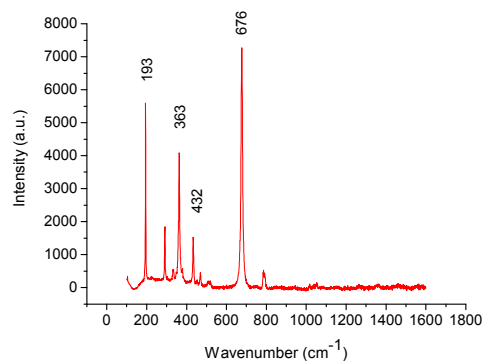
Figure 18b: Raman-spectrum obtained from talc inclusion in Santa Terezinha emerald.

3.3. Socoto (Brazil)

The first results of examinations of inclusions in Socoto emeralds were presented by Schwarz et al. (1990). The great variety of different mineral inclusions is found to be the most characteristic feature. However, mica is the most frequently observed inclusion. Micas are usually biotite and phlogopite, and less frequent they can be margarite or muscovite. This is due to the fact that the largest portion of the Socoto emeralds is found in a biotite/phlogopite schist host rock.

Normally, the mica crystals occur in the form of rounded or irregular-shaped platelets. Their colour is generally light to dark brown. Margarite and muscovite are practically colourless. Only rarely occur the mica crystals isolated, mostly they form agglomerations. It is the agglomerations of mica that sometimes make the host emerald crystal have dark brown colour (figure 19) and partially appear almost opaque. Sometimes, tubes are observed orientated in the direction of the c-axes and are accompanied with mica. Beside mica, chlorite inclusions are observed, which are

sometimes not distinguishable from mica without the help of confocal-Raman microscopy.
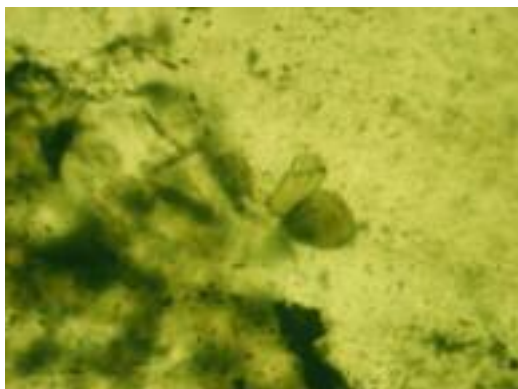
Figure 19: Only rarely isolated occurring mica crystals, usually forming agglomerations, darkening the crystal. x50

Figure 20: Fissure system parallel to the c axis in emeralds from Socoto. x10

Other inclusions found in Socoto emeralds are actinolite, tremolite, apatite, talc, quartz, albite, molybdenite and hematite/goethite/lepidocrocite, in which molybdenite is least frequently observed and considered as a rare mineral inclusion. Actinolite/tremolite sometimes forms thick needles or rods that are practically colourless and transparent. They normally occur isolated (figure 23a) but sometimes are found to be bundles of numerous crystals showing no preferred orientation. Besides the colourless, transparent crystals, others of greenish to light brownish crystals occur that sometimes show the characteristics of a bamboo-like appearance.
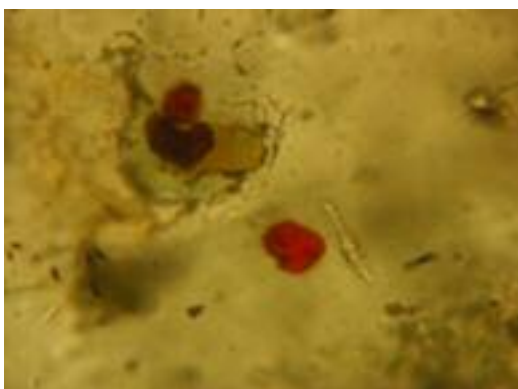
Figure 21: Lepidocrocite (FeOOH) with very intensive red colour, with brownish hematite (Fe_2O_3). x50

Figure 22: The dark brown core zone is caused by the conglomeration of mica and some carbonate minerals. x50

Observation in all samples indicates that the importance of actinolite/tremolite as mineral inclusions falls clearly behind that of micas. This fact is in accordance with

the investigation Schwarz (1990) made in the emerald mining areas showing that actinolite schist is rarer as an emerald host rock than is the mica schist.

The appearance of isolated albite crystals and of fractures filled with feldspar in the emeralds can be explained also by the fact that the Socoto emeralds are partly found in feldspar masses. Hematite occurs as small, irregular crystals that can be found mostly within fissures or dispersed over the surface of the emerald crystals. Lepidocrocite can be found sometimes to be associated with hematite and shows a very strong red colour (figure 21). Apatite occurs as prismatic crystals that are sometimes slightly corroded and rounded. They are colourless and they almost always show cleavage planes parallel to the basal phase. Based on their appearance within the emerald host crystal we can define them as protogenetic inclusions. Besides the mineral inclusion mentioned above, there are talc crystals occurring in the form of transparent, colourless platelets. According to Schwarz et al. (1990), Eidt and Schwarz (1986), tourmaline and orthite can be observed as rare inclusions in emeralds from Socoto also. Fluid inclusions were found to be of two-phase or three-phase composition, in which two-phase inclusions are more abundant. Nevertheless, there are still many fractures that generally have no orientation and that are mostly unhealed and other fissures that occur very abundant in a certain place orientated parallel to the c axis of host crystal (figure20). In the samples which were cut perpendicular to the c axis we found the trace of concentric colour zoning, reflecting the hexagonal symmetry of the host crystals (figure 22). The core with darker colour is caused by the high inclusion density, in general, they are dark brown mica, and may be carbonate minerals, or others. The presence of the core zone as well as the growth layer shows that the growth process of Socoto emeralds is characterized by the repeated abrupt alterations of the forming environment.
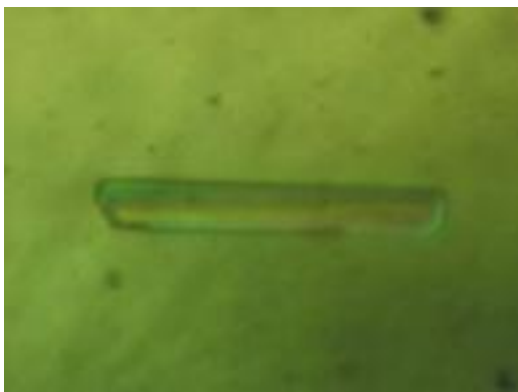
Figure 23a: Single tremolite crystal in Socoto emerald. x50
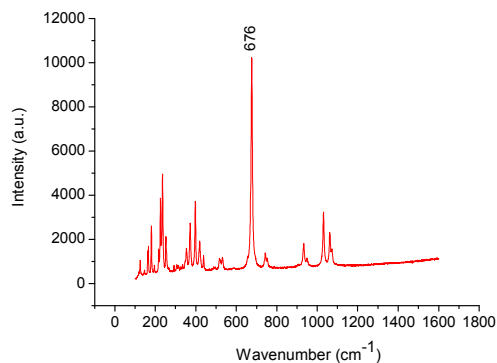
Figure 23b: Raman-spectrum obtained from tremolite inclusion in Socoto emerald.

3.4. Carnaiba (Brazil)

In Carnaiba emeralds there are silky to white tracks or clouds to be seen with the naked eye which is found to be characteristic for emeralds from this locality. Under the microscope it becomes obvious that these tracks are composed of numerous tiny particles (figure 24) which are mostly cavities with one or two-phase (liquid and gas) fillings. These particles are so tiny that only with magnification 50x or more, they become individually obvious, and even with 50x magnification it is hard to find cavities that are filled with two phases. The compact agglomeration of these tiny particles is responsible for the lack of transparency of the majority of emeralds from Carnaiba.

Mineral inclusions are quite rare in Carnaiba emeralds. This is in contrast what may be expected considering the host rocks and geology events: those of Carnaiba are the same like those of Socoto and both deposits are found in mica-schist. In fact, there are numerous mineral inclusions in Socoto emeralds, but in Carnaiba emeralds there are only mica, quartz and goethite. Other minerals such as tourmaline, actinolite, and apatite had been seen only one time in the whole investigation. Mica presents as plate-like crystals with irregular, rounded outline and possess no preferred orientation. These mica plates (biotite) which obviously are protogentetic inclusions show more or less intensive brown colour.

Figure 24: Numerous particles (one- or two-phase inclusions) marking tracks or clouds in emeralds from Carnaiba causing a lack of transparency.
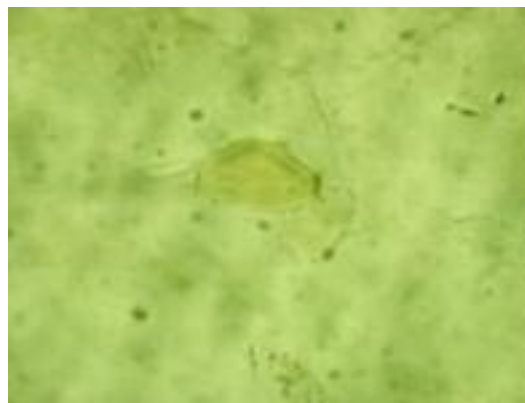
Figure 25: Mica plate (biotite), one of the rare mineral inclusions in Carnaiba emeralds.

Apart from these inclusions, growth structures such as growth pyramids in the form of zigzag lines, growth lines parallel to the basic face or a concentric striation parallel to the faces of the prism, are other common features of Carnaiba emeralds.

3.5. Capoeirana (Brazil)

Capoeirana emeralds belong to the schist-hosted type. This study brings out quartz, mica (biotite) and fluid inclusions in emeralds from Capoeirana. At the first sight, the liquid inclusions of emeralds from this location are like those observed in emeralds from Itabira. Both locations contain liquid inclusions having a broad diversity of forms. However, three-phase or multi-phase inclusions containing two liquids, which are a very abundant type in Itabira emeralds, were not found in Capoeirana. What make liquid inclusions in Capoeirana emeralds look like those in Itabira emeralds, is that they can be seen also in rectangular bordered cavities, almost cubic negative crystals (figure 26) or in acicular fissures, or in growth tubes oriented parallel to the c-axis. They are usually two-phase and sometimes can be three-phase inclusions. The solid phase in the three-phase Capoeirana inclusions did not appear to be cubic, unlike those common to Nigerian or Chivor emeralds.

Quartz inclusions are colourless, transparent, and can be found either as rounded grains or in long prismatic forms. Rounded quartz grains were found usually in groups, distributed irregularly within host crystals (figure 27). Long prismatic quartz crystals were found as singly transparent ones, orientated parallel to the c-axis. In

31

some cases, quartz was found to be associated with fracture systems or liquid inclusions.

Mica inclusions were found less frequently than quartz. Not only in one sample but also in the whole sample set, quartz inclusions were found to be dominant over those of mica. Micas were observed as transparent to translucent slightly greyish brown flakes and booklets or somewhat rounded grains and they are not distributed in any certain place inside the host crystal. Growth tubes are abundant and oriented parallel to the c-axis, sometimes found together with mica booklets.

In addition to mica and quartz, siderite crystals are found as atypical mineral inclusions from this region. In the study of Epstein (1989), the slightly rounded, translucent greyish white crystals which were determined as calcite and dolomite were also found in a few cases. They all belong to carbonate group, but, nevertheless by Raman spectroscopy, in this study only siderite has been analyzed.
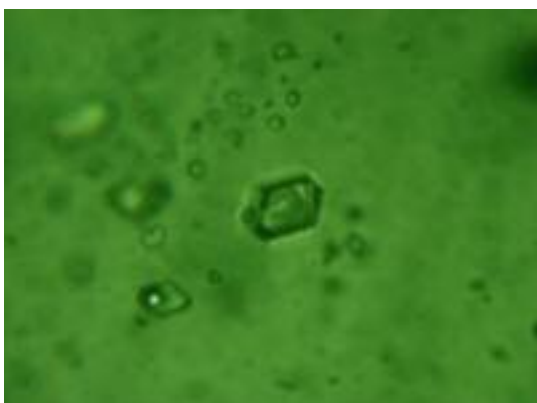
Figure 26: Liquid inclusions in negative crystals in emeralds from Capoeirana. x50

Figure 27: Group of quartz grains in Capoeirana emerald. x10

3.6. Itabira (Brazil)

These emeralds are like those from Capoeirana and in general, are easily distinguished from those from Santa Terezinha, Carnaiba and Socoto based on inclusion features. Under the microscope Itabira emeralds were found to contain relatively few types of inclusions. The most frequent observed inclusions are liquid, quartz and micas. Other mineral inclusions, which were found much less frequent, are apatite, tremolite and hematite. According to Schwarz (1987) andesine may also be found.

Liquid inclusions built the most abundant group in Itabira emeralds which exhibit a large variety of forms. This indicates a complex and multiphase formation history of emeralds in this region. Among liquid inclusions, two-phase type (liquid-gas) seems to occur more often. They are widely and irregularly distributed within host crystals, and can be observed in various-sized tubes or in almost rectangular bordered cavities as well as in more or less perfectly formed negative crystals. Three-phase inclusions were sometimes found, and differently, they are usually composed of two fluids and a bubble (figure 29), in case of four-phase inclusions, liquid phases are still dominant: 2 liquids, a solid, and a bubble. The type of liquid inclusion containing solid substance is occasionally observed in Itabira emeralds. In general, liquid inclusions are so small that all attempts to determine their phases by confocal-Raman spectroscopy failed.
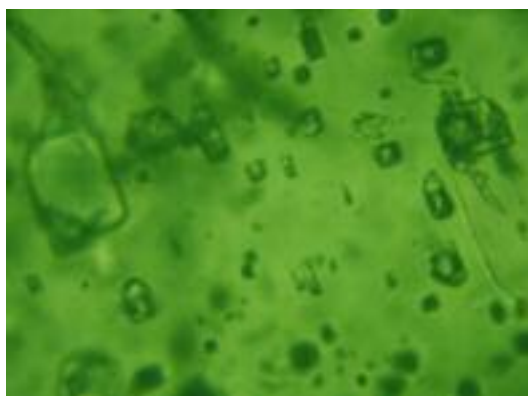
Figure 28: Almost rectangular bordered cavities filled with two or three phase inclusions in Itabira emeralds. x10

Figure 29: Multi-phase inclusions were found often containing two liquids and gas. x50

Among mineral inclusions of emeralds, micas were found to be the most common. They vary in a large diversity of forms and colours. Not only does the colour of mica inclusions vary from sample to sample but also within the same sample itself. The colour may be composed of various shades of brown, from yellowish, grey to dark brown. The mica flakes are usually strongly rounded or irregular. In some samples, micas are elongated or have a disc-shaped form and are (001)-oriented parallel to the basic face (001) of the emerald. The strongly rounded micas which show no preferred orientation are considered as protogenetic inclusion and often possess a deep brown colour. The thickness of mica slabs are also very different, some mica slabs are so thick that they appear almost opaque and show very clearly cleavage surfaces (figure 30). Another appearance of protogenetic mica is that the mica crystals are in a state of dissolution (figure 31). The syngenetic micas are mostly thin and transparent flakes

which are either elongated or partly exhibit a distorted pseudo-hexagonal shape. These flakes show the following orientation within host crystal: the elongated crystals lie parallel to the c axis, and the pseudo-hexagonal crystal lie parallel to the basal plane. Micas have been determined by Raman spectroscopy as biotite and phlogopite.

Quartz is another type of frequently observable inclusion, but is much less frequently observed than mica is. Quartz crystals occur normally colourless, elongated or rounded and sometimes are found to be associated with liquid inclusions. Another type of inclusion in Itabira emeralds are various fissures which remained unhealed. This indicates that these fissures were formed when the crystal growth process had been stopped, thus the crystal had no longer contact with any liquid environment. In a few samples, tremolite, apatite and hematite are rarely found.
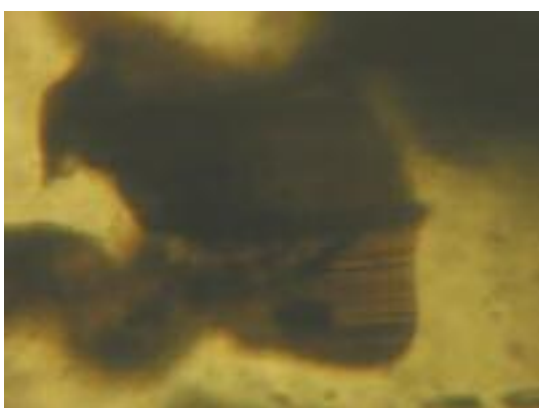
Figure 30: Thick brown mica flake with cleavage or growth surface. x50
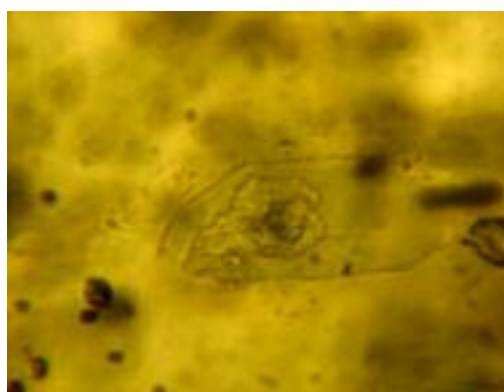
Figure 31: Mica flake with corrosion. x50

3.7. Mananjary (Madagascar)

Abundant types of mineral inclusions are the most striking internal characteristic observation in Mananjary emeralds. Most of the inclusion features are similar to those found in emeralds from other schist-type deposits. Nevertheless, not all of Mananjary emerald inclusions can be found in any other locality. The association of numerous mineral inclusions such as quartz, mica (biotite, phlogopite), amphibole (actinolite, tremolite) and other minerals such as feldspar (albite, oligoclase), carbonate minerals (magnesite, calcite, dolomite), talc, molybdenite, tourmaline and fluid inclusions is a special feature of emerald from this occurrence.
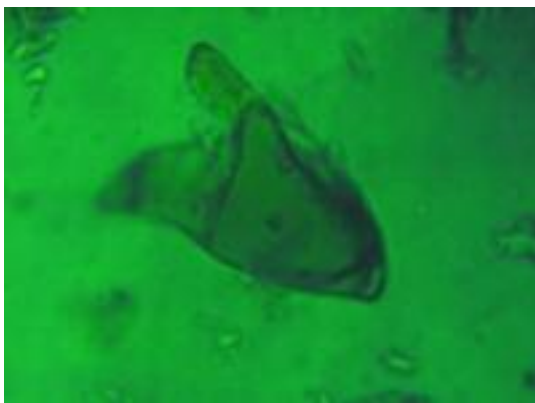
Figure 32: Thin plate of mica inclusion in Mananjary emerald. x50
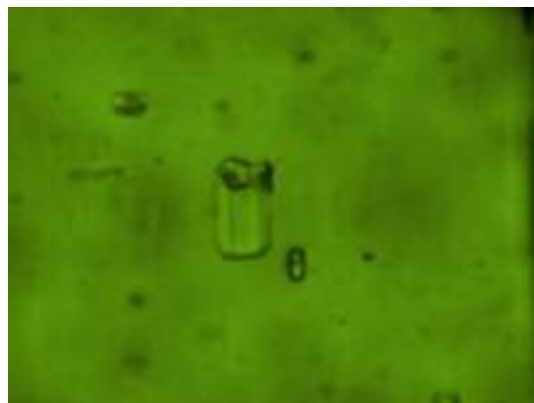
Figure 33: Quartz appears with fluid inclusions in prismatic form. x50

Quartz inclusions are mentioned in almost all emeralds from different localities (Schwarz and Henn, 1992). In Mananjary emeralds, quartz appears in a diversity of morphologies. Quartz inclusions can appear as transparent, colourless, elongated (or prismatic) parallel to the c-axis of the host emerald crystals, often associated with primary fluid inclusions (figure 33). They occur as isolated crystals, irregularly distributed throughout the host crystal or dispersed over the planes of healing fissures. The others are postgenetic inclusions that show irregularly rounded crystals, some of which have a badly corroded rough surface. Quartz inclusions can also be observed in groups of small grains. They are well rounded or almost spherical.

Nevertheless, the appearance of mica inclusions in Mananjary emeralds is even more frequent than that of quartz. They belong to the most common group of mineral inclusions. Micas were determined by Raman spectroscopy to be usually biotite and phlogopite. They often appear as thin plats with usually somewhat rounded edges, or may also have a almost perfect sharp outline (figure 32).

Not only mica schists are host rocks of emeralds in Mananjary but also amphibole schists (although less frequent). Consequently, amphiboles also belong to the main inclusions in emeralds; the observed amphiboles are actinolite and tremolite. They arrange as chaotic tubular crystals which always knit with others. But that distribution of amphibole is only in certain areas of the host crystals, not in the whole sample as those in emeralds from Habachtal.
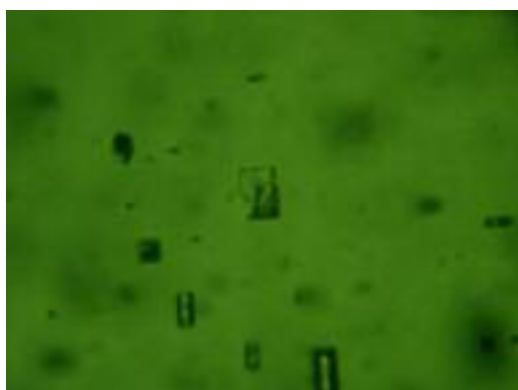
Figure 34a: Oligoclase (KAlSi$_3$O$_8$) found to be with two-phase inclusions. x50
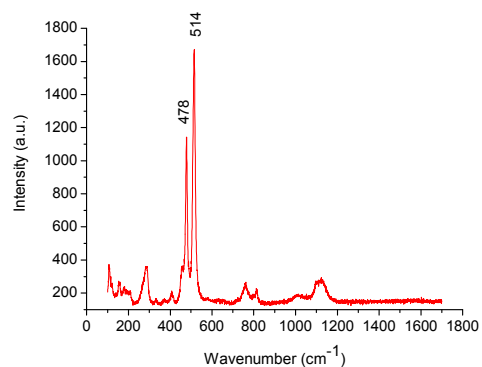
Figure 34b: Raman-spectrum obtained from oligoclase inclusion in Madagascar emerald.

In comparison with the above mentioned inclusions, carbonate minerals, feldspar and molybdenite are less frequent. Carbonate minerals are most irregular or rounded grains, although they show some relatively well-developed rhombohedral crystals. In general, they appear transparent and colourless. The surface corrosion made some carbonate crystals appear slightly brown. Feldspar is determined normally to be either albite or oligoclase. They are usually irregular in shape and often very rounded or corroded (figure 34a). Molybdenite occurs as grey or silver platelets with typical metallic luster. They may be slightly rounded or show a well developed hexagonal outline. Tourmaline has been identified in Mananjary emeralds (Schwarz, 1994; Hänni and Klein, 1982). Nevertheless, this inclusion is found occasionally during this study among widely different occurrences including Mananjary emeralds.

Figure 35a: Occasional case of tourmaline crystal found in emeralds from Mananjary. x50
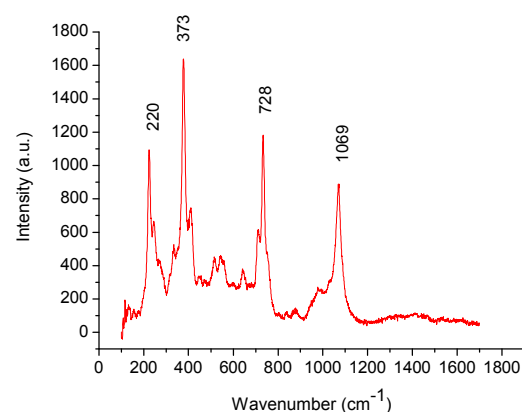
Figure 35b: Raman-spectrum obtained from tourmaline inclusion in Mananjary emeralds.

Fluid inclusions are also abundantly observed in Madagascar emeralds. Primary fluid inclusions are often associated with quartz crystals. These inclusions are typically elongated – that is, within growth tubes – in the direction parallel to the c-axis of the host emerald crystal. Fluid inclusions can be two-phase or three-phase inclusions.

3.8. Habachtal (Austria)

Being one of the typical schist-hosted types, Habachtal emeralds show more or less the same feature of inclusion types which were described in other familiar localities. Nevertheless, the main portion of emerald samples were found in amphibole schist, consequently, the inclusions which were found to be typical are amphibole (tremolite, actinolite), biotite and liquid, as expected.

The most recognizable feature of Habachtal emeralds is the image which is teeming with masses of amphibole needles (figure 36). They rarely occur solitaire but often congregate in clusters and bundles. Their colour is always green and varies from pale to dark shades. The picture of an amphibole cluster as shown in figure 36 is absolutely unique for Habachtal emeralds. Thus this is the most distinguishable character of emerald in this locality. In other localities which were described above, amphibole can be found singly and itself can not be the clue to conclude the origin of host emerald crystals. The frequent appearance of amphibole can be seen again in emeralds from Kafubu or Ural which will be described later in this chapter. But such appearance of numerous amphibole needles in Habachtal emeralds is still a very prominent feature.

Apart from amphiboles, micas, which are mainly biotite, are characteristic of Habachtal emeralds, showing the familiar features with that of mica schist-hosted emerald inclusion. By this study, biotite is found out to be either brown or completely colourless in lamina forms and usually hides in the clusters of amphibole. The amount of mica can not be compared with those of amphibole but mica strew singly throughout the crystals.

Mica lamina can be found to be accompanied with liquid inclusions in the amphibole clusters. Liquid inclusions are either irregular cavities or negative crystals very often forming two-phase inclusions and frequently are very tiny (figure 37). The appearance

of liquid inclusions is also common in all schist-hosted types. Other mineral inclusions which may be rarely found are oligoclase, apatite, epidote, sphene. They are considered as atypical inclusions in emeralds from Habachtal.
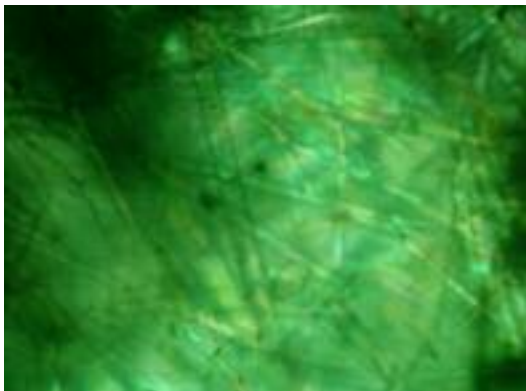
Figure 36: Amphibole inclusions in Habachtal emeralds. x10

Figure 37: Two-phase inclusions observed in Habachtal emerald. x50

3.9. Kafubu (Zambia)

The microscopic in situ observation in Kafubu emeralds leads to the conclusion that the most significant inclusions are liquids. In general, the features of liquid inclusions in Kafubu emeralds are more or less alike with those in Gwantu (Nigeria) or Itabira emeralds: they all display wide variations in shape and appearance. Nevertheless, the features of fluid inclusions in Kafubu emeralds allow this locality to be discriminated from the others. The well shaped forms of negative crystals which are very common in Gwantu or Itabira emeralds were found less frequent in Kafubu emeralds.
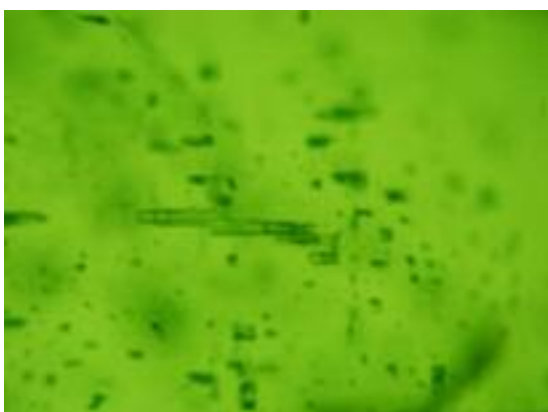
Figure 38: Fluid inclusions in Kafubu emerald. x10
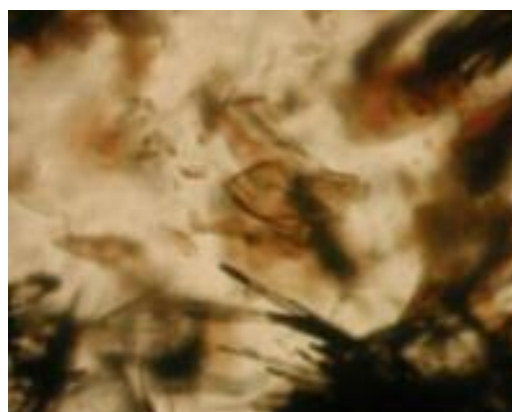
Figure 39: Amphibole and mica occasionally found singly but usually in groups in emeralds from Zambia. x50

38

Furthermore, the ratios of volume of gaseous phase (bubble) to liquid phase in multi-phase inclusions of Kafubu emeralds are smaller than those in Gwantu or in Itabira emeralds. As mentioned, the rectangular bordered cavities or the well-formed negative crystals were found less frequent than the elongated filled fractures (figure 38). Usually, elongated fluid inclusions are orientated parallel with the c axis. The small tiny fractures were partially filled and marked by planar groups of wispy or irregularly shaped fluid inclusions that often show optically a low relief.

Mineral inclusions are also common in emeralds from Kafubu; biotite, and amphibole were found to be most common. Biotite and amphibole (Raman spectroscopy indicated amphiboles are both actinolite and tremolite) were occasionally found solitaire but always grouped together. In some cases amphiboles are practically abundant and they knit together to form clusters, this makes Kafubu emeralds more or less alike with those from Habachtal. Amphibole appeared colourless to a light green colour, and either typical straight needles or bamboo-like forms (figure 40a).
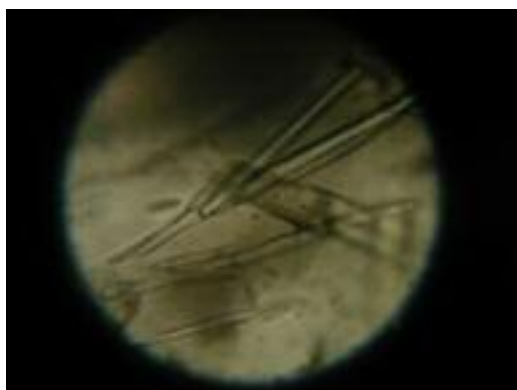
Figure 40a: Apatite crystal with amphibole needles in Kafubu emeralds.
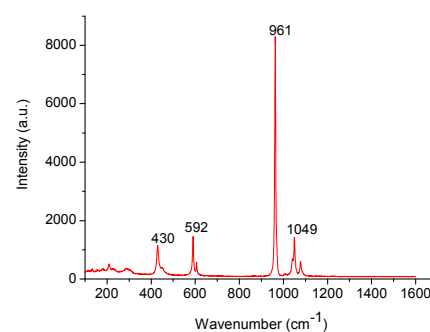
Figure 40b: Raman-spectrum obtained from apatite inclusion in Kafubu emerald.

Less abundant than biotite and amphibole are apatite, albite, quartz, hematite and lepidocrocite. Quartz is found as small grains associated with liquid inclusions. According to Zwaan et al. (2005) and Koivula (1982), tourmaline is a mineral inclusion in Kafubu emeralds as well; and this is in agreement with one of the host rock types of Kafubu emerald which is tourmaline-bearing mica schist. Furthermore, pyrite and talc are identified as rare mineral inclusions. Another widespread feature in Kafubu emeralds is parallel growth lines with a fine lamellar appearance. These

exhibited moderate to strong narrow zoning of straight, alternating light green to green bands which are oriented parallel to the prism faces of crystal.

3.10. Gwantu (Nigeria)

Gwantu emeralds show a large variety of fluid inclusions with tubular or irregularly shaped forms. The tubular shaped ones are orientated with the c-axes of the emerald host crystal, and therefore, they are considered as the primary filled cavities. Most of the fluid inclusions in the Gwantu emeralds have strong relief and appear almost opaque in the transmitted light. This is due either to the difference between the refractive index of the cavity filling and the surrounding emerald or to the irregular walls of the cavities. The most abundant type of inclusion in Gwantu emerald is one containing a liquid, a gas bubble and one or two crystals (figure 41).

Figure 41: Multi-phase inclusion in Nigerian emerald, fingerprint is also shown. x10

Figure 42: Fluid inclusion in Nigerian emeralds in elongated cavities. x50

Minerals contained in multi-phase inclusions show very well-formed cubic or rectangular crystals. The gas bubbles are identified as carbon dioxide by this study. According to Schwarz and others (1996), the minerals are probably halite. Such multiphase inclusions are also found in emeralds from Chivor, Columbia. The ratios of gas bubble to the volume of solid substances are relatively high in comparison with other localities. In addition to the large liquid inclusions, fingerprints were also frequently observed in Gwantu emeralds. By studies of Lind et al. (1986, 1984) two different types of two-phase inclusions were described. The first type forms irregular feathers, in most cases in the core of the crystals. The second type was generally

observed at the rims of crystal and forms elongated, often jagged cavities parallel to the prism face.

Beside the liquid inclusions, growth structures are also common in Gwantu emeralds. The most frequent observed structures are the bands parallel to the basal-pinacoid, prism and pyramidal faces. One can observe that during the growth of the crystal, many fluid inclusions have been incorporated. In comparison with liquid, mineral inclusions are much less frequent. There were samples in which even only liquid inclusions were observed. The most common minerals, according to Schwarz and others (1996) are fluorite (figure 43a) and albite (however, they were found in less than 10 percent of 1000 samples).
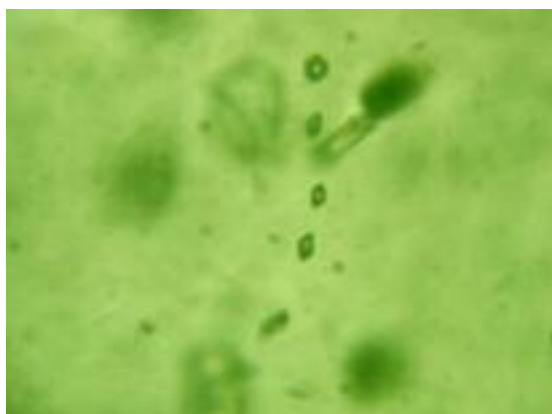
Figure 43a: The appearance of euhedral fluorite in such groups is very rare in Gwantu emerald, normally they are found singly. x50
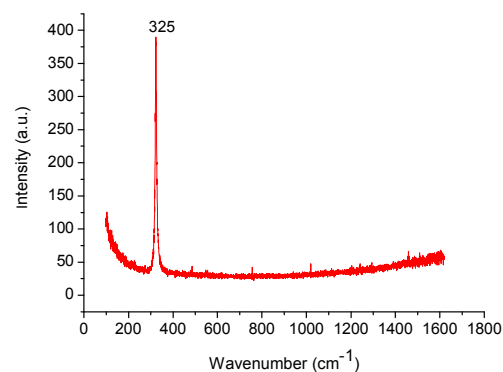
Figure 43b: Raman-spectrum obtained from a fluorite inclusion in Gwantu emerald.

Other minerals such as mica, ilmenite, quartz and tourmaline were found in less than a few percent of the samples. By the present study, biotite, fluorite, albite and tourmaline were found among which fluorite seemed to be the most common; the others were all found only occasionally.

3.11. Transvaal (South Africa)

As emeralds hosted in biotite schist, Transvaal emeralds present the typical inclusions for this origin: fluids and mica (biotite, muscovite) as well as atypical ones such as calcite, quartz, talc. Notably, fluid inclusions in Transvaal emeralds were found fewer in comparison with mineral inclusions in one sample itself or in comparison with

those in other localities of the same host rock (for instances, Kafubu, Itabira). These appear usually to be small, containing two phases, a liquid (water or liquid CO_2) and a CO_2 bubble. Sometimes, they can be seen in elongated cavities. Liquid inclusions in veil-like type or in tubular fissures were also seen. These make groups of irregularly shaped tiny inclusions which look like curved veils. This type of inclusions has also been observed in "emerald" crystals grown by the flux methods, which will be mentioned later in the part on synthetics. Three-phase inclusions were occasionally found, when found, they show the solid phase to be of square or rectangular shapes as those in Chivor or Gwantu emeralds. Three-phase inclusions were described by Schrader (1985) as unexpected inclusion of emeralds from South Africa.

Figure 44: Growth zoning in emeralds from Transvaal. x10
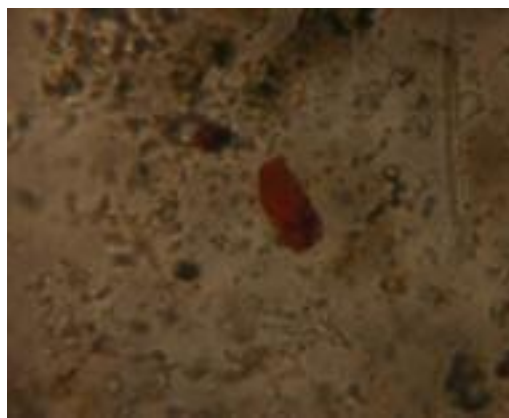
Figure 45: Lepidocrocite, with light brown flakes of mica. x50

Micas are considered as the most frequently observed inclusion, as been described in many localities; they appear with typical brown colour. Calcite and quartz show more or less well-formed crystals. Quartz crystals present the preferred orientation in host crystals parallel to the c axis.

Growth zoning is another feature of emeralds from Transvaal. They almost appear as fine-scaled parallel lines (figure 44). The colour between the lines is slightly varying. This indicates that the forming environment of Transvaal emeralds was not harshly changed. Hematite and lepidocrocite with the typical red colour were found commonly (figure 45).

3.12. Ural (Russia):

Uralian emerald is another one belonging more to the schist-hosted type. These emeralds were found to contain several types of liquid and two-phase inclusions. The most noteworthy were found in the form of flat cavities orientated on planes parallel to the pinacoid. In general, extremely thin channel-like structures running parallel to the c-axis, that is, perpendicular to the flat cavities, are confined to these planes. These cavities consist of liquid or two-phase (1 liquid and one bubble) inclusions and they have less frequently three-phase inclusions. Channel-like growth tubes parallel to the c-axis and elongated fluid inclusions trapped on growth planes were observed. In addition, numerous, partly healed fractures were observed irregularly traversing through most of the crystals.

Figure 46: Elongated mica inclusion in Uralian emerald. x50

Figure 47: Tiny particles (fluid inclusions) in Uralian emeralds resembling those in emeralds from Capoeirana. x50

In a few cases, fluid inclusions in Uralian emeralds were found to be alike with those in emeralds from Itabira: three-phase inclusion containing 2 liquids and a gas bubble. The gaseous and liquid phases in these inclusions are CO_2. The solid phase in three-phase inclusions is halite, but the halite crystals found here are not in the cubic form as those in Chivor or Gwantu emeralds. The feature of clouds or trails caused by tiny particles found in Carnaiba emeralds were also found in Uralian emeralds (figure 48). As described, these particles are the tiny one or two-phase liquid inclusions that make the host crystals look partially translucent only.

Mineral inclusions were found only rarely in Uralian emeralds. The most frequently observed minerals are several forms of mica which were determined by confocal-Raman spectroscopy as phlogopite (and muscovite with the smaller portion) which are

known to originate from mica schist host rocks. In general, phlogopites are virtually colourless, only a few of those show the brown hue. Normally, they appear as the more or less corroded flakes which are considered to be the typical form of mica. But sometimes they can appear as small rounded grains which at the first glance look like quartz grains. In other cases, the elongated form makes them to be confused with amphibole (if remembering that amphibole schist is one of the host rocks of these emeralds) (figure 46). Nevertheless, true grains of quartz and actinolite also occur. Actinolite crystals are found usually to occur individually. Due to the much less frequent appearance of mineral inclusions in comparison with liquid ones and the features of liquid inclusions, Uralian emeralds present themselves to be most alike with emeralds from Carnaiba.

3.13. Malipo (China):

The frequent appearances of protogenetic needle-formed tourmaline make emeralds from Malipo deposit very different not only from emerald of schist type but also from their other non-schist type partners. Tourmaline is not a common inclusion of emeralds and has been found only in few localities, such as Carnaiba (Brazil), Mananjary (Madagascar), Gwantu (Nigeria) as occasional inclusion. So, the frequent appearance of tourmaline can be used as the first criterion for the differentiation of this locality from others.

Perpendicular to the c axis cracks and fissure systems are very widespread. Together with the fissure system, there appear quartz, and members of the carbonate group (calcite, dolomite). These make the investigated samples from Malipo emeralds not transparent, in some cases even only translucent. Other mineral inclusions sometimes found in Malipo emeralds are apatite, scheelite, arsenopyrite, zircon, fluorite and sphene. Except apatite, fluorite and sphene which can be found in emeralds from some Brazilian localities and in some stones from Habachtal, Kafubu, Gwantu, these inclusions have not been seen in other localities.

Figure 48a: Tourmaline in emerald from Malipo. x10
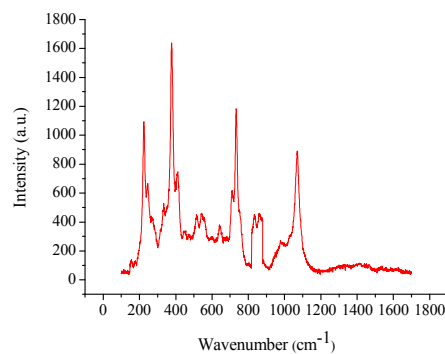
Figure 48b: Raman-spectrum obtained from tourmaline inclusion in emerald from Malipo.
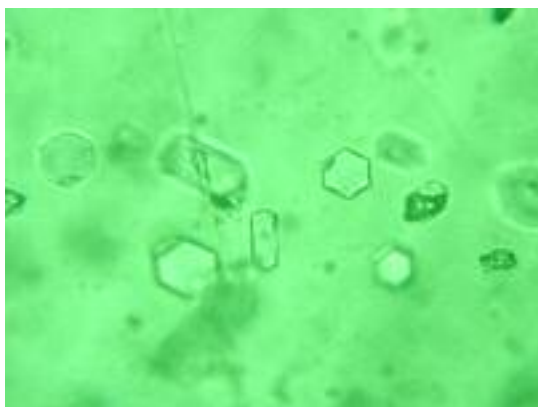
Figure 49: Quartz crystal (hexagonal form) and carbonate mineral (dark grains). x10

Figure 50: Eye-like three-phase inclusion in Malipo emerald. x50

Two- and three-phase inclusions are also frequently found in elongated forms in emeralds from Malipo, normally together with the fissure system. The eye-like three-phase inclusion shown above is an interesting case found in Malipo emeralds but the form is not typical for multi-phase inclusions in material from this region. The solid phase was determined in most cases to be quartz and sometimes halite.

3.14. Flux-grown syntheses

Numerous nail-head spicules are very typical for synthetic emerald like products which are never found in the natural samples. Fracture systems are also widespread in the flux synthetic samples. The whole crystal may contain many two-phase inclusions in wisp- or veil-like configurations. These wispy veils - more precisely, secondary flux-lined healed fractures - are typical of flux-grown synthetic stones (Graziani et al., 1987; Duyk, 1965).

45

(a) x50

(b) x10

(c) x10

(d) x10
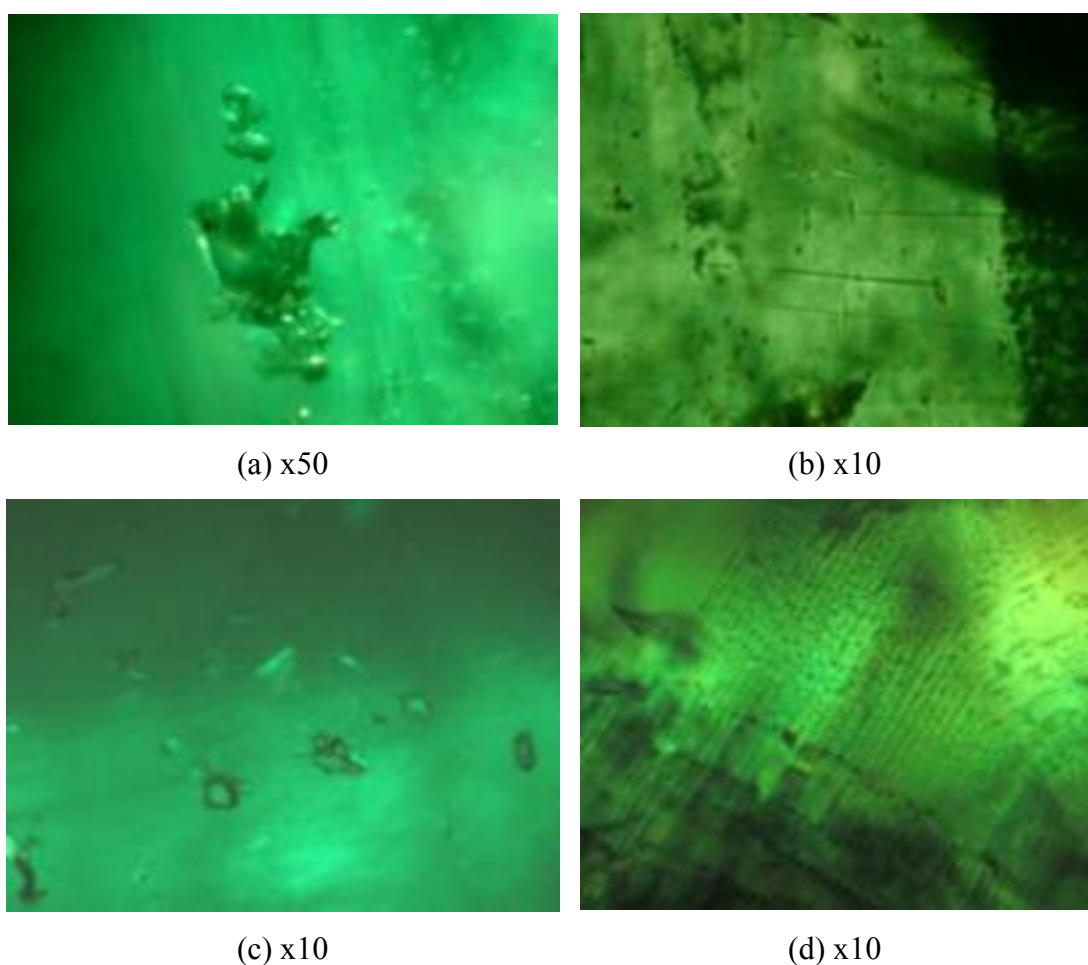
Figure 51: Inclusions in flux-grown "emeralds"; (a) undetermined inclusion in Gilson-emerald supposed to be rest melt substance (molybdate) which is very common in flux synthetic emerald and may be an indicator for Lennix-emeralds by Graziani et al. (1987); (b) phenakite crystals which show the typical appearance in nail-head spicules in Lennix-emerald; (c) cluster of phenakite crystals in Gilson-emerald; (d) tiny particles forming fingerprints composed of tiny two-phase inclusions (look like those in natural emeralds but in fact are flux fillings and completely solid) in Lennix-emerald.

Twisted veil-like structure elements are another characteristic of the flux synthetic "emerald". The presence of multiphase inclusions can be explained as the result of the rest of the melt substances which have been incorporated during crystal growth. Besides, sometimes there are crystals of platinum (from the crucible) as guests in the synthetic hosts.

In the samples of Chatham flux, multiphase inclusions are found arranging within the growth zoning. The zoning lines may be straight or angular in conformity to the hexagonal prism. Otherwise in Chatham flux, multiphase inclusion can occur individually in three-phase inclusions. In Lennix flux, quartz crystals and fog- or wisp-like forms of liquid drops were found. In comparison with other flux samples,

Gilson Flux is relatively poor in inclusions. Nevertheless, flux material and fractures are still found. A part of filled fractures shows the very characteristic stripe pattern.

3.15. Hydrothermally-grown syntheses

(a) x50

(b) x10

(c)

(d)

(e)

(f)
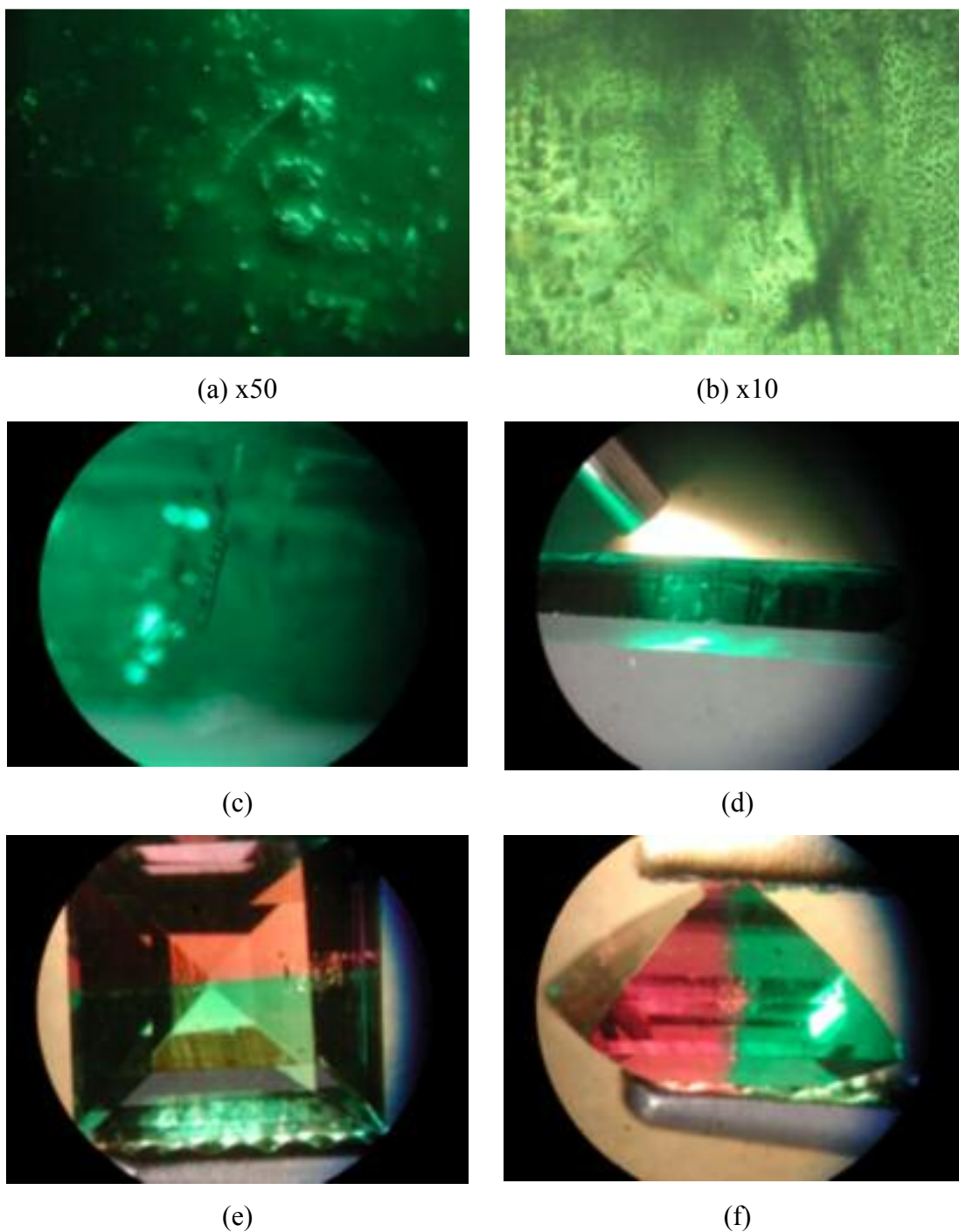
Figure 52: Inclusions in hydrothermally-grown "emeralds"; (a) undetermined particle with metal lustre in Biron "emerald"; (b) fingerprints in Biron "emerald"; (c) black grain substance swarming from one metal needle in Tairus "emerald"; (d) many metal needles found in one Tairus "emerald"; (e) chevron-like growth zoning in Tairus "emerald"; (f) two differently coloured parts in one Tairus stone with chevron feature indicating that the green part was firstly grown and then the red part.

The parallel chevron-like feature of growth lines is a very special character of hydrothermal samples (Fumagalli et al., 2003; Sechos, 1997; Koivula et al., 1996). In addition, there are phenakite crystals, fingerprints, 2-phase inclusions (gas and liquid) which are found in almost all samples.

The faceted Biron synthetic "emeralds" examined range in clarity from those with prominent inclusions, growth features and colour zoning, to those that were remarkably clean and appeared to be nearly flawless with no growth features. Two-phase inclusions consisting of a fluid and a gas bubble were observed to have three distinct appearances: 1. forming fingerprint patterns and wispy veils; 2. as large, irregular voids containing one or more bubbles and 3. trapped within the tapered portion of nail-head spicules. The nail-head spicules are formed by a single crystal or a group of phenakite crystals. Growth features are observed in one or in combination of the following forms: straight, parallel and uniform; angular, straight and intersecting, parallel needle-like particles, veil structures and dark metallic inclusions can be found. Tairus samples can be distinguished in 2 types. In type 1 "emerald" is extremely clean; multiphase inclusions do not occur.

Beside the step-like growth lines there are only tiny opaque solid inclusions with metallic lustre which have been determined by Schmetzer et al. (2006) as native copper. In type 2, there are many needle-like metal inclusions and chemical analysis by means of ICPMS brings out this metal as an alloy of iron (80 wt%), nickel (15 wt%) and chromium (5 wt%). In addition, there are also bubbles and/or two-phase inclusions.

Discussion

Microscopical research on the phases, the types of inclusion in emeralds can help to separate the localities or the origin of host crystal minerals by means of association of certain inclusions or in some cases, by appearance of special inclusions itself. Geologically, typical emerald mineralization can be roughly classified into schist-hosted and non-schist-hosted types, based on the major host rocks. Acording to this very coarse discrimination, typical schist-hosted emeralds come from Brazil, Austria

(Habachtal), Madagascar (Mananjary), Russia (Ural), South Africa (Transvaal), and Zambia (Kafubu). The others, from not clearly shist-hosted deposits, usually come from Nigeria (Gwantu), Colombia (Chivor) and China (Malipo) belong to the non-schist-hosted type.

For the schist-hosted type endmembers, the inclusion suit of quartz, mica, amphibole, fluid inclusions are normally abundant and considered as the typical inclusions for emeralds of all of these localities. And, because the localities have the same inclusion suit, then, the appearance of these inclusions has only a little value in distinguishing each locality from the others. Nevertheless, in the mean of association with other types of inclusions, or by some special appearances of typical inclusions themselves, and especially, with increasing personal experiences, the possibility of proper discrimination is growing. For instances, the cluster of amphibole in Habachtal emeralds is one distinguishable feature. The feature of abundant multi-phase inclusions containing two liquids, developed in well-formed negative crystals; more or less square, rectangular cavities is characteristic for Itabira emeralds. In the contrary, beside the typical mineral suit, there are the individual minerals that exist only in certain localities and could be a great value to limit the range of emerald location, for instance, pyrite is found only in emeralds from three locations, that are Santa Terezinha, Kafubu and Chivor.

Furthermore, those emeralds coming from a geological environment that is characterized by the association of different metamorphic schists, for examples Mananjary, Transvaal, etc, with principally biotite/phlogopite schists and subordinately amphibole-bearing or amphibole schist, and pegmatite veins, probably show the typical inclusions such as quartz, biotite, phlogopite, rods or needles of actinolite, tremolite, crystal grains of chromite, feldspar. Other localities such as Kafubu in which the host rock of emeralds are partly tourmaline bearing mica schist could be noted additionally by the tourmaline inclusions.

For the non-schist-hosted branch of emerald deposits, such as Malipo, Gwantu and Chivor emeralds, mineral inclusions are not characterized by mica or amphibole, but different suits instead. Carbonate minerals, tourmaline, feldspars, scheelite are minerals characterized for emeralds from Malipo. A great part of fluid inclusions

together with the less frequent mineral inclusions in emeralds from Gwantu can be used to separate this locality from the others.

Country	Brazil					Zambia	Madagascar	South Africa	Russia	Austria	China	Colombia	Nigeria	Syntheses				
Locality or deposit	Santa Terezinha	Socoto	Carnaiba	Capoeirana	Itabira	Kafubu	Mananjary	Transvaal	Ural	Habachtal	Malipo	Chivor	Gwantu	Chatham	Syn. Gilson	Syn. Lennix	Syn. Biron	Syn. Tairus
Quartz	.	.	.	●	●	.	●	.	.		●	.	.			.		
Biotite	●	●	.	●	●	●	●	●		●			.					
Muscovite		●	.						●	.		.						
Phlogopite		●			●		●			.								
Margasite		.																
Calcite	●			.			.	.			●	●						
Dolomite	●			.			.				●	●						
Magnesite	●						.											
Siderite				.														
Hydrozincite	.																	
Talc	●	.				.	.	.										
Scheelite											.							
Albite	.	.				.	.				.	●	.					
Oligoclase	.						.			.								
Andesine				.														
Clinochlore												.						
Chlorite		.																
Zircon											.							
Pyrite	●					.						●						
Molypdenite		.					.											
Apatite		.	.		.	.				.	.							
Magnetite	.																	
Hematite	.	.			.	.		.				.						
Goethite	.	.	.															
Lepidocrocite		.				.		.										
Arsenopyrite											.							
Actinolite	.	.	.			●	●		.	●								
Tremolite	.	.			●	●	●			●								
Tourmaline			.			.	.				●		.					
Epidote										.								
Sphene										.	.							
Fluorite										.		.						
Phenakite														.	.		.	.
Pargasite												.						
Chromite	●																	
Ilmenite													.					

Table 3: Mineral inclusions in emeralds from various deposits and different methods of production with probability of observed inclusion frequency. (●) more significant; (.) less significant

Carbonate minerals, feldspars and pyrite are minerals characteristic for emeralds from Chivor. Mica and amphibole are even considered as rare mineral inclusions in non-schist-hosted emeralds.

Briefly, good knowledge on the host rocks of emeralds as well as on the forming conditions is a good base for research on provenance discrimination based on inclusions or internal features of emeralds.

Inclusions provide the most effective means of separating the synthetic ones against the natural counterparts. So far the inclusions observed in synthetic "emeralds" are fingerprints, veils, and fracture; single occurrence of large two-phase inclusions, nail-head spicule inclusions with gas and liquid phase, phenakite crystal, numerous types of growth features, negative crystals, metals, etc.. In contrast to flux-grown synthetic products, in which the fingerprints and veils are healed fractures with flux fillings, the fingerprints and veils in hydrothermal synthetic "emeralds" generally consist of many small two-phase inclusions that are usually concentrated at chevron and planar interfaces; although flux inclusions may be similar in appearance, they are completely solid. The fingerprints and veils in hydrothermally grown "emeralds" in some case are remarkably similar in nature and appearance to those observed in natural emeralds.

4. CHEMICAL PROPERTIES OF INVESTIGATED EMERALDS

Laser ablation-inductively coupled plasma-mass spectrometry (LA-ICP-MS) and electron microprobe analysis (EMPA) were used to determine the concentration of 30 elements, i.e. Li, Be, B, Na, Mg, Al, Si, P, K, Ca, Sc, Ti, V, Cr, Mn, Fe, Co, Ni, Ga, Ge, Rb, Sr, Y, Zr, Nb, Mo, Cs, Ba, La and Ta, in 36 emerald samples from various localities and different types of synthesis. Basing on the idea that the concentration of principle elements may allow us to specify whether the stone is natural or synthetic in the first place, it might be possible to classify natural emeralds whether of "schist-type" or of "non-schist-type" due to the concentration of Na, K and Mg, for example. Other localities, such as Chivor and Malipo could be specified due to low and high concentration of Fe and V, respectively.

Using chemical properties to distinguish natural emeralds from synthetic counterparts has been performed by a number of researchers (Stockton, 1984; Schrader, 1983; Hänni, 1982). The theory that one can discriminate chemically between synthetic and natural gem materials is based on the premise that some chemical elements which are nonessential for the crystal compound can be found only in natural but not in synthetic material, and conversely; some other elements which are used in synthetic manufacture, then contaminated during production are normally found to be more plenty in synthetic than in natural material (Stockton, 1984). Furthermore, we truly see that emeralds from different localities show different qualities and colours, it may be hue or transparency, colour zoning or intensity. These differences could be the result of the forming condition of each emerald, especially the incorporation of colour relevant trace elements. Therefore, at least theoretically, chemical analyses may even present additional criteria that could be used to distinguish between natural emeralds according to their geological setting and formation.

Chemical analyses were carried out by means of Laser Ablation - Inductively Coupled Plasma - Mass Spectrometer (LA-ICP-MS) and Electron Microprobe. Using LA-ICP-MS is to identify Li, Be, B, Na, Mg, Al, P, K, Ca, Sc, Ti, V, Cr, Mn, Fe, Co, Ni, Ga, Ge, Rb, Sr, Y, Zr, Nb, Mo, Cs, Ba, La and Ta. Electron microprobe analysis was used

to identify the most important element Si and other elements as well to have a reference matrix between LA-ICP-MS and EMPA measurements.

Ablation was achieved with a New Wave Research UP-213 Nd:YAG laser ablation system, using a pulse repetition rate of 10 Hz producing 100 μm crater diameters. Analyses were performed on an Agilent 7500ce inductively coupled plasma - mass spectrometer in pulse counting mode (one point per peak and 10 ms dwell time). Data reduction was carried out using the software "Glitter". The amount of material ablated in laser sampling is different for each spot analysis. Consequently, the detection limits are different for each spot and are calculated for each individual acquisition. Detection limits generally range between 0.001 and 0.5 ppm (μg/g). ^{28}Si was used as internal standard. Analyses were calibrated against the silicate glass reference material NIST 612 using the values of Pearce et al. (1997), and the US Geological Survey (USGS) glass standard BCR-2G was measured to monitor accuracy.

Microprobe analyses were achieved with a JEOL JXA 8900RL - electron beam - Microprobe with wavelength dispersive analyse technique. The chemical composition of each sample was then corrected by PAP program. The samples were measured by an acceleration voltage of 20 KV and 20 nA filament current. The detection limits differ for each element and are affected by the overall composition of a sample and the analytical conditions. For most elements, the detection limits for wavelength-dispersive (WD) spectrometers is between 30 and 300 parts per million (ppm). The precision depends on counting statistics, particularly the number of X-ray counts from the standard and sample, and the reproducibility of the WD spectrometer mechanisms. The minimum obtainable precision is about 0.5 percent, although it is higher for elements at trace concentrations. Therefore, EPMA is specially used in this study for detecting the main element Si.

In the following diagrams, the chemical data for the most important elements are displayed and shortly discussed; the numbers of the samples are shown next to Figure 53.

4.1. Silicon (Si)

Figure 53: Diagram showing the content of silicon in emeralds from various
deposits and manufactures, sample-numbers (x-axis) are given below.

Colombia (Chivor): 1-5	Madagascar (Mananjary): 22, 23
Nigeria (Gwantu): 6-10	Zambia (Kafubu): 24, 25
China (Malipo): 11, 12	South Afirca (Transvaal): 26, 27
Brazil (Santa Terezinha): 13	Syn. Lennix: 28
Brazil (Socoto): 14	Syn. Gilson: 29, 30
Brazil (Capoeirana): 15	Syn. Chatham: 31, 32
Brazil (Carnaiba): 16	Syn. Biron: 33, 34
Brazil (Itabira): 17	Syn. Tairus: 35, 36
Russia (Ural): 18, 19	
Austria (Habachtal): 20, 21	

The ideal composition of beryl, i.e emerald, shows a content of 67% silicon by
weight. However, values of real compositions of natural emeralds are rather constant
and usually content an amount of silicon less than the theoretic values. These values in
"schist-type" emeralds are from 62,72 wt% to 64,41 wt% and in "non-schist-type"
emeralds are from 64,99 wt% to 66,25 wt%. However, emeralds from China could be
classified geologically as "non-schist type" emeralds but the content of silicon is
somewhat more like those of "schist-type" ones (63,52 – 63,91 wt%). Synthetic
"emeralds" achieve approximately the ideal composition in which the content of
silicon lie in the range from 66,30 wt% to 66,83 wt%.

4.2. Aluminium (Al)

Figure 54: Diagram showing the content of aluminium in emeralds from various
deposits and manufactures, sample numbers are shown next to figure 53.

Again, to compare with the ideal amount of aluminium in theory (18,9 wt%), the content of aluminium in "schist-type" emeralds which was detected to lie between 14,01 wt% to 17,05 wt% is much far from the theoretical value, while in "non-schist-type" emeralds these values are from 16,23 wt% to 17,79 wt%. Synthetic "emeralds" have from 17,28 wt% to 19,30 wt% of aluminium content. One Chinese emerald has 19,87 wt% of this element. In general, "non-schist-type" emeralds contain more aluminium than "schist-type" ones do and therefore these lie closer to the ideal value.

4.3. Beryllium (Be)

Unlike the results investigated for the aluminium and the silicon content, the beryllium content shows to be very variable in both "schist-type" and "non-schist-type" emeralds. And also the beryllium contents variation between natural and synthetic samples is not of high significance: In natural samples the amount of beryllium varies from 12,75 wt% to 15,64 wt% while the beryllium content for synthetic ones is from 13,61 wt% to 14,55 wt%. The theoretical content of this element is 14,1 wt%.

55

Figure 55: Diagram showing the content of beryllium in emeralds from various
deposits and manufactures, sample numbers are shown next to in figure 53.

4.4. Lithium (Li)

Lithium was found in almost all emeralds (up to 0,174 wt%) with only one exception
(synthetic Tairus) showing an amount under the limit of detection for this element (1
ppm). The favourite flux using in flux synthetic manufactures is lithium molybdate,
but flux syntheses did not show to contain high lithium contents compared with
natural emeralds of "schist-type". Among the samples studied, some Brazilian
(Itabira, Socoto, Carnaiba) emeralds were found to have the highest values. Except the
Tairus sample mentioned above, "non-schist-type" emeralds have the least lithium
values compared with all others (from 0,007 wt% to 0,025 wt%).

Figure 56: Diagram showing the content of lithium in emeralds from various deposits and manufactures, sample numbers are shown next to figure 53.

4.5. Sodium (Na)

Sodium was found in all natural emeralds with varying amounts from 0,096 wt% to 1,696 wt%. The "non-schist-type" emeralds have been found to contain 0,096 to 0,924 wt% whereas "schist-type" emeralds have distinctly more, from 1,048 wt% to 1,696 wt%. Nigerian emeralds were found to contain least sodium among natural samples (up to 0,132 wt%). Some synthetic "emeralds" show Na-amounts to be very small, up to 0,066 wt%, some other synthetic stones were almost free of this element (containing only some ppm).

Figure 57: Diagram showing the content of sodium in emeralds from various deposits and manufactures, sample numbers are shown next to figure 53.

57

4.6. Magnesium (Mg)

Magnesium was absolutely not found in Chatham samples, other syntheses were found to contain less than 0,032 wt%. "Schist-type" emeralds show amounts from 0,349 wt% to 0,550 wt%; "non-schist-type" emeralds show the amounts from 0,002 wt% to 0,308 wt%. Nigerian emeralds were found to contain least magnesium among natural emeralds (up to 0,044 wt%). Generally, Nigerian emeralds can be easily distinguished from other natural emeralds from other countries with the variation of magnesium which is significantly from 0,022 wt% to 0,048 wt%.

Figure 58: Diagram showing the content of magnesium in emeralds from various deposits and manufactures, sample numbers are shown next to figure 53.

4.7. Gallium (Ga)

Gallium was contained in both natural and synthetic "emeralds". In natural emeralds the amount of gallium was detected between 7 ppm to 28 ppm whereas in synthetic "emeralds" a slightly lower range of 0 ppm to 21 ppm was found.

4.8. Caesium (Cs)

Chinese emeralds were found to have the largest concentrations of caesium among the samples investigated (up to 1338 ppm), followed by Brazilian and Zambian emeralds. The amount of caesium was found to vary strongly in emeralds from Madagascar

(from some ppm to some hundred ppm). Emeralds of "non-schist type" (Colombia and Nigeria) and Tairus content less than 100 ppm of caesium. Flux "emeralds" were found to content less than 1 ppm of this element.

4.9. Iron (Fe)

Iron has been found in all samples with considerable variation in stones of different origins or even in the same locality. These amounts range from 0,002 wt% to 0,893 wt%. Colombian emeralds have least iron among natural stones with a variation from 0,023 wt% to 0,149 wt%. Flux samples (Chatham and Gilson) were found to contain also small contents varying from 0,02 wt% to 0,054 wt%. Obviously, it is not easy to discriminate emeralds from each other due to the overlap of iron contents among them. This, of course, is also a problem of the area under investigation in a single crystal of emerald, where the influence of very small inclusions (iron-compounds etc.) may be very large.

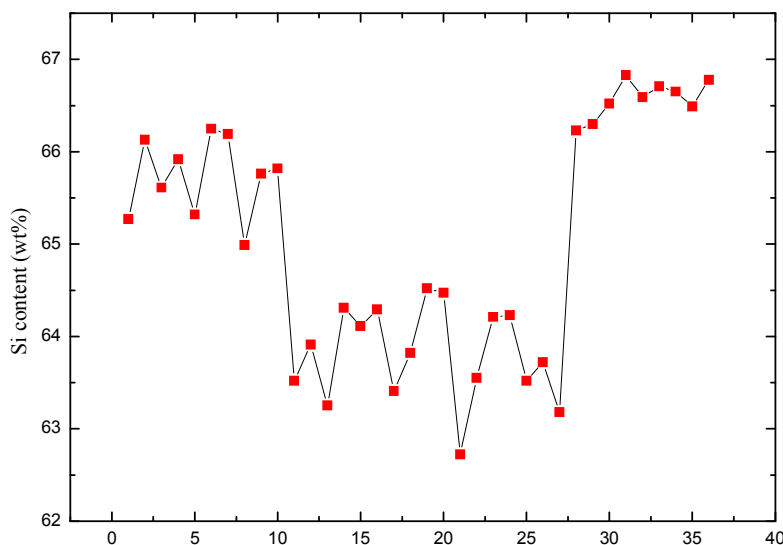*Figure 59*: Diagram showing the content of iron in emeralds from various deposits and manufactures, sample numbers are shown next to figure 53.

4.10. Niobium (Nb) and Strontium (Sr)

Niobium was found only in some Tairus samples with very variable amounts, from some ppm to 128 ppm. Strontium was found in Austrian samples with a maximum amount of about 7 ppm.

59

4.11. Titanium (Ti)

Although titanium was found in all specimens, the content of titanium in samples is not considerably varying from some ppm to some ten ppm, except some synthetic specimens (Tairus, Biron, Gilson) among which the Biron sample contains remarkably high titanium contents of about 199 ppm. In general the content of titanium in emerald does not enable to distinct between occurrences of natural emeralds.
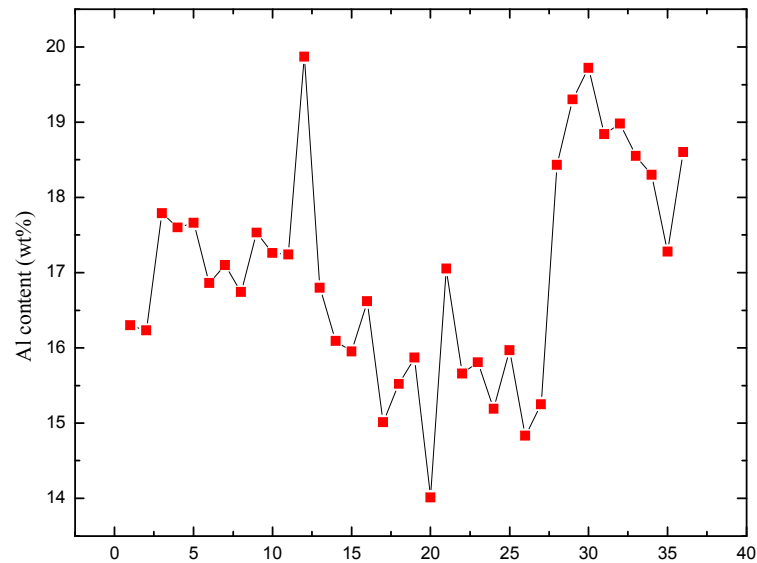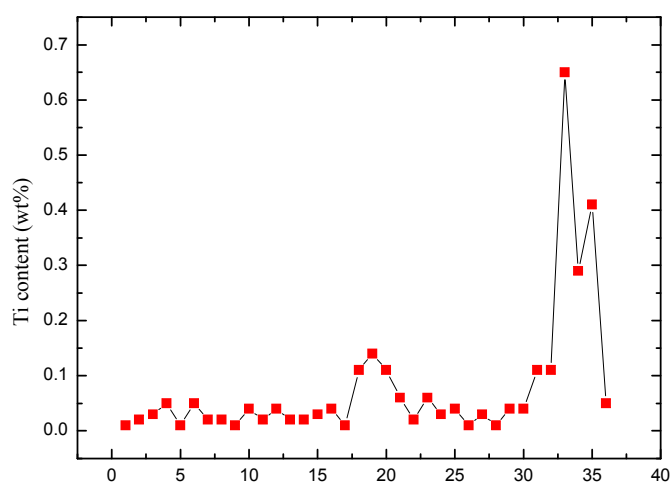

Figure 60: Diagram showing the content of titanium in emeralds from various deposits and manufactures, sample numbers are shown next to figure 53.

4.12. Nickel (Ni)

In almost all samples nickel was found with strong variations. Within the studied samples, hydrothermal syntheses have the highest amounts of nickel, from 792 ppm to 1370 ppm (the highest nickel values are found in a Tairus sample). Differently, flux syntheses were found to contain small amounts of this element. In Gilson samples less than 15 ppm and in Chatham samples less than 1 ppm of nickel was detected. Among natural stones the amount of nickel in "schist type" emeralds (up to 175 ppm) is relatively higher than that of "non schist type" ones (less than 10 ppm), a distinctly low content of nickel was found in Nigerian samples (less than 1ppm).

4.13. Rubidium (Rb)

This element was found most frequently and with a relatively high concentration in emeralds from Madagascar with values up to 138 ppm. Other "schist-type" emeralds contain some tens ppm. Compared with "non-schist-type" emeralds, "schist-type" emeralds contain less rubidium (Colombian emeralds have less than 3 ppm, Nigerian emeralds less than 16 ppm). Normally synthetic "emeralds" do not contain any rubidium, the maximum being represented by less than 3 ppm.

4.14. Vanadium (V)

Among the investigated samples, vanadium was found with extremely high values in Chinese specimens, up to 0,587 wt%. This element was not found in almost all synthetic "emeralds" except one sample of Gilson (0,113 wt%). Other natural emeralds contain vanadium amounts varying from 0,011 wt% to 0,082 wt%.
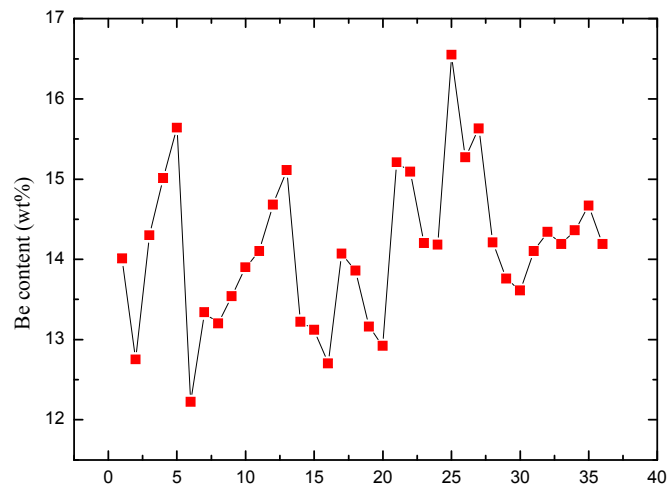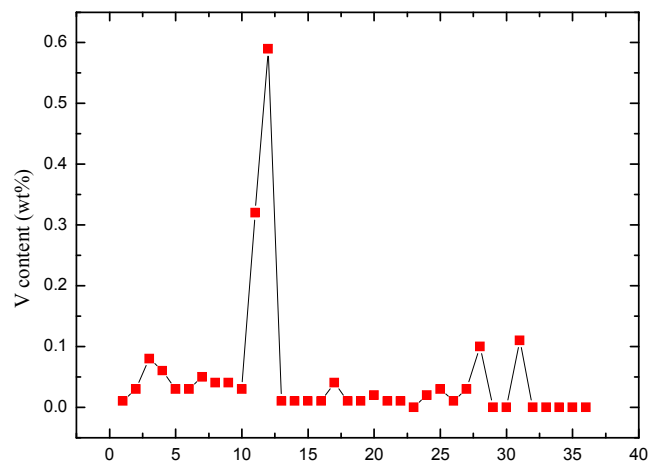

Figure 61: Diagram showing the content of vanadium in emeralds from various deposits and manufactures, sample numbers are shown next to figure 53.

4.15. Molybdenum (Mo)

As to be expected, molybdenum was found only in flux synthetic "emeralds", in Chatham samples this element amounts up to 4118 ppm whereas in Gilson samples the maximum molybdenum content was 120 ppm. Molybdate can be used as flux components; therefore the present of Mo in a sample could be used to distinguish between natural and certain synthetic "emeralds". However, not all flux samples were

found to content molybdenum; therefore the absence of this element is not provable for the natural origin of an emerald.

4.16. Potassium (K)

The potassium contents detected in emeralds of this investigation are relatively high compared with other studies (Hänni, 1982; Schrader, 1983; Stockton, 1984), and reach up to 0,285 wt%. High contents of potassium are found in samples from Zambia, Madagascar, and Austria, whereas emeralds from Chivor and Nigeria have been found to contain less potassium. Chivor stones with potassium contents varying from 0,006 wt% to 0,013 wt% could be said to be the emeralds with the lowest potassium values among natural samples. Potassium amounts in synthetic stones are almost in the same variation with Colombian ones, from 0,001 wt% to 0,014 wt%, with one exception of a Gilson sample, showing up to 0,041 wt%.
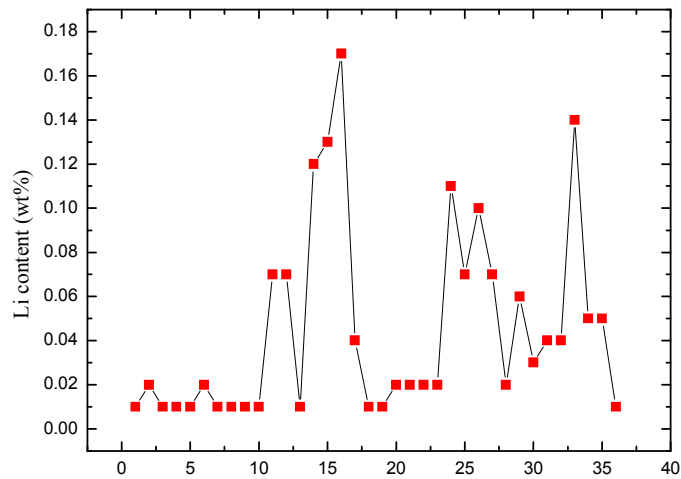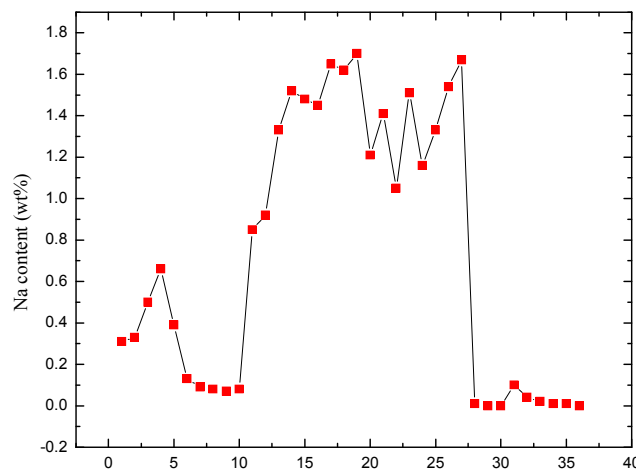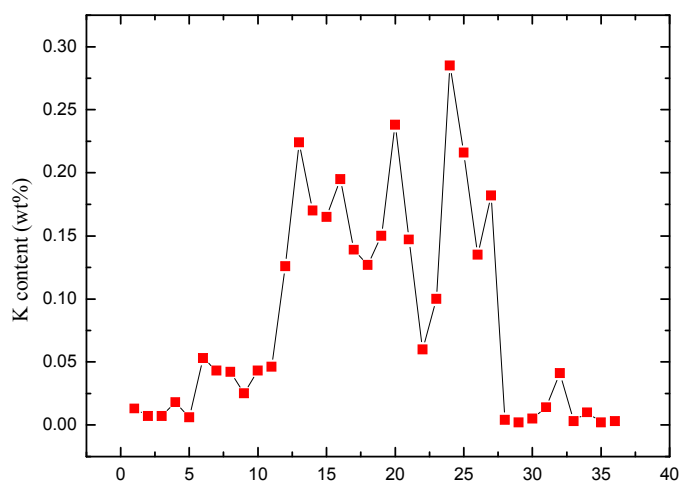

Figure 62: Diagram showing the content of potassium in emeralds from various deposits and manufactures, sample numbers are shown next to figure 53.

4.17. Manganese (Mn)

In flux syntheses and emeralds from Colombia only traces of manganese were found (< 1 ppm), whereas the manganese contents in hydrothermal syntheses were found to lie between 171 ppm to 206 ppm (i.e. 0,022 w% to 0,025 wt%) and in other natural emeralds between some ppm to some hundred ppm. Nigerian emeralds have 3 ppm to

7 ppm and Austrian emeralds have 100 ppm to 380 ppm are the emeralds with lowest and highest manganese contents, respectively.

4.18. Chromium (Cr)

Chromium has been found in all the examined specimens with considerable variation in stones either in different provenances or even in the same locality. The amount of chromium in natural samples varies from 0,006 wt% to 0,424 wt%, the lowest and the highest chromium containing stones were found to be one emerald from China and one from Madagascar, respectively. In synthetic samples the amount of chromium varies from 0,165 wt% to 0,413 wt%.
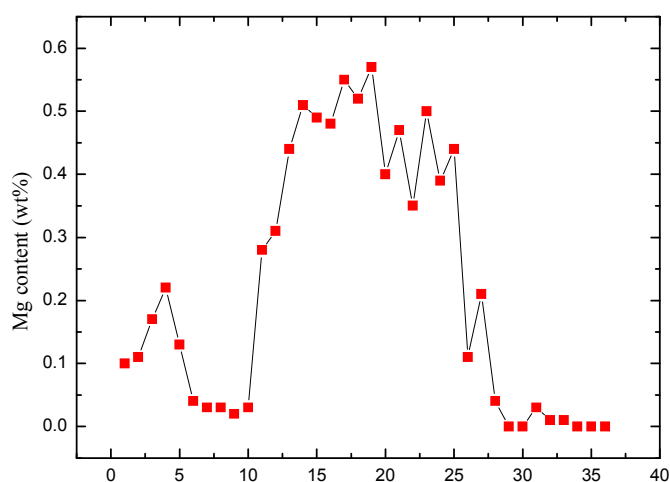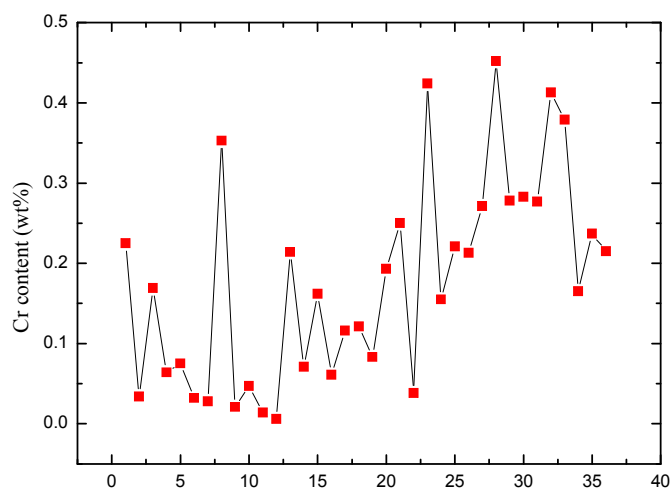

Figure 63: Diagram showing the content of chromium in emeralds from various deposits and manufactures, sample numbers are shown next to figure 53.

4.19. Scandium (Sc)

All natural and synthetic emeralds were found to contain scandium in varying amounts. The amount of scandium in synthetic "emeralds" lies between 0,001 wt% to 0,004 wt%, whereas in natural emeralds between 0,001 wt% to 0,066 wt% in which emeralds from all Brazilian localities and China have distinctly higher values.
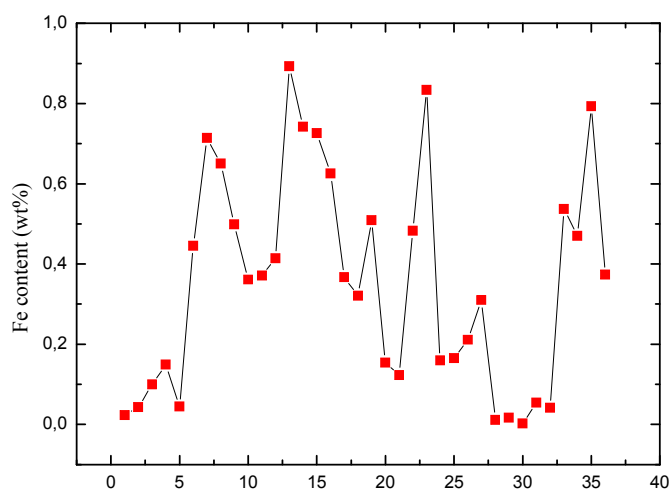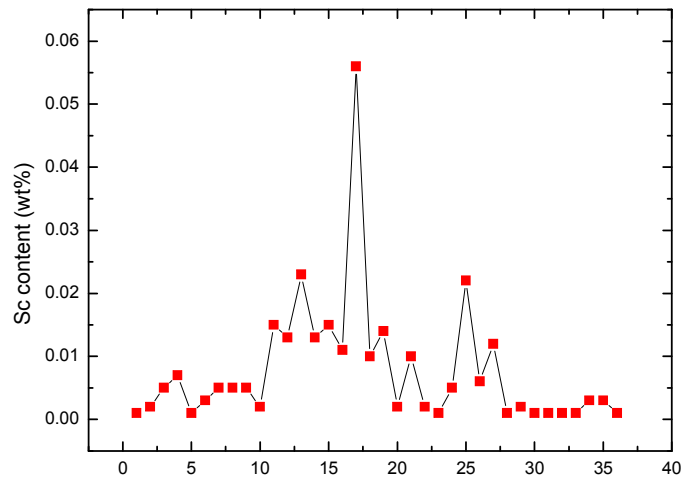
Figure 64: Diagram showing the content of scandium in emeralds from various deposits and manufactures, sample numbers are shown next to figure 53.

Discussion

Emeralds from occurrences in Brazil, Madagascar, Zambia, Russia and South Africa belong to the so-called "schist-type" deposits, which are located in regions where acidic magmas have penetrated country rocks in the vicinity of basic and ultrabasic rocks, Be-enriched fluids derived from these acidic magmas have generated metasomatism of Cr-bearing mafic and ultramafic wall-rocks leading to the formation of emeralds. The ore bodies usually consist of phlogopite-bearing rocks, related to a peculiar metasomatic association in ultrabasic rocks surrounding, containing actinolite or tremolite and variable quantities of talc, chlorite, quartz, albite, chromite, ilmenite, magnetite, apatite, fluorite, etc.. Emeralds of "non-schist-type" provenance, which are those from Colombia and Nigeria are generated within the regime of carboneous rock suites or within a pegmatite which is not associated with schistic bodies.

In contrast to the emeralds from the "schist-type" deposits, which have relatively high magnesium (0,349-0,550 wt%), sodium (1,048-1,696 wt%) and potassium (0,053-0,285 wt%) contents, emeralds from "non-schist type" are characterized by lower contents of these elements, magnesium (0,002-0,308 wt%), sodium (0,096 wt%), and potassium (0,006-0,054 wt%). Therefore, the content of these elements may be used

64

as a good criterion to discriminate emeralds on a obviously not completely homogenious scale between the two endmembers "schist type" and "non-schist type".

Besides, other elements such as Fe, Cr and V could be also good criteria for some peculiar regions. Among natural samples, the Fe content is found to be extremely low in emeralds from Colombia (0,023-0,149 wt%) while in other localities this values ranges from 0,123-0,893 wt%. Chromium is the element responsible for the green colour of emeralds. However, all samples from the Chinese deposit are characterized by low chromium values, and contain relatively high amounts of vanadium, about 0.3 to 0.5 wt% which contributes to their colour.

The amounts of main elements (Si, Al, Be) in synthetic "emeralds" are approximately near to the ideal amounts whereas these values are more different in natural emeralds. This is probably a result of the substitution of site replacements by "impurity ions", since the amount of non essential elements ("impurities") is much higher in natural emeralds, especially in "schist-type" emeralds, than that in synthetic ones. The Si content in synthetic samples varies from 66,30 wt% to 66,83 wt%, i.e., only 0,7 wt% to 0,17 wt% different to the ideal amount, while in natural samples these amounts are up to 5 wt% less. Similarly, Al and Be content in natural samples can be up to 4% and 2% by weight less than ideal amount, respectively, while in synthetic "emeralds", these values are more or less 1% different.

The differences of cation amounts in emeralds from various localities could be the result of the isomorphic substitutions. Nevertheless, it is impossible to give out the exactly substitutions in emeralds for each particular locality. As Be^{2+}, Si^{4+}, Al^{3+} have ionic radii in tetrahedral sites of 0,27; 0,26; 0,53 Å, respectively, and Na^+, K^+, Rb^+, Cs^+ have ionic radii of 0,99; 1,51; 1,52; 1,67 Å, resp. (Shannon, 1976), it is clear that none of these alkali metal ions can substitute for beryllium, silicon or aluminium in the beryl crystal structure. It is highly probable that most of the alkali ions in beryl are located in structure channels and play their part as charge compensation for other ions in other substitutions. Only lithium with an ionic radius of 0,59 Å can substitute in some positions of main elements within the architecture of the main, channel surrounding crystal structure. On the charge and radius requirements Al^{3+} could be substituted not only by trivalent elements (Cr^{3+}, V^{3+}, Fe^{3+}) but also by divalent

elements Mn^{2+} (0,66 Å), Mg^{2+} (0,57 Å), Fe^{2+} (0,63 Å) according to the scheme: Al^{3+} $\rightarrow$ Mg^{2+} + (R^+ + H_2O) since the charge compensation is saved by R^+ alkali ions (Sherriff et al., 1991).
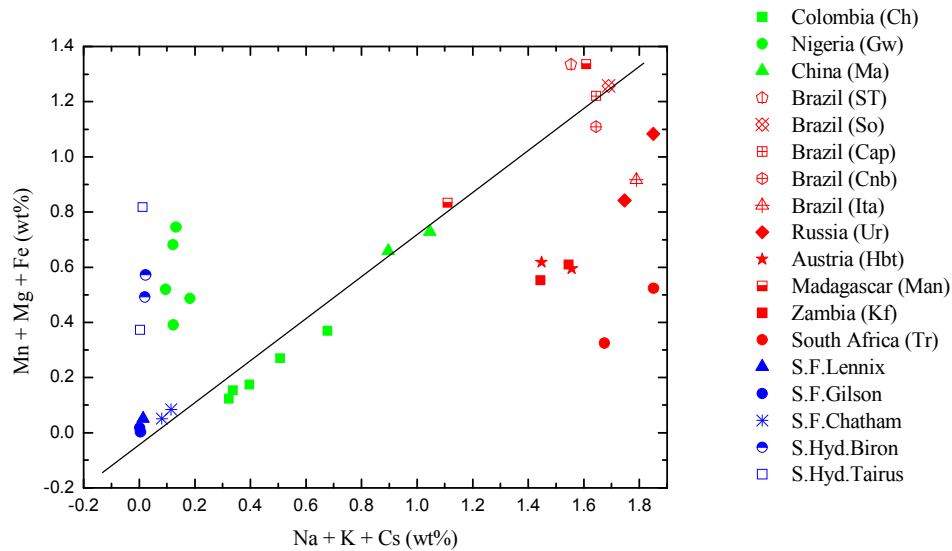
Figure 65: Plot of alkali content (Na, K and Cs) versus the contents of Mn, Mg and Fe showing for a part of investigated samples the trend of more channel alkali ions with more divalent structural ions.

Nevertheless, the ionic replacements in beryl are fairly complicated and this supposed substitution is probably only one of the possibilities since the plot of alkalis versus the amounts of Mn, Mg, Fe show only in a part of the samples investigated the positive correlation between alkali contents and the amount of the divalent ions (Figure 65). In addition, the contents of alkalis are not correlated negatively with the aluminium contents. In these cases, the substitution of aluminium must be more complicate and may be accompanied by other cations, such as: $Al^{3+} + R^+ \Leftrightarrow Si^{4+}$, $Be^{2+} + R^+ \Leftrightarrow Al^{3+}$ (Shatskiy et al., 1981 and Schmetzer and Bernhard, 1994).

Howthorne and Cerny (1977) supposed a substitution for beryllium in its tetrahedral site: $Li^+ + R^+ \Leftrightarrow Be^{2+}$ in which Be^{2+} is substituted by Li^+ and the alkali in channel (R^+) is a charge compensator. Other substitutions in beryl are proposed by Shatskiy et al. (1981): $Be^{2+} \Leftrightarrow \square + 2R^+$; $3\ Be^{2+} \Leftrightarrow 2\ Li^+ + Si^{4+}$; $Be^{2+} + 2R^+ \Leftrightarrow Si^{4+}$; $Be^2 + Si^{4+} \Leftrightarrow 2\ Al^{3+}$. All these possibilities make it very difficult to predict or model the substitutions in beryl on a structural and chemical base.

5. RAMAN MICRO-SPECTROSCOPY OF EMERALDS

Raman spectroscopy is one of the non-destructive methods using the light induced vibrations and interactions of the visible light with bondings influenced by the neighbourhoods and the lattice or more general, neighbourhood in a certain materials structure. Using this method allows to characterize for example different water types in channel sites of beryls from different localities and from different producers. The differences in Raman spectra of emeralds are observable for the Raman shifts in the range 200-1600 cm^{-1} and the range of water vibrations at 3500-3800 cm^{-1}. In correlation with the chemical data, results achieved by Raman spectroscopy lead us to conclude that the controversially discussed Raman shift at 1067 cm^{-1} – 1072 cm^{-1} is generated by the Si-O bonding and not by the Be-O bonding as mentioned in some publications. This Raman-shift occurs in "schist-type" emeralds around 1069-1072 cm^{-1} while in "non-schist-type" emeralds and synthetic emeralds it occurs around 1068-1070 cm^{-1} and around 1067-1068 cm^{-1}, respectively. The Full Width at Haft Maximum (FWHM) data vary from about 19 to 26 cm^{-1} in "schist-type" emeralds, from 11 to 14 cm^{-1} in synthetic and from 12 to 15 cm^{-1} in "non-schist-type" emeralds, respectively. Peaks of water motion show also different characters among emeralds of various deposits. Raman spectroscopy therefore can be used as a strong destruction free spectroscopic method in discriminating emerald origins. In addition, behaviour of water molecules under different temperatures are studied and two types of water can be assigned by means of Raman spectroscopy.

The Raman spectra presented were done in the confocal mode by means of a Jobin Yvon (Horiba group) LabRam HR 800 spectrometer. The system was equipped with an Olympus BX41 optical microscope and a Si-based CCD (charge-coupled device) detector. Spectra were excited by the Ar^+ ion laser emission with 514 nm as a green laser with a grating of 1800 grooves/mm. Due to these parameters and the optical path length of the spectrometer a resolution of 0.8 cm^{-1} is achieved. The spectra acquisition time was set 240 seconds for all measurements. Two ranges are separately measured: one from 200 cm^{-1} to 1600 cm^{-1} – the range of structural vibrations, and the spectra of this range were recorded under room temperature; the other from 3500 cm^{-1} to 3700 cm^{-1} to obtain the Raman-bands of the water and hydroxyl-groups and these spectra were measured under different temperatures, from 78 K to 300 K in steps of 25 K.

Peak analysis was performed with an Origin-lab 7.5 professional software package. The single or overlapping peaks were fitted using Gauss-Lorentz function.

5.1. Raman spectra in the range from 200 cm^{-1} to 1600 cm^{-1}

The vibrational spectra of beryl have been studied by various authors. Narayanan (1950) provided a low-frequency spectrum of beryl with little detail. Griffith (1969) presented powder Raman spectra in which some main bands of the silicate ring stretches were indicated. Adams and Gardner (1974) identified all of the lines predicted by factor group analysis in single crystal spectra. Hofmeister et al. (1987) studied vibrational spectra of several beryllium aluminosilicates including beryl. The later authors mention that despite the data presented in the literature and general agreement among references, it remains controversial to assign modes to bands, especially for high frequencies where both Si-O vibrations and mixed Si-O, Be-O modes can exist. Hagemann et al. (1990) reported the effect of impurities on the Raman spectrum of beryl and some spectral differences between his samples were presented. Kim et al. (1995) calculated normal modes for beryl and correlated the vibrational properties of the crystal structure with those of the isolated Si_6O_{18} ring. Charoy et al. (1996) produced some spectroscopic characterizations including channel occupancy characteristics in beryl.

Nevertheless, using Raman spectroscopy efficiently to distinguish natural emeralds from synthetic ones and to determine localities of natural emeralds has just been recently established by Moroz et al. (2000). Their way to separate localities of emeralds is to compare spectra among specimen of various deposits and figure out peculiar bands that occur in each locality. Our method for this purpose was to define the FWHM and the position of certain bands in Raman spectra (bands around 1067-1072 cm^{-1}), since it is found that in synthetic "emeralds" (both hydrothermal and flux) the band position is at lower frequency (at 1067-1068 cm^{-1}) and FWHM (about 11 to 14 cm^{-1}) is smaller in comparison with those of natural stones (in "schist-type" stones, these values are 1069-1072 cm^{-1} and 19-26 cm^{-1}, respectively; in "non-schist type" stones, these values are 1068-1070 cm^{-1} and 12-15 cm^{-1}, respectively, with an exception in the case of emeralds from Malipo and this will be discussed more later). In addition, peculiar band criteria were also used as additional method to distinguish

between emeralds from different localities and manufactures although the reason for these peculiar bands has not been understood yet. Another contribution of this study is assigning the band around 1067-1072 cm^{-1} to Si-O which has been previously reported and controversially discussed.

5.1.1 Comparisons of Raman spectra up to 1600 cm^{-1}.

Geometrical factors were strongly controlled in all Raman measurements. An optical polarizer was used allowing only the laser beam with definitive vibrational direction (N-W) pass through (the precision of polarizer is about 99,8%). Experiments were then conducted with different orientations of the beryl crystals (i.e orientations of c axis) with regard to E, the electric vector. Whatever the crystallographic orientation is parallel or normal to the c axis, some Raman bands are always seen, although their relative intensity may be changed. They are those around 321-325 cm^{-1}, 395-398 cm^{-1}, 441-446 cm^{-1}, 683-688 cm^{-1}, 1003-1008 cm^{-1} and 1067-1072 cm^{-1} (figure 66 and 67). These bands are the so-called main Raman bands of emerald, in which bands around 321-325 cm^{-1}, 395-398 cm^{-1} and 683-688 cm^{-1} have been assigned to ring vibrations by all investigators (Moroz et al., 2000, Adams and Gardner, 1974, Griffith, 1969, Charoy et al., 1996, Kim et al., 1995), bands around 1003-1008 cm^{-1} to Si-O (Adams and Gardner, 1974), while 1067-1072 cm^{-1} is a controversially assigned band and will be discussed more below, and the band around 441-446 cm^{-1} is still indefinite.

Other bands which are seen in all samples, when the crystal is oriented normal to the laser beam (E⊥c), and not seen when the crystal is oriented parallel to the laser beam (E//c), are those around 416-422 cm^{-1}, 769-772 cm^{-1}, and 1236-1244 cm^{-1}. There is no controversial situation, i.e. there is no band which is seen when the crystal is oriented parallel to the laser beam but not seen when the crystal is oriented normal to the laser beam. To find out the peculiar bands, the spectra obtained from normal orientation of all samples are compared. The band at 237 cm^{-1} is present only in samples from Russia, the band around 247-250 cm^{-1} is shown in some beryls and syntheses, including Nigeria, Brazil (Socoto), Zambia and two producers, that are Tairus and Chatham. Almost all of the natural samples, except those from Russia, Nigeria and Brazil (Carnaiba) show bands around 269-271 cm^{-1}, but all synthetic ones absolutely do not.
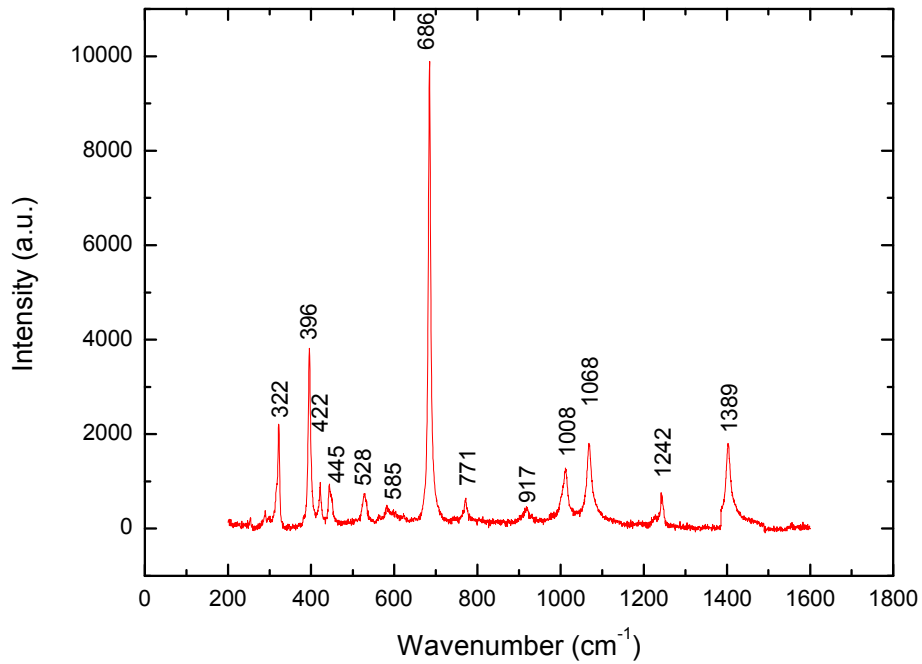
Figure 66: A Raman spectrum of Nigerian emerald (E⊥c) in the range 200-1600 cm^{-1}, sample Gw650.
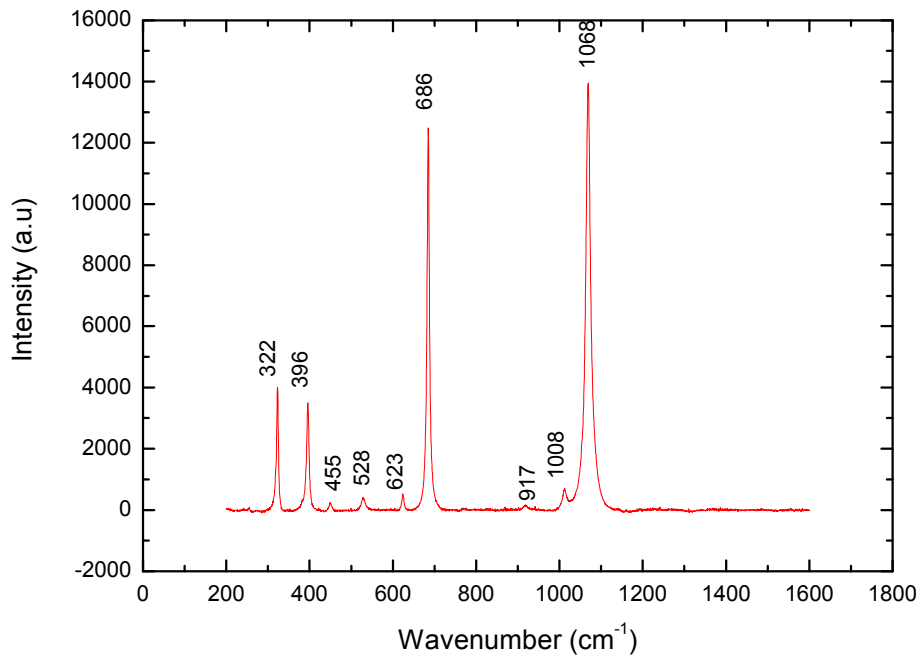
Figure 67: A Raman spectrum of Nigerian emerald (E//c) in the range 200-1600 cm^{-1}, sample Gw650.

70

Origin	Ring rotation (AD)			Ring (H,AG)		Ring				
China (Ma)		269	291	324		398	416	442		575
Nigeria (Gw)	250		289	321		396	422	445	528	583
Colombia (Ch)		270	290	322		396	420	443	528	578
Brazil (Ita)		269	290	322		397	416	442	525	573
Brazil (Cap)			291	325		400	419	441	527	580
Brazil (Cnb)			292	323		399	418	442	525	576
Brazil (So)	247	269		323		398	416	442	525	575
Brazil (ST)		270	291	325		400	416	441		583
Austria (Hbt)		268	291	324		398	418	442		
Russia (Ur)			293	323		400	419	443		577
South Africa (Tr)		271	293	324		397	419	444		577
Zambia (Kf)	247	269	291	325		400	416	441	525	582
Madagascar (Man)		269	292	325		400	416	441		
Tairus	250			322	382	395	422	446	527	598
Biron				320		395	417	441	525	592
Lennix				322		396	421	444	530	
Gilson			289	320		395	421	443	528	563
Chatham	243		299	320		395	420	444	528	581

Table 4: Raman bands of emeralds from different deposits and manufactures in the range between 200-600 cm[1]. The measurements were conducted with normal orientation of the laser beam to the c axis (E⊥c).

Origin	Ring	Ring	Al-O			SiO BeO	Shoulder	CO_2	CO_2
China (Ma)		685	765	906	1003	1070	1129	1236	
Nigeria (Gw)		685	771	918	108	1069		1242	1389
Colombia (Ch)	622	686	769	912	1005	1069		1239	1385
Brazil (Ita)		686	765	913	1003	1070	1127	1237	1385
Brazil (Cap)		684	770	917	1004	1072		1242	
Brazil (Cnb)	619	687			1003	1071		1238	
Brazil (So)		688	767	916	1007	1071	1124	1234	
Brazil (ST)		687			1003	1071	1106	1234	1386
Austria (Hbt)		687			1003	1072		1238	
Russia (Ur)	621	687	767	910	1003	1071		1238	
South Africa (Tr)	620	687			1003	1072	1132	1236	1387
Zambia (Kf)		687		915	1008	1072	1129	1238	
Madagascar (Man)		688			1003	1071	1091	1236	1386
Tairus	626	684	772	918	1008	1068		1240	
Biron	620	682	767	916	1003	1068		1239	
Lennix	618	685	772		1004	1067		1244	
Gilson	605	684	770	913	1003	1068		1243	
Chatham		684	769	917	1010	1067		1243	

Table 5: Raman bands of emeralds from different deposits and manufactures in the range between 600-1600 cm^{-1}. The measurements were conducted with normal orientation of the laser beam to the c axis (E⊥c).

Other bands at 289-291 cm^{-1} were found in almost all samples, except for those from Brazil (Socoto), and those from some synthetic producers including Lennix, Biron, and Tairus. None of the investigated samples, except Tairus syntheses, have bands around 382 cm^{-1}. All synthetic "emeralds" and natural emeralds from Colombia, Nigeria, Zambia, Brazil (except Santa Terezinha stones) exhibit additional bands around 525-528 cm^{-1}. Bands at 563-598 cm^{-1} appear in all samples, except for the Lennix syntheses and samples from Austria and Madagascar. One can see the band around 600-622 cm^{-1} (ring-bound) in the samples from Colombia, Brazil (Carnaiba), Russia, South Africa, and in Tairus, Biron, Lennix, Gilson syntheses but not in samples from China, Nigeria, Brazil (Itabira, Socoto, Capoeirana, Santa Terezinha), Zambia, Madagascar and synthetic Chatham. There is an additional band at 906-918 cm^{-1} in samples from China, Nigeria, Colombia, Brazil (Itabira, Socoto, Capoeirana), Russia, Madagascar, and in samples of Tairus, Biron, Gilson, Chatham. The shoulder at 1091-1132 cm^{-1} can be seen in samples from China, Brazil (Itabira, Socoto, Santa Terezinha), South Africa, Zambia and Madagascar.
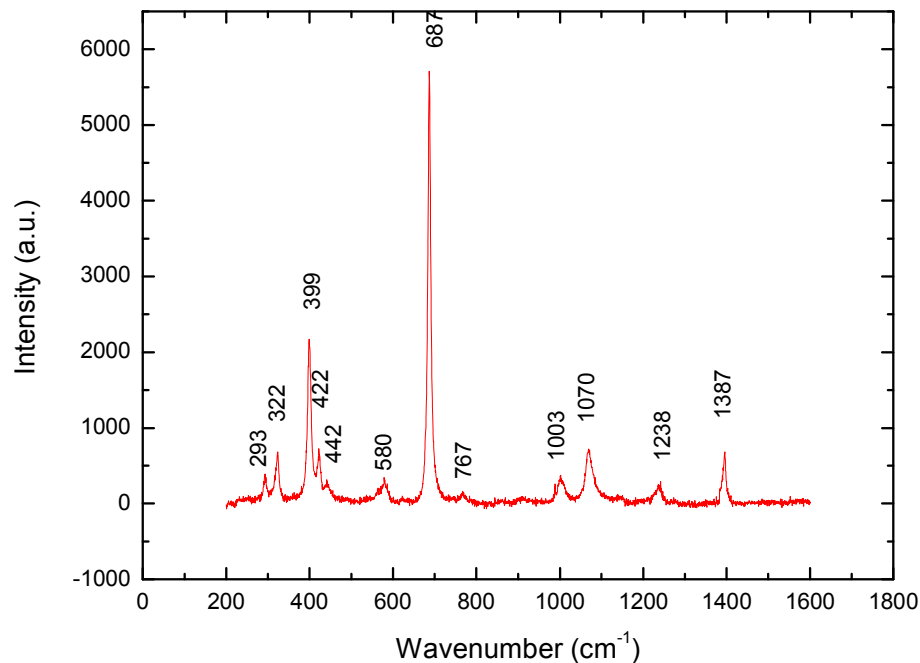
Figure 68: Raman spectrum of Maxixe-type emerald (E⊥c) shows to contain the two bands of CO_2 at about 1238 cm^{-1} and 1387 cm^{-1}.

Other bands can be seen in higher ranges, that are around 1224-1243 cm^{-1} and 1385-1387 cm^{-1} in which the former one is seen in all natural and synthetic samples. The later one is not seen in samples from China, Brazil (Carnaiba, Socoto), Austria, Russia, Zambia and in all synthetic samples. These bands are seen only when E is normal to the c axis, and they absolutely disappear when E is parallel to the c axis. According to Charoy et al. (1996) these bands are generated by the vibration of CO_2 molecules existing in the channels of the crystal structure. To elucidate the idea of Charoy et al. (1996), we made a Raman measurement of maxixe-type emerald (figure 68), which has been known to contain CO_2 in the structurally provided channels. The result was that the spectrum of maxixe-type emerald also shows these bands. The disappearance of these bands when E is parallel to the c axis supports the fact that the CO_2 molecule is oriented normally to the c-axis. However, the reason for the disappearance of the band at 1385-1387 cm^{-1} in some origins is not explained by this.

5.1.2 Bands around 1067-1072 cm^{-1}

A particular interest in the range between 200-1600 cm^{-1} hits the band around 1067-1072 cm^{-1} which is assigned by Kim et al. (1974), Moroz et al. (2000) as a band of the Be-O bond, and by Adams and Gardner (1974), Charoy et al. (1996) as a band related to the Si-O bond, in contrast. In "schist-type" emeralds this band shifts around 1069-1072 cm^{-1} while in "non-schist-type" emeralds (Nigeria, Colombia) and in synthetic ones this bands shifts around 1068-1070 cm^{-1} and 1067-1068 cm^{-1}, respectively.

In other words, in natural samples this band shifts to higher frequency than it does in synthetic ones, and it tends to shift to the highest frequency in "schist-type" samples. Moreover, the width of this band also changes among stones of different provenances. The FWHMs of synthetic emerald samples range from 11 cm^{-1} to 14 cm^{-1}. All "schist-type" emerald samples show the FWHMs from 19 cm^{-1} to 26 cm^{-1}. Emerald samples from Nigeria and Colombia ("non-schist-types") show significantly lower values from 12 cm^{-1} to 15 cm^{-1}. A special case delivers emeralds from China; they may be characterized petrographically as being of "non-schist type" but the peak position and FWHMs are similar to those of "schist-type" stones, 1070 cm^{-1} and 17-21 cm^{-1}, respectively.
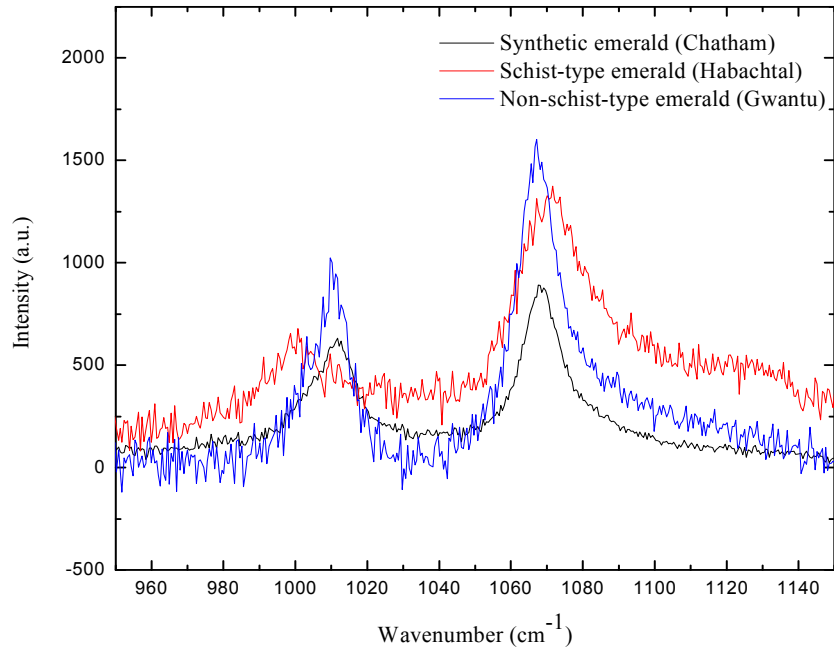
Figure 69: Diagram showing the Raman shift differences around 1068 cm^{-1} between synthetic "emeralds" (black line) and natural emeralds ("schist type": red line; "non-schist type": blue line).
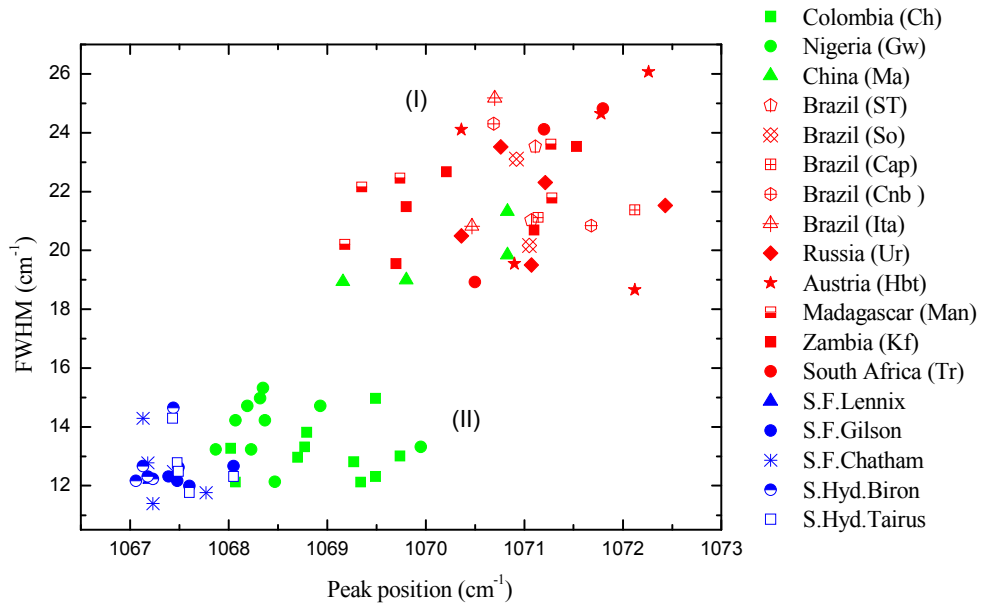
Figure 70: Diagram showing the plot of peak position versus FWHM value for emeralds from various deposits and for synthetic "emeralds" of different methods.

Based on FWHM values and Raman positions of this band, we can separate the samples studied into two ranges: range I including "schist-type" emeralds and Chinese emeralds are those of high FWHMs and high peak position; range II including synthetic and "non-schist-type" emeralds are those of low FWHMs and low peak position.

The peak position and value of FWHM shows to be correlated with the silicon contents, that is, in the samples where the content of silicon is high the peak position and FWHM are low and in the samples where the content of silicon is low the peak position and FWHM are high (figure 71).
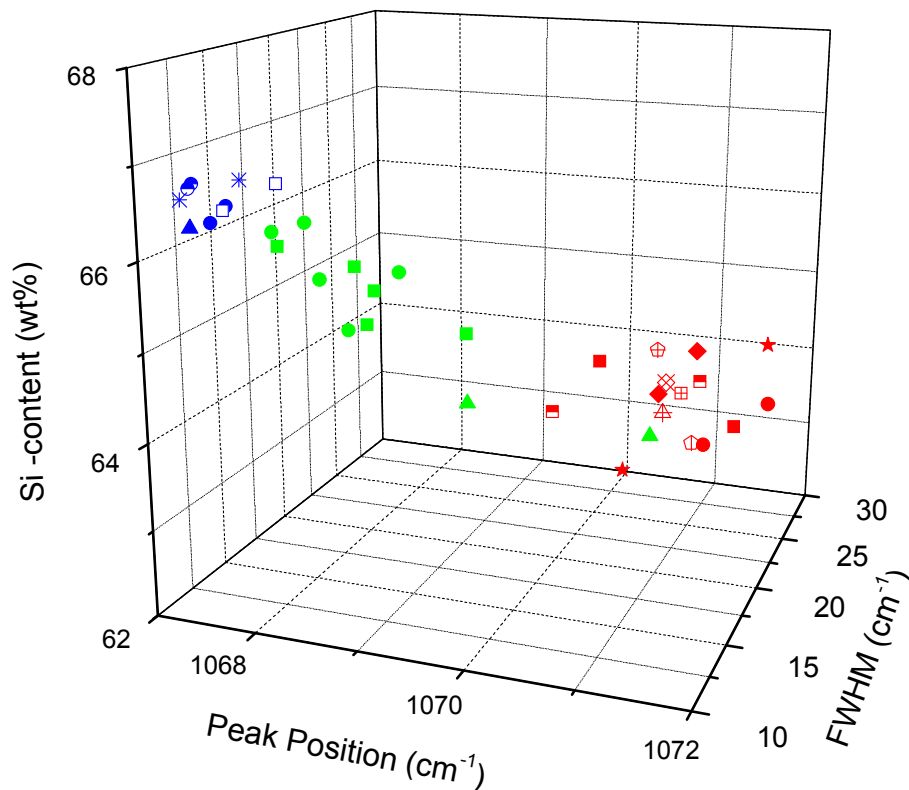
Figure 71: 3D-Diagram showing the correlation between the content of silicon, peak position and FWHM value of the Raman-peak.

The silicon content of emeralds of range I varies from 62,72 (wt %) to 64,41 (wt %), and silicon content of range II varies from 64,99 (wt %) to 66,83 (wt %). The FWHM values and position of this band show a clear relation with the silicon content, but not with the beryllium content (figure 72). Therefore; it is assumed, that this band arises from Si-O bond but not from Be-O bond interaction.

75

The shifting and broadening (increasing in FWHM) of the Raman band are primarily the results of positional disorder. Since the band shifting and broadening are seen in low silicon containing samples, there are actually other elements than silicon occupying the silicon sites in the crystal structure. The amount of positional disorder in each sample is the amount of lost silicon (in comparison with the ideal silicon amount). Other elements which may substitute Si^{4+} are Al^{3+} and, under special conditions, Be^{2+}, while Li^+ is a very doubtful replacement partner. Charge compensators may be served by alkali ions (mainly Na^+, K^+, Cs^+) which find their structural place in the channels of the structure. That means, the lost of silicon in the emerald structure could be compensated by other substituting elements (Al^{3+}, Be^{2+}, Li^+, ect.) together with charge compensating ions (Na^+, K^+, Cs^+).
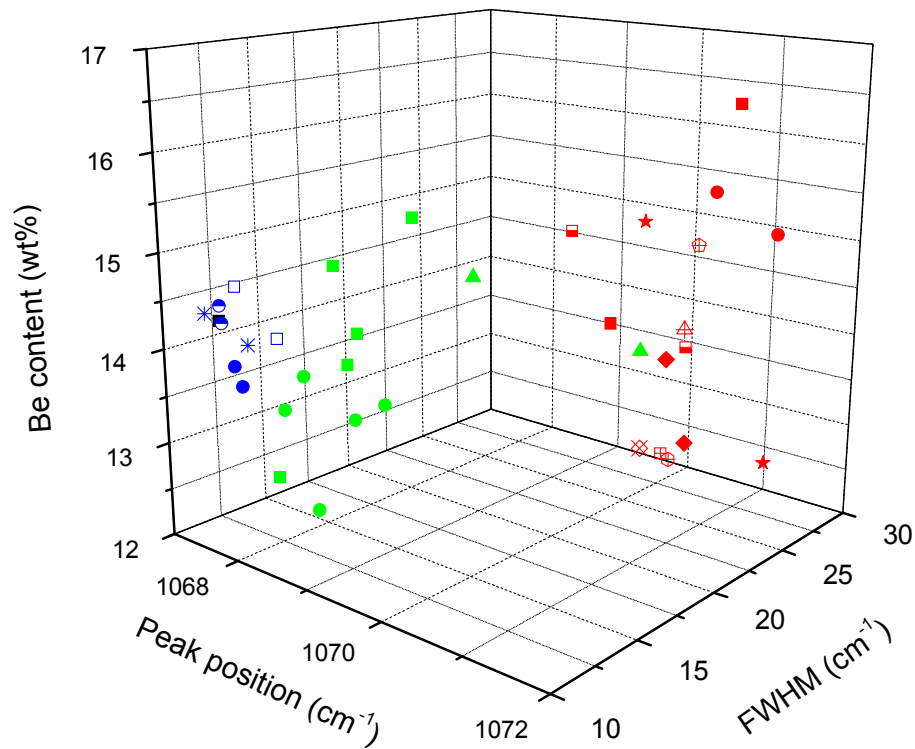
Figure 72: Diagram showing no correlation between the content of beryllium with the FWHM values and the Raman-peak positions.
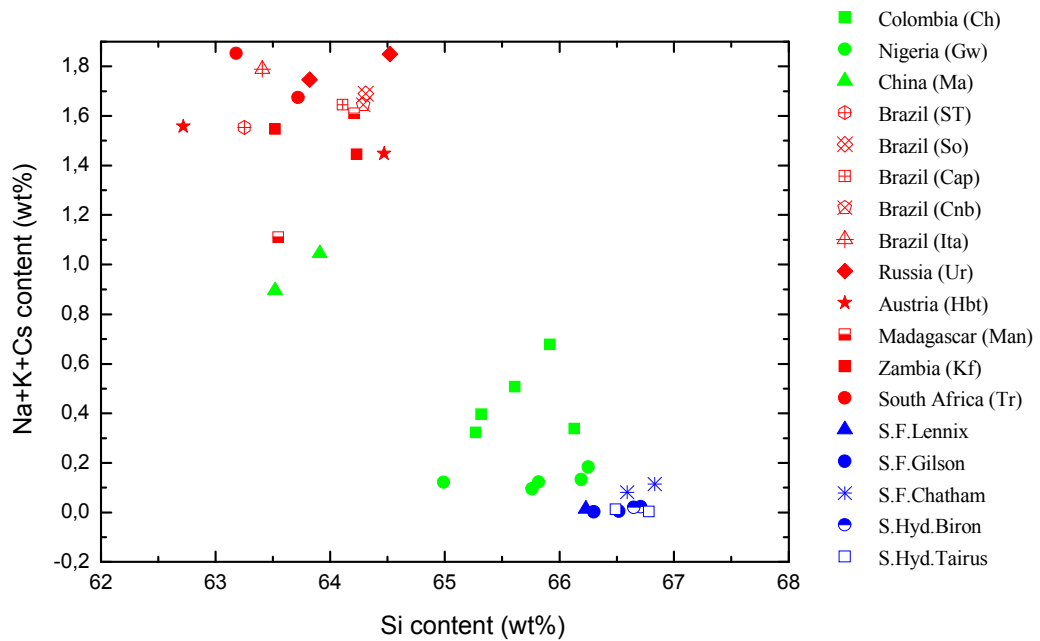
Figure 73: Diagram showing the alkali contents (Na, K, Cs) versus the Si contents for emeralds from various deposits and for synthetic "emeralds" of different methods.

The correlation between Si- and alkali ion contents elucidated this fact, since in samples where the Si content is low, the alkali content is high (figure 73). Nevertheless, as discussed above, Al^{3+}, Be^{2+}, Li^+ do not play the only role as the substituting elements for silicon, therefore, these do not show diagrammatically a significant correlation with silicon.

5.2 Raman spectra of emeralds at high Raman shift: 3500-3700 cm^{-1}.

5.2.1. Measurements under room temperature.

Under room temperature all samples of this investigation were measured to obtain the spectra in the range of OH⁻ and water molecule vibration (from 3500 cm^{-1} to 3700 cm^{-1}). All measurements were conducted with E normally to the c axis. Two bands may be seen in this range (although not always equally among all samples): one at about 3608 cm^{-1} and the other at 3598 cm^{-1} (figure 74).
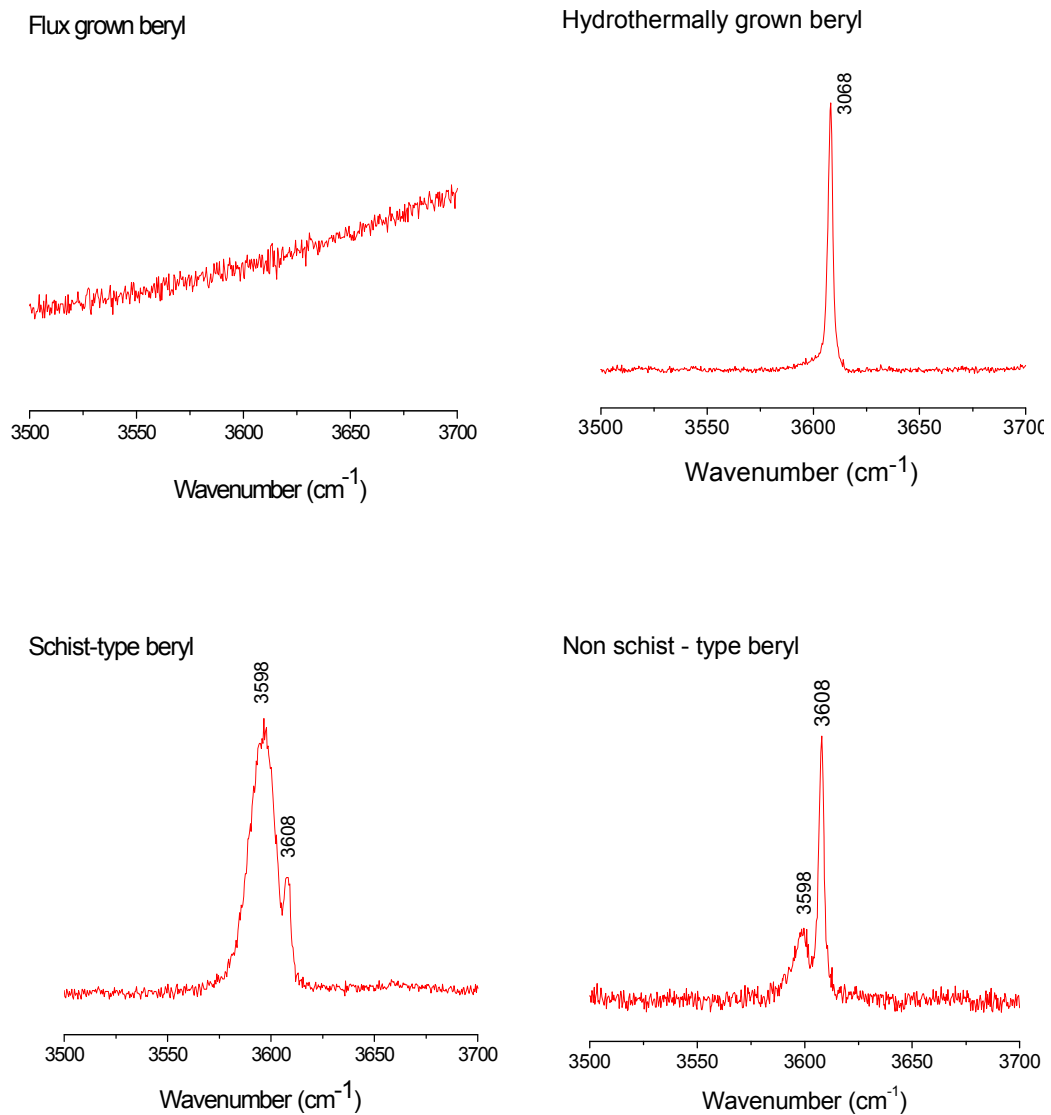
Figure 74: Raman spectra of emeralds in the "water range" (E ⊥ c axis)

All natural stones show both bands; however, the intensity ratios of the two bands are very different between "schist-type" stones and "non-schist-type" ones. In more detail, the intensity of band 3608 cm^{-1} is seen to be higher than that of the band at 3598 cm^{-1} in all "non-schist-type" samples (including Chinese emeralds), while it is lower among "schist-type" samples.

All flux synthetic "emeralds" do not show any Raman bands in this range other than the signal of luminescence. This elucidates the fact, that there is no water in flux grown "emeralds". Hydrothermally grown synthetic "emeralds" show one band at 3608 cm^{-1}.

By considering the chemical data, it is obvious that the appearance of the band at 3598 cm^{-1} and also the intensity ratio of the two bands (3598 cm^{-1} and 3608 cm^{-1}) depend on the amount of alkali ion. Band 3598 cm^{-1} is detectable only in alkali containing samples, in alkali-free samples (hydrothermal syntheses) this band absolutely disappears while band 3608 cm^{-1} truly exists. This band increases in intensity as the alkali content of emerald increases, and the more alkali ions are present in sample, the higher is the ratio I_{3598}/I_{3608}.

In those samples with the amount of alkali ions higher than 1,1 wt% (all "schist-type" emeralds), the intensity of band 3598 cm^{-1} is higher than that of band 3608 cm^{-1} ($I_{3598}/I_{3608} > 1$), and conversely; in those samples with the amount of alkali ions lower than 1,1 wt% (all "non-schist-type" and synthetic "emeralds") the intensity of band 3608 cm^{-1} is higher than that of the band at 3598 cm^{-1} ($I_{3598}/I_{3608} < 1$) (figure 75).

According to this observation and to the classification of Wood & Nassau (1967, 1968), it can be stated here, that the Raman band at 3608 cm^{-1} is generated by water type-I (those water molecules without any presence of alkali ions nearby) and the Raman band at 3598 cm^{-1} is generated by water type-II (water molecules with alkali ions nearby).
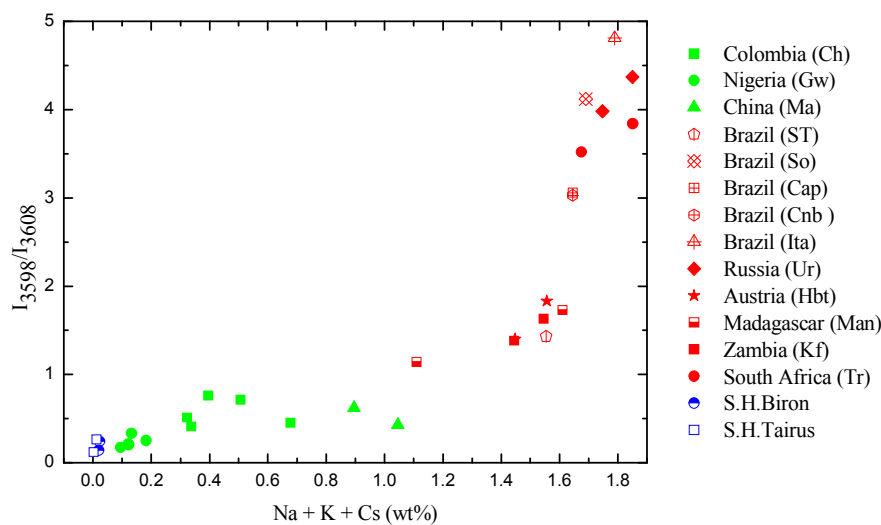
Figure 75: Diagram showing the ratio of two water bands versus the amount of alkalis in emeralds.

In both, "schist-type" and "non-schist-type" stones, the band at 3598 cm^{-1} (water type II) shows to be much broader than the band at 3608 cm^{-1} (water type I). The FWHM values of band 3598 cm^{-1} range from 11,2 cm^{-1} to 14,8 cm^{-1} while those of band 3608 cm^{-1} (water type I) range from 1,6 cm^{-1} to 2,8 cm^{-1}. The reason that the Raman band of water type II is broader than band of water type I may be due to the vibrational characteristics of each water type itself. This means, since there is the appearance of alkali ions nearby (in cases of water type II), the orientation of water molecules is changed; the vibration energy and/or state of vibration of water molecules are therefore actually changed. This explains why water type-II molecules generate Raman band at different positions and different FWHMs than water type-I molecules do. Nevertheless, it may be also the case that, the broadening of band 3598 cm^{-1} is caused by the combination of more than one band, since its width is not normal for a single typical Raman band. According to the study of Schmetzer & Kiefert (1990) on water by means of Infrared spectroscopy, water type II can be subdivided into type II a (H_2O-Na-OH_2) and type IIb (H_2O-Na-). Therefore, it is supposed here, that the band at 3598 cm^{-1} is not a single band but in fact a combination of at least two bands, one due to type-IIa water and other due to type-IIb.

5.2.2 Measurements under low temperatures.

To investigate the behaviour of this broad band, Raman measurements were carried out under different temperature levels. One sample of "schist-type" beryl was chosen for low temperature experiment; the position of the sample was kept constant (in the way that the crystallographic c axis is normal to the vibration of the laser beam) during measurement. Figure 76 shows 10 spectra measured from 300 K down to 78 K, i.e. 27 $^{\circ}$C to -195°C.
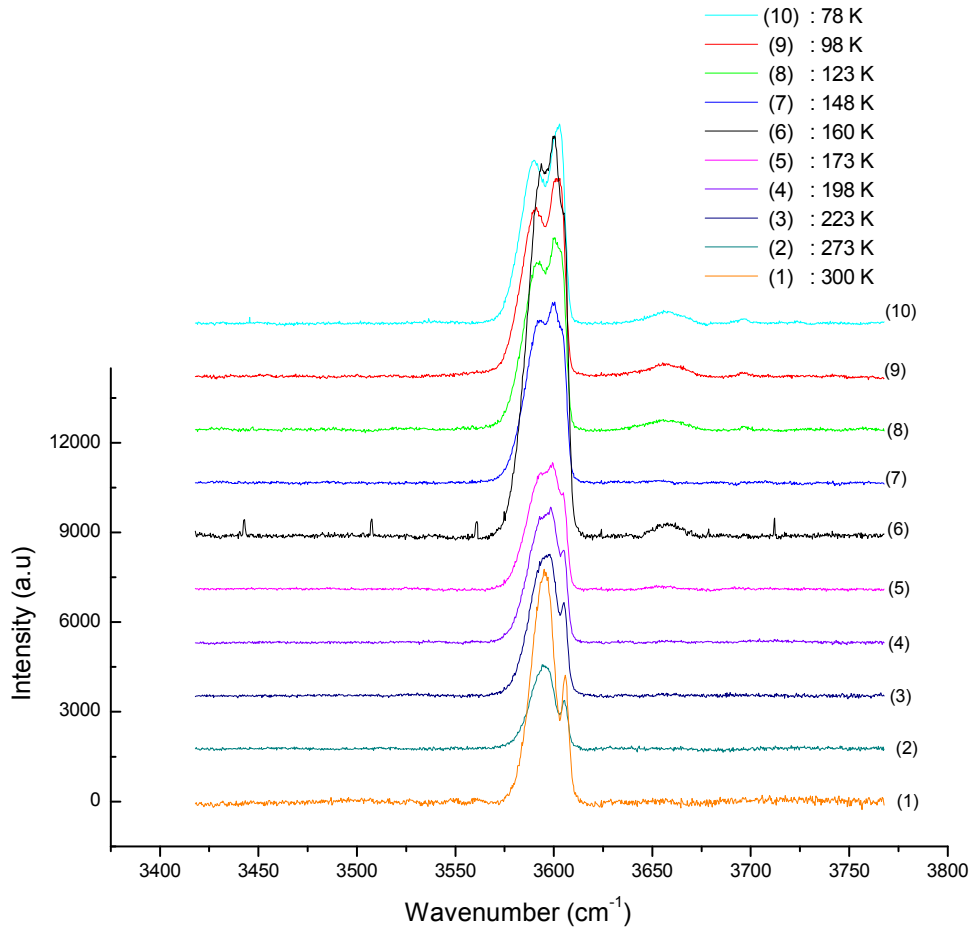
Figure 76: Raman spectra of a "schist-type" emerald under different temperatures: (1): 300 K; (2): 273 K; (3): 223 K; (4): 198 K; (5): 173 K; (6): 160 K; (7): 148 K; (8): 123 K; (9): 98 K; (10): 78 K.

From 300 K to 223 K the spectra show to maintain 2 peaks (figure 77), although the FWHM values and the positions of the two peaks change under different temperatures. In addition, the lower the temperature is, the closer the two peaks come together (from 11,6 cm^{-1} when measured under room temperature to 10,3 cm^{-1} when measured at 223 K). The FWHM of band 3596 cm^{-1} is increased while that of band 3608 cm^{-1} decreased. The changes of position and FWHM of peaks are shown in table 6.
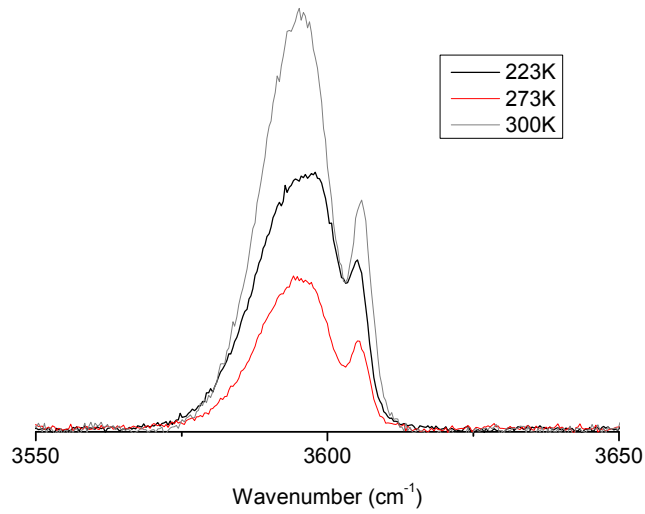
Figure 77: Raman spectra of beryl in the range of water molecules resonance show two peaks from room temperature (300 K) down to 223 K.

	Peak positions (cm^{-1})	Distance between peaks (cm^{-1})	FWHM (cm^{-1})
300 K	3596,6 / 3608,2	11,6	14,3 / 3,3
273 K	3596,5 / 3607,8	11,3	15,1 / 2,9
223 K	3597,1 / 3607,4	10,3	16,3 / 2,5

Table 6: Changes of peak data under different measuring temperatures

From 198 K to 123 K, the spectra clearly contain 3 peaks (figure 78); only lower than 198 K the splitting of the band of water type II are present.

	Peak position (cm^{-1})	Distances between peaks (cm^{-1})	FWHM (cm^{-1})
198 K	3594,6/3602,1/3607,5	7,5/5,4	15,5/8,0/3,3
173 K	3593,5/3601,6/3605,9	8,1/4,3	17,1/6,7/3,5
148 K	3594,4/3602,8/3607,0	8,4/4,2	16,9/7,0/3,9
123 K	3594,1/3603,1/3606,9	9,0/3,8	17,6/6,0/3,8

Table 7: Changes of peaks under different measuring temperatures.
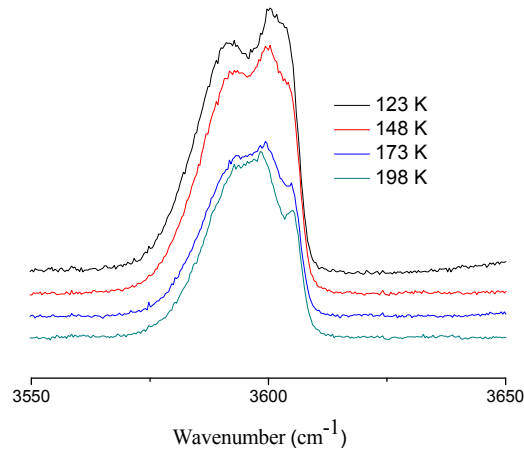
Figure 78: Three peaks of water molecules are detectable under lower temperatures between 198 K and 123 K
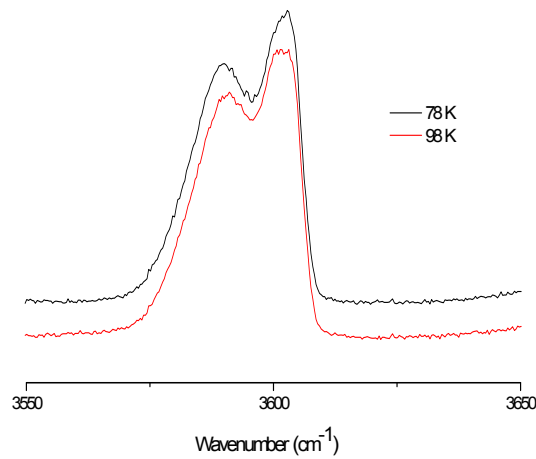
Figure 79: From 98 K to 78 K again 2 Raman peaks of water molecules are present, but the intensity ratios of the two peaks have changed

Below 98 K, again only two peaks are detectable, one at 3593 cm^{-1} with lower intensity and another at 3604 cm^{-1} with higher intensity. The changes are shown in the following table.

	Peak position (cm^{-1})	Distances between peaks (cm^{-1})	FWHM (cm^{-1})
98 K	3593,0/ 3604,4	11,4	17,9 / 6,9
78 K	3592,9/ 3604,6	11,7	17,9 / 6,8

Table 8: Changes of peak-parameters between 98 K and 78 K.

83
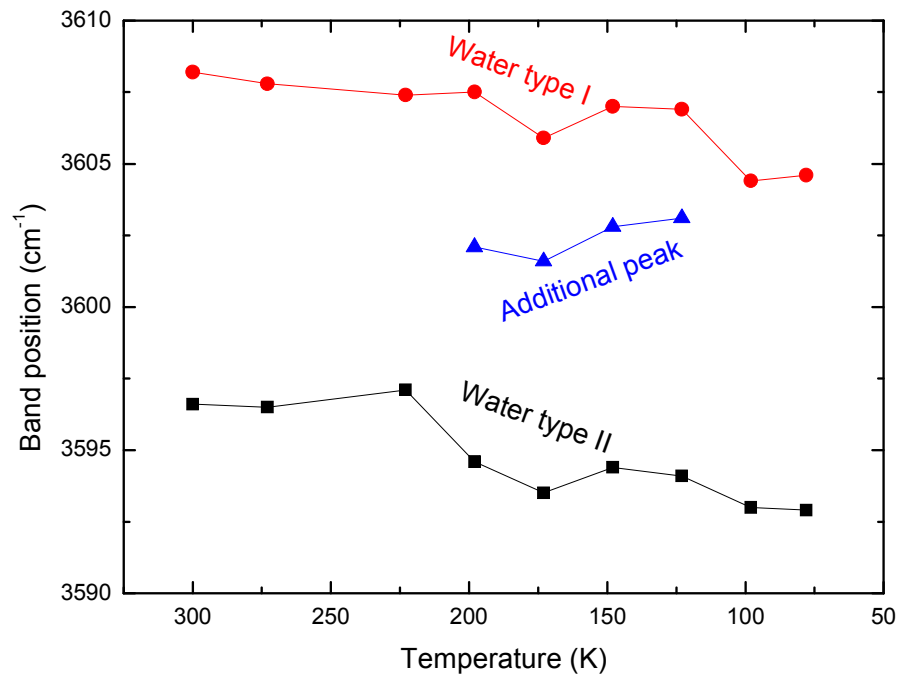
Figure 80: Diagram showing the plot of peak positions derivable from water bonds versus temperature.
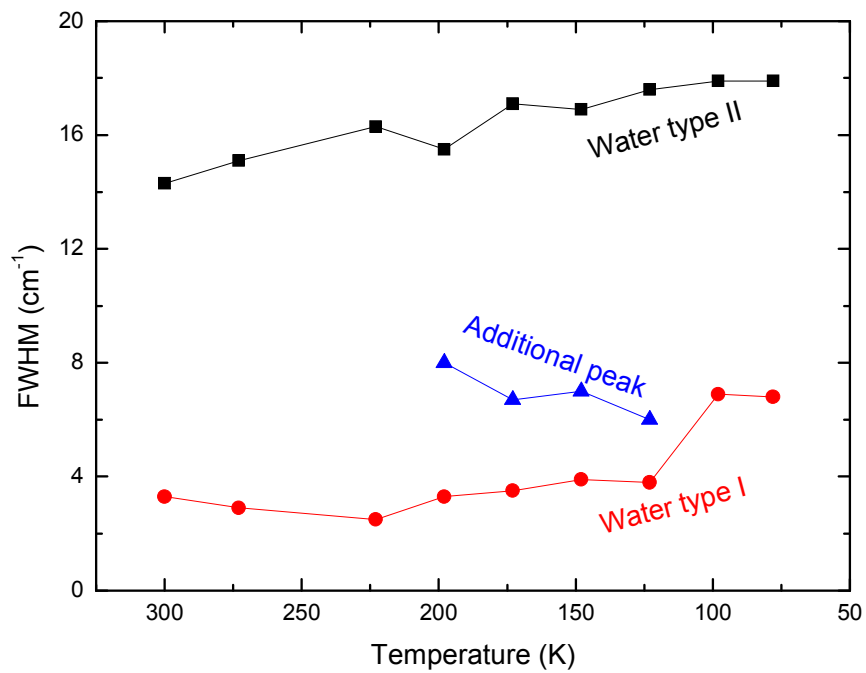
Figure 81: Diagram showing the plot of FWHM of the peak of water bonds versus temperature.

84

Figures 80 and 81 illustrate the diagrams showing the appearance of the additional peak between 123 K and 198 K and the changes of band positions and FWHMs of two types of water bands according to the change of temperature. There are some proposals for the appearance of the additional peak as followings. However, it has to be underlined, that the presented proposals need further experimental confirmation. We need a strictly accurate polarizer filter. 1. Following the study of Schmetzer & Kiefert (1990) in which 3 types of water have been assigned, type I, type IIa and type IIb by means of IR spectroscopy, the additional peak seen in Raman spectroscopy therefore could be assigned for the third type of water. And, the peak which is detected at room temperature at 3598 cm^{-1} is the overlap of two water types IIa and IIb. 2. At low temperatures, the silicate structure of emerald is slightly constricted. Accordingly, deformation or reorientation of water type II molecules may took place (remember that water type II molecules oriented in such a way that their two-fold symmetry axis is parallel to the crystallographic six-fold axis of the emerald structure). This means, the parallel position changes slightly to the diagonal position. This new position with new vibrational energy generates a new energy which is recordable as an additional peak in the spectrum.

6. INFRARED SPECTROSCOPY OF EMERALDS

Beside Raman spectroscopy, Infrared spectroscopy is also a strong method in investigating vibrations of dipole bondings in material and has been applied for research on beryl, especially on water in beryl, since around 40 years ago. (Flanigen, 1967, Wood and Nassau, 1967 and 1968). In this study this method is used to investigate the features of water in channel sites of beryl as well as features of bands around 1200 cm^{-1} and a significant shoulder at 1140 cm^{-1} which may help to resolve the problems concerning the separation of the provenance of the samples as well as the separation between synthetic stones from natural ones. In general, the separation is based on the presence or absence of bands of different types of water molecules in the spectra (Schmetzer and Kiefert, 1990). Further contributions of this chapter are the assignment of the band at 1200 cm^{-1} to Si-O vibrations.

Prior to now, using Infrared (IR) spectroscopy to distinguish natural emeralds from synthetic counterparts has been applied mainly due to the characteristics of water absorption bands which were investigated by many authors using powdery emerald material mixed with KBr (KBr pellet technique) or thin plates.

In flux synthetic "emeralds" no water absorption band can be observed. This elucidates the lack of water in the crystal growth process itself. In hydrothermal synthetic "emeralds", only bands of type-I water (water molecules which are not associated to alkali ions) are seen, elucidating that the growing media is free of alkali ion. In natural emeralds, bands of both, type-I and type-II waters (water molecules which are bound to alkali ions) can be seen (Wood & Nassau, 1967, 1968; Flanigen, 1971). Vibrations of water molecules were investigated by these authors between 1500 cm^{-1} to 1700 cm^{-1} and between 3500 cm^{-1} to 3800 cm^{-1} in which vibrations in the former range were assigned to deformation modes of water molecules and vibrations in the later range were assigned to stretching modes of water molecules.

Later, in the studies of Schmetzer (1989) and Schmetzer & Kiefert (1990) it was found that the intensity ratios of bands in the range 3500 cm^{-1} to 3800 cm^{-1} change in samples of different localities. They contributed additional criteria not only to separate

synthetic "emeralds" from natural ones, but also to determine the origins of natural emeralds. The criteria were elucidated later by the study of Mashkovtsev & Lebedev (1993). Furthermore, comparing the intensity ratios of three water absorption bands in the range between 3500 cm^{-1} to 3800 cm^{-1} it was concluded that one or more additional types of water or hydroxyl group are present in beryl.

Features of carbon dioxide, registered usually at about 2200-2400 cm^{-1}, may be used as criteria to discriminate distinct synthetic "emeralds" and natural ones and were supposed by Leung et al. (1983), and Stockton (1987). By using a conventional double-beam infrared spectrophotometer to obtain transmission spectra of faceted samples, Leung et al. (1983) found that no synthetic "emerald" (hydrothermal and flux synthesis) shows any band at about 2356 cm^{-1} which he assigned to CO_2 in the channel. Stockton (1987) used a Fourier transform infrared instrumentation also for faceted samples and found that two bands of CO_2 at about 2358 cm^{-1} and 2340 cm^{-1} were seen in both synthetic and natural emeralds, however, in natural emeralds the band at 2358 cm^{-1} is always stronger than the band at 2340 cm^{-1}, while in synthetic "emeralds" this relationship is reversed. One other band of unknown vibration occurred in the same range with carbon dioxide (2293 cm^{-1}) and has been supposed by Stockton (1987), and Koivula et al. (1996) as a signal to determine synthetic "emeralds" from natural ones since this band could be found only in natural stones. Nevertheless, according to Duroc-Danner (2006), new hydrothermal synthetic products of Tairus show to have this band. Therefore this signal has no longer its discriminating character.

Many studies of Mashkovtsev and others, using chemical analysis and polarized infrared spectroscopy for thin plates, brought out features of bands of chlorine in the range between 2500 cm^{-1} to 3100 cm^{-1} (Mashkovtsev & Sohntsev, 2002; Mashkovtsev & Smirnov, 2004; Adamo et al., 2005) and ammonium in the range between 2500 cm^{1} and 3300 cm^{-1} (Mashkovtsev & Sohntsev, 2002; Mashkovtsev et al., 2004) and were propagated to be new criteria to separate some hydrothermal synthetic "emeralds".

Nevertheless, none of the mentioned authors used the characteristics of spectra in the vibration range of the silicate structure as criteria to separate natural emeralds from their synthetic counterparts. In our study, we investigated the features of water bands

and also bands in the range of the silicate structure to contribute to the separation of emerald origins. Besides, by correlating with chemical data we tried to assign 2 bands at 1200 cm^{-1} and 1140 cm^{-1} to certain vibration modes.

IR spectra of emeralds were recorded in the whole range, from 400 cm^{-1} to 4000 cm^{-1} using a PERKIN ELMER FT-IR Spectrometer 1725X with 100 scans and 4 cm^{-1} resolution. Band fittings were done by using the fitting program Origin 7.5 with Gauss-Lorentz function. The samples were prepared as pellets made out of 2 mg of powdered emerald mixed with 200 mg KBr powder to minimize polarization effects.

In the recorded region, there are four notable ranges showing different significant features for natural and synthetic emerald samples: 1) from 400 cm^{-1} to 1300 cm^{-1}; 2) from 1500 cm^{-1} to 1700 cm^{-1}; 3) from 2200 cm^{-1} to 2400 cm^{-1}; and 4) from 3500 cm^{-1} to 3800 cm^{-1}. One band in the range 3430 cm^{-1} to 3470 cm^{-1} is always seen and is the result of water absorbed in KBr powder which is hardly prevented.
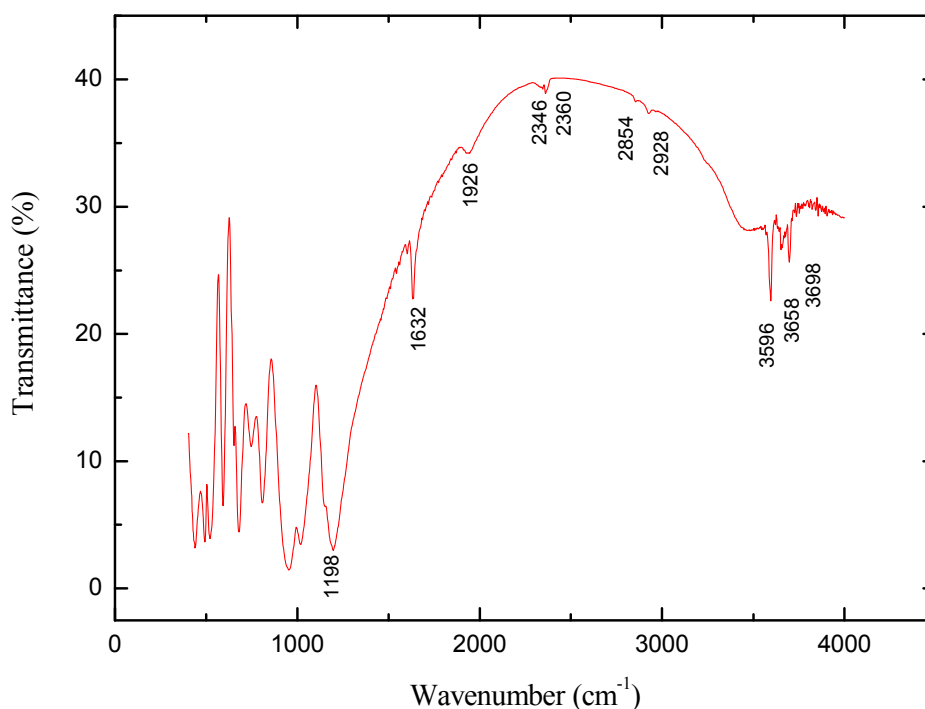
Figure 82: IR spectrum of a 200mg KBr-pellet with 2mg of a natural emerald from China (sample Ma04) in the mid-infrared range 400-4000 cm^{-1}.
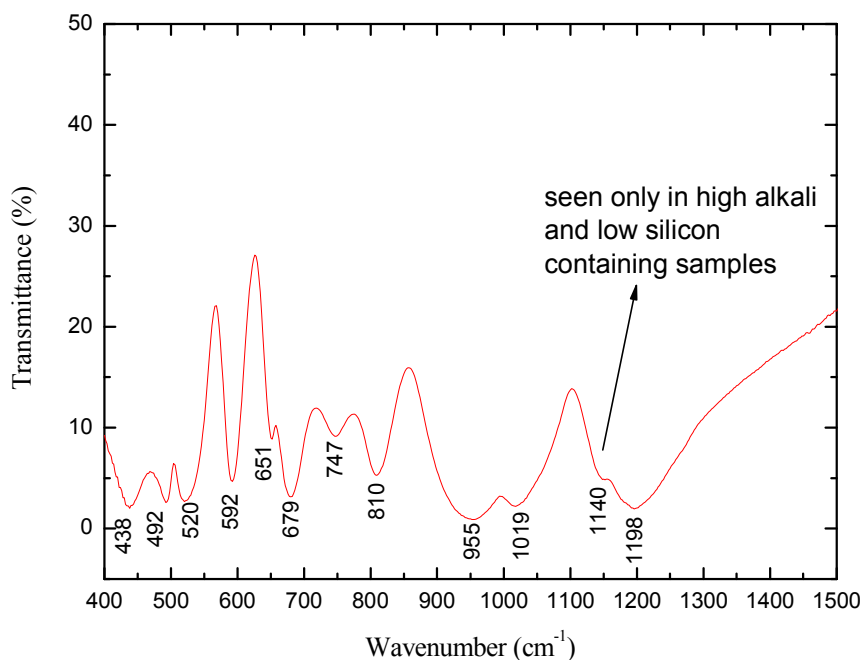
Figure 83: IR spectrum of one emerald from China (sample Ma04) in the range
400-1500 cm^{-1}

6.1. IR absorption spectroscopy in the range 400-1500 cm^{-1}

Various bands are observed in the range between 400-1500 cm^{-1}. Although bands in this range have been calculated and studied by many scientists, the assignments for the origin of these vibration modes are still controversial.

Figures 82 and 83 show the IR spectra of one special emerald (Chinese provenance). The bands in the range between 800-1300 cm^{-1} have been assigned to the internal Si-O vibrations by many authors (Gervais & Pirou, 1972; Adams & Gardner, 1974; Hofmeister et al., 1987; Aurisicchio et al., 1994), but according to Plyusnina (1964), Plyusnina & Surzhanskaya (1967) this range was due to vibrations of the BeO$_4$ tetrahedral coordination polyhedron. This range shows two dominating bands at about 1200 cm^{-1} and 955 cm^{-1}. Other complementary bands could be are around 1019 cm^{-1} and 1140 cm^{-1} which form shoulders of the main bands. Moreover, the band around 1140 cm^{-1} is well observed in high alkali and low silicon containing samples ("schist-type" emeralds and Chinese emeralds); in low alkali containing samples this band is not observable (all investigated synthetic samples and samples from Nigeria, Colombia). Bands reported by other authors (Manier-Glavinaz et al., 1989) at 1170 cm^{-1} and 1050 cm^{-1} do not appear in all of our investigated samples. One band at

about 1450 cm^{-1} was seen in a sample from Santa Terezinha, and has not been discussed and mentioned yet.

The bands appearing at about 810, 750, and 680 cm^{-1} were ascribed to the Be-O cluster by Hofmeister et al. (1987) or to Al-O coordination by Plyusnina & Surzhanskaya (1967). Beside all of these bands, one sample from Santa Terezinha shows other additional bands at 731 and 882 cm^{-1}.

In the range between 600 - 400 cm^{-1} the bands were said to correspond to LiO$_4$ vibrations as determined by Tarte (1965). Nevertheless, according to Gevais & Pirou (1972) two bands at 525 and 500 cm^{-1} belonged to vibrations of SiO$_4$ tetrahedrons, and following Plyusina & Surzhanskaya (1967), these bands correlated with Si-O-Al stretching.

	Aurisicchio et al., 1994	Manier-Glavinaz et al.,1989	Hofmeister et al., 1987	Adams & Gardner, 1974	Gervais & Pirou 1972	Plyusnina & Surzhanskaya, 1967; Plyusnina, 1964	Tarte, 1965
1200	Si-O	Si-O	Si-O	Si-O	Si-O	Be-O	
1147		Si-O	Si-O		Si-O		
1019		Si-O	Si-O		Si-O		
955	Si-O	Si-O	Si-O		Si-O	Si-O	
810	Be-O		Be-O	Si-O	Si-O	Be-O	
747			Be-O				
679			Be-O				
651							
592							Li-O
520	Al-O				Si-O	Si-O-Al	Li-O
492	Al-O				Si-O	Si-O-Al	Li-O
438							Li-O

Table 9: Assignments of vibrations to bands according to different studies.

Bands around 1200 cm^{-1}and 1140 cm^{-1}: This study focuses on the band around 1200 cm^{-1} which has assigned to Be-O vibrations by Plyusnina (1964), Plyusnina & Surzhanskaya (1967) and to Si-O vibrations by other authors. This investigation proves that this band around 1200 cm^{-1} in fact varies in its actual position from 1171-1207 cm^{-1}. In more detail, all synthetic samples show the band around 1200 cm^{-1} to about 1207 cm^{-1}, and natural emeralds show the band around 1171 cm^{-1} to 1203 cm^{-1}. In addition, all "schist-type" emeralds show a shoulder at about 1140cm^{-1}. This shoulder can be seen in Chivor (Colombian), Chinese emeralds but not in Nigerian emeralds ("non-schist-type" emeralds) and absolutely disappears in synthetic ones. Moreover, the band at 1200 cm^{-1} shows to be clearly more slender in synthetic "emeralds" than in natural ones. Relating to chemical data, it is found that in the samples with a high content of alkali ions and a low content of silicon (usually "schist-type" emeralds) the shoulder at 1140 cm^{-1} is clearly present and also the position of the band at 1200 cm^{-1} shifts backward to lower wavenumbers. In contrary, in the samples with a low content of alkali and a high content of silicon, the shoulder disappears and the position of the band at 1200 cm^{-1} shifts toward higher wavenumbers.
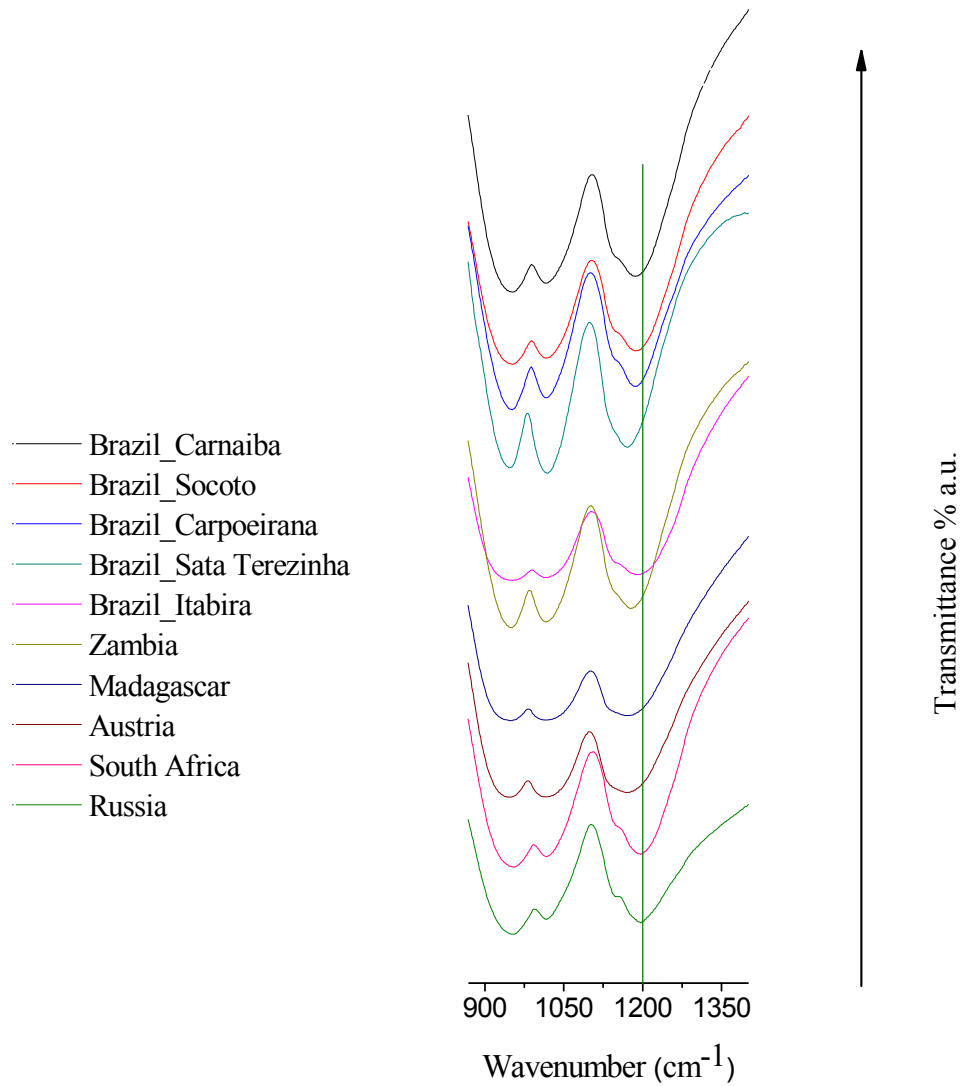
Figure 84: IR spectra of "schist-type" emerald powder in KBr pellets from various deposits in the range between 900-1350 cm^{-1} show to contain the shoulder at about 1140 cm^{-1} and the band at about 1200 cm^{-1} is very asymmetric.
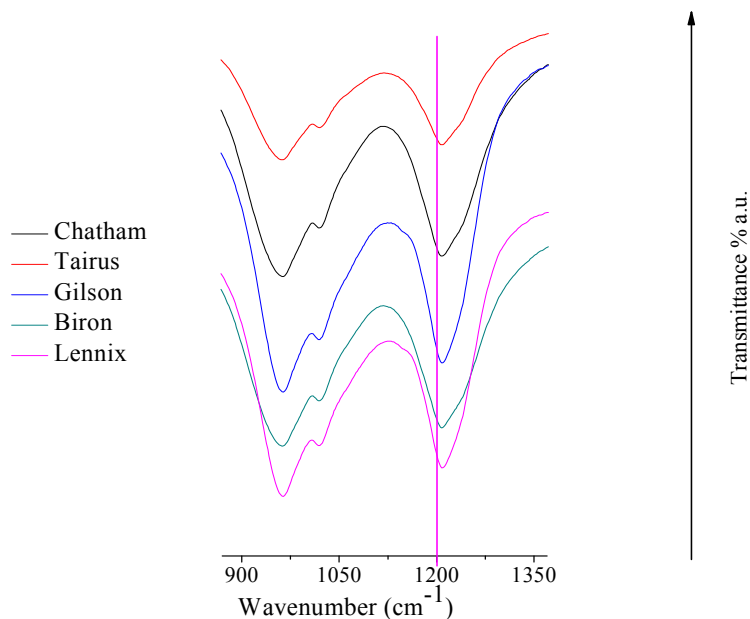
(a)
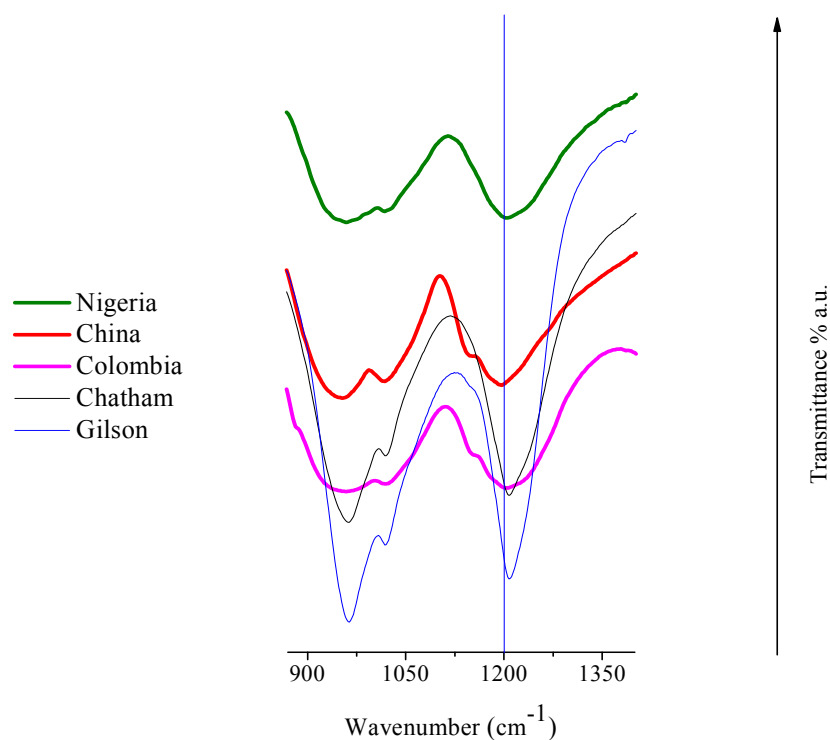
(b)

Figure 85: (a) IR spectra of synthetic "emerald" powder in KBr pellets from different manufactures in the range between 900-1350 cm^{-1} do not show the shoulder at 1140 cm^{-1}. (b) IR spectra of "non-schist-type" emerald powder in KBR-pellets from different deposits compared with synthetic "emeralds" of Chatham and Gilson manufactures in the range between 900-1350 cm^{-1} in which the spectrum of a Nigerian sample does not show the shoulder at 1140 cm^{-1}; the band at 1200 cm^{-1} tends to be less asymmetric and more slender in synthetic samples.

93

Nevertheless, in all spectra of natural and synthetic samples containing or not containing the shoulder, this band is more or less asymmetric. In natural samples, the flank of the band at 1200 cm^{-1} can reach 1500 cm^{-1} while in synthetic samples it is limited to about 1300 cm^{-1}. The asymmetry of the band may be due to the following effects:, 1. The shoulder at 1140 cm^{-1} may cause the shift of the band at 1200 cm^{-1} and produce therefore the asymmetry of this band; 2. This shoulder may exist in all samples but when its intensity is very low, it has no influence. 3. Because the flank of the band at 1200 cm^{-1} is very large, shoulders may be hidden.

Origin 7.5 Peak Fitting with Gauss-Lorentz function has been used to smooth the IR spectra in the whole range between 850-1500 cm^{-1} to obtain the exact values of intensity, FWHM and position of the possible bands in this range. Fitting results manifest the trends which are shown above, i.e. band 1200 cm^{-1} still shifts backward in natural samples and toward higher wavenumbers in synthetic samples.
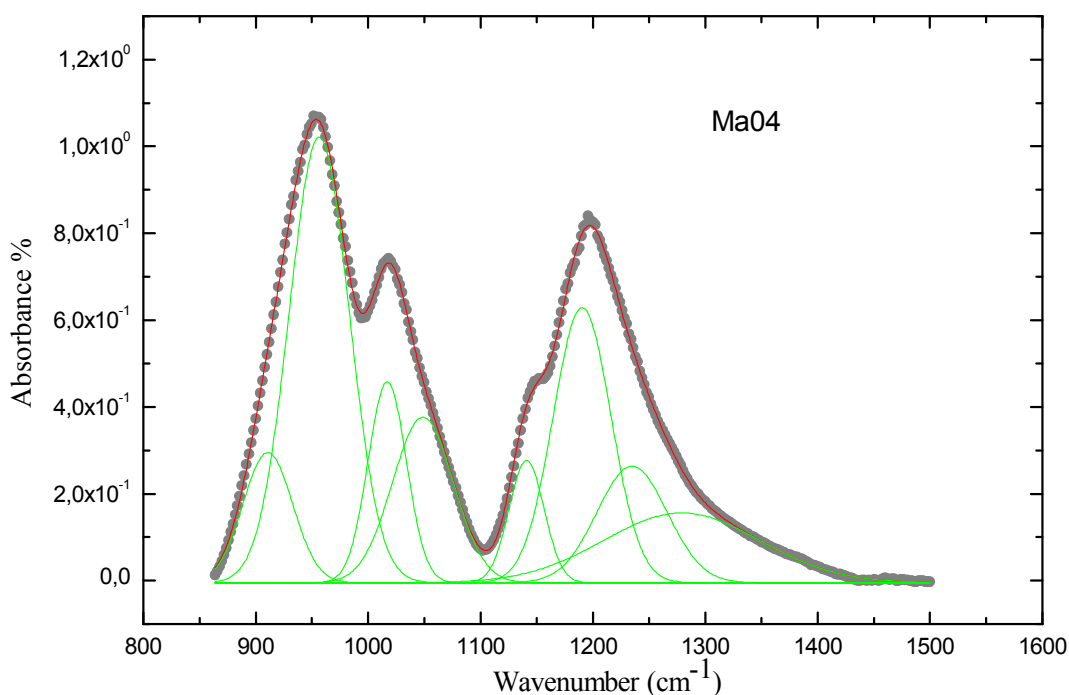
Figure 86: Diagram illustrating IR spectra in the range 850-1500 cm^{-1} of a Chinese sample (grey dots), the proposed peaks (green lines) and the sum of the proposed peaks (red line).
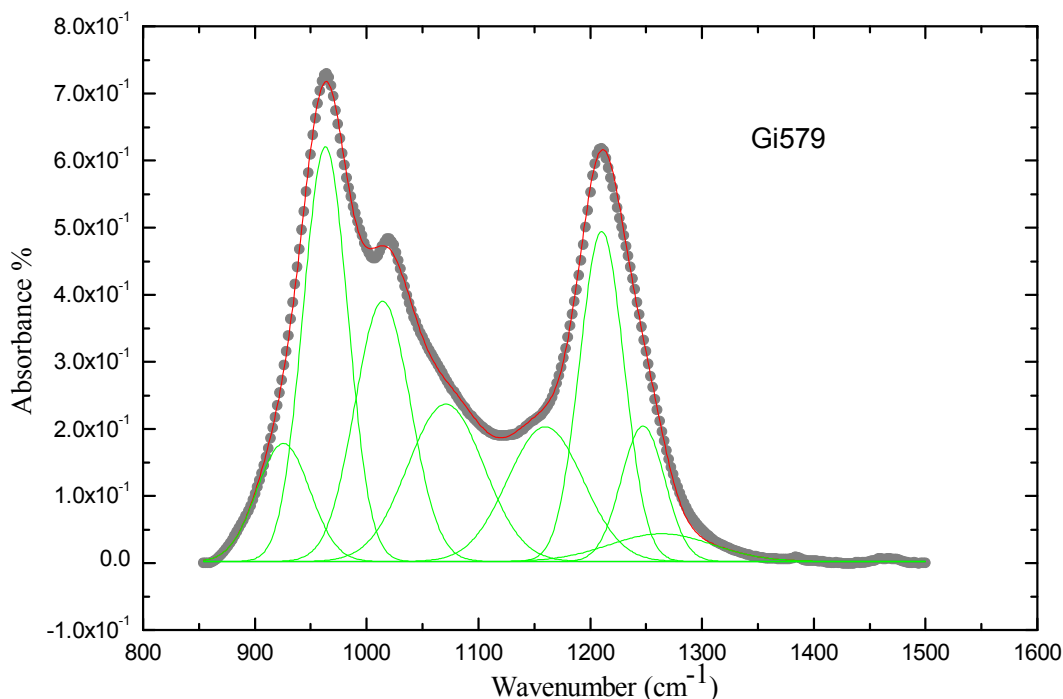
Figure 87: Diagram illustrating IR spectra in the range 850-1500 cm^{-1} of a synthetic sample from Gilson (grey dots), the proposed peaks (green lines) and the sum of the proposed peaks (red line).

A plot of the position of the 1200 cm^{-1} band versus the Si content shows a clear trend. For high Si-containing samples, the band around 1200 cm^{-1} and the shoulder at 1140 cm^{-1} shift both toward higher wave numbers. Besides, these bands do not show any relation with the content of Be. Therefore, the assignment of this band to Si-O vibration is preferred rather than to Be-O vibrations. Again, this observation is corresponding with experience and interpretation of the band at 1067-1072 cm^{-1} in Raman spectroscopy. Beside, the plot of intensity ratios of the band at 1200 cm^{-1} and the shoulder at 1140 cm^{-1} versus the Si content shows a positive linear trend, i.e. this intensity ratio is high in high Si-containing samples. So, not only the band at 1200 cm^{-1} but also the shoulder at 1140 cm^{-1} has a relationship with the Si content. Similarly, the plot of ratios of the band at 1200 cm^{-1} and the shoulder at 1140 cm^{-1} versus the alkali contents (mainly sodium and potassium) shows a negative linear trend, i.e. this intensity ratio is high in low alkali-containing samples. Therefore, the existence of the shoulder at 1140 cm^{-1} in all "schist-type" emeralds and "non-schist-type" emeralds from 2 localities (Colombia and China) could be related also to alkali ions. The existence of this shoulder could be explained as follows: 1. The shoulder is generated

by a vibration X-O in which X is a divalent or trivalent cation substituting in the Si position.
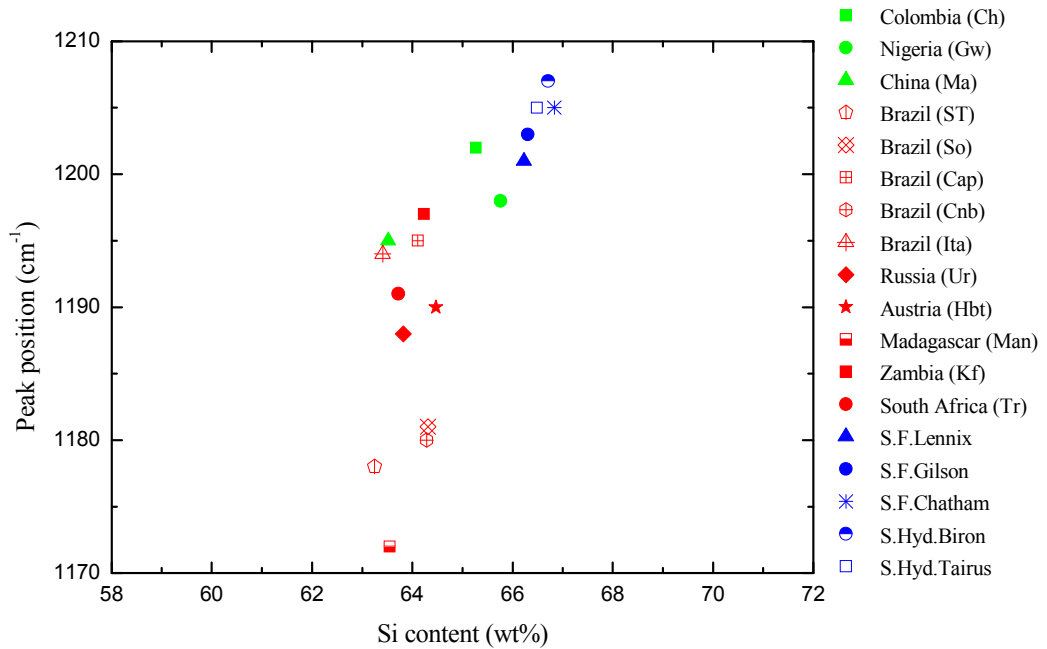
Figure 88: IR-band positions around 1200 cm^{-1} versus Si content.
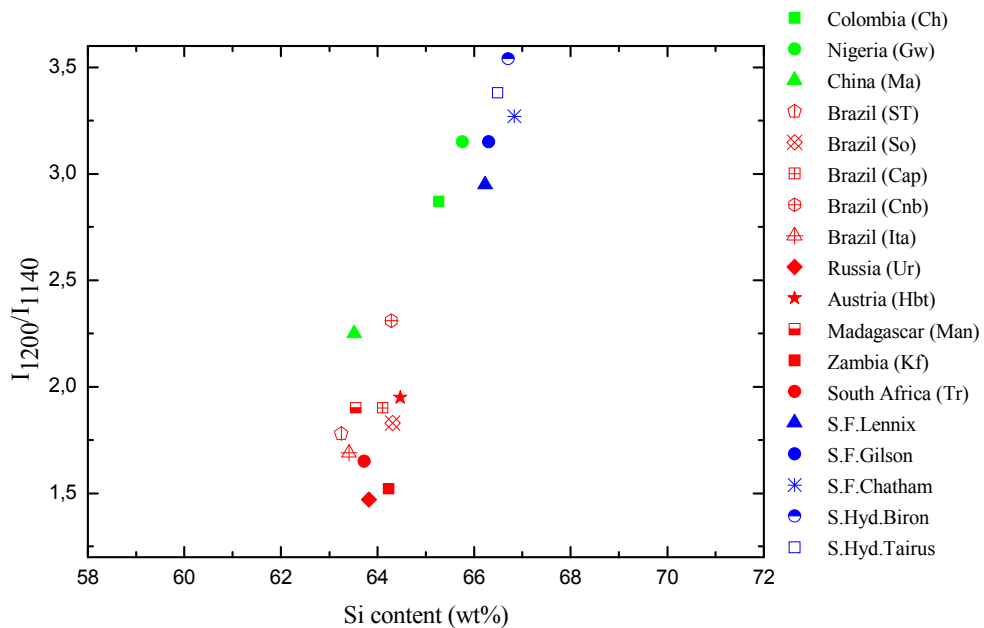
Figure 89: Intensity ratios of IR-bands at 1200 cm^{-1} and shoulders at 1140 cm^{-1} versus Si content.

96
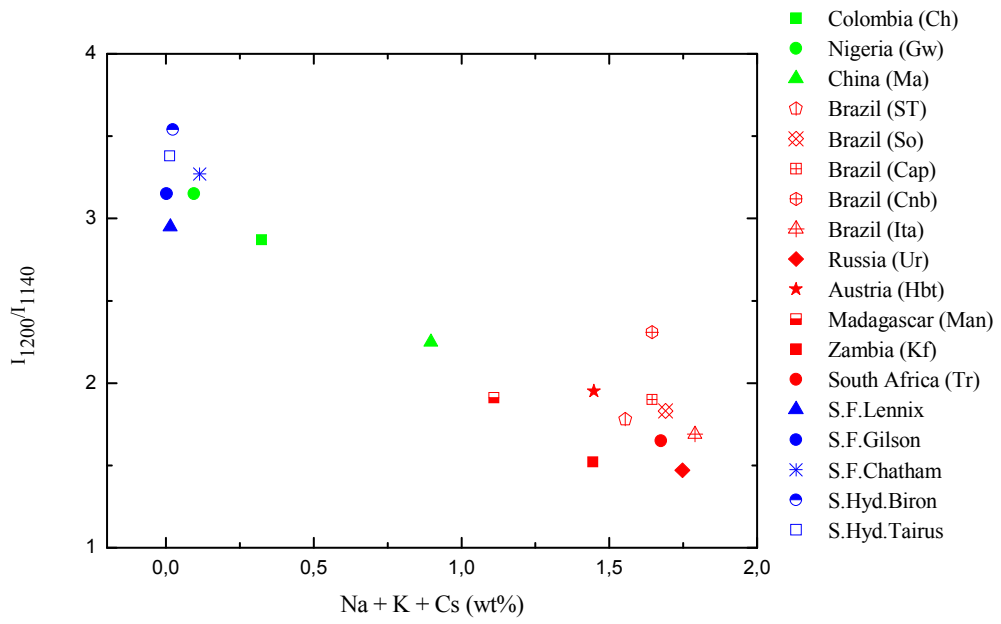
Figure 90: Intensity ratios of IR-bands at 1200 cm^{-1} and shoulders at 1140 cm^{-1} versus alkali content.
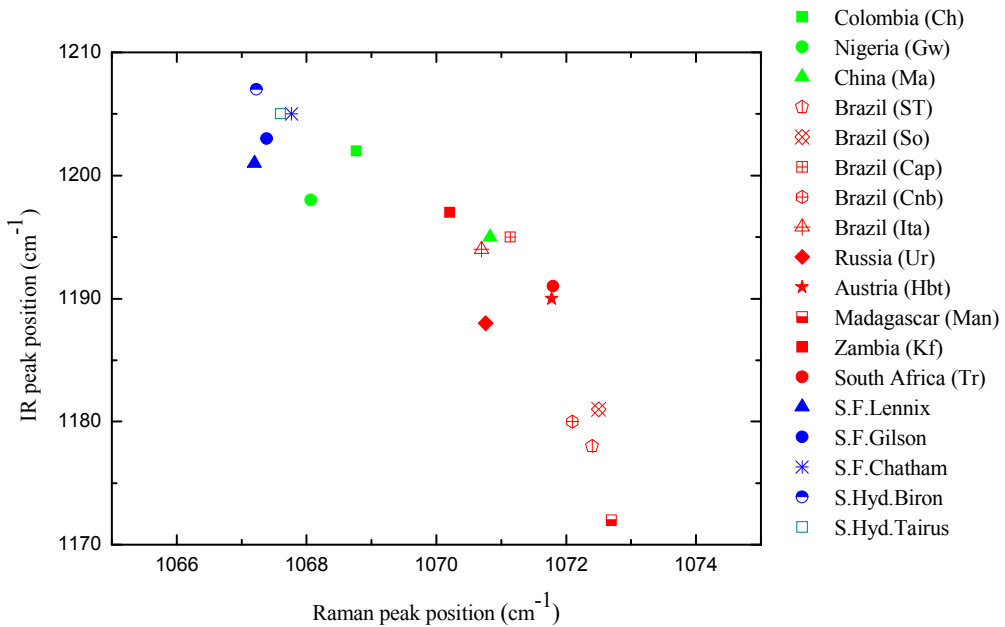
Figure 91: IR band positions around 1200 cm^{-1} versus Raman band positions at 1068 cm^{-1}.

The charge compensation is served by alkali ions (Na, K, Cs) in the channel. 2. The shoulder is generated by M-O vibrations in which M is the alkali ion in the channel.

97

6.2. IR absorption spectroscopy in the ranges 1500-1700 cm^{-1} and 3300-3800 cm^{-1}.
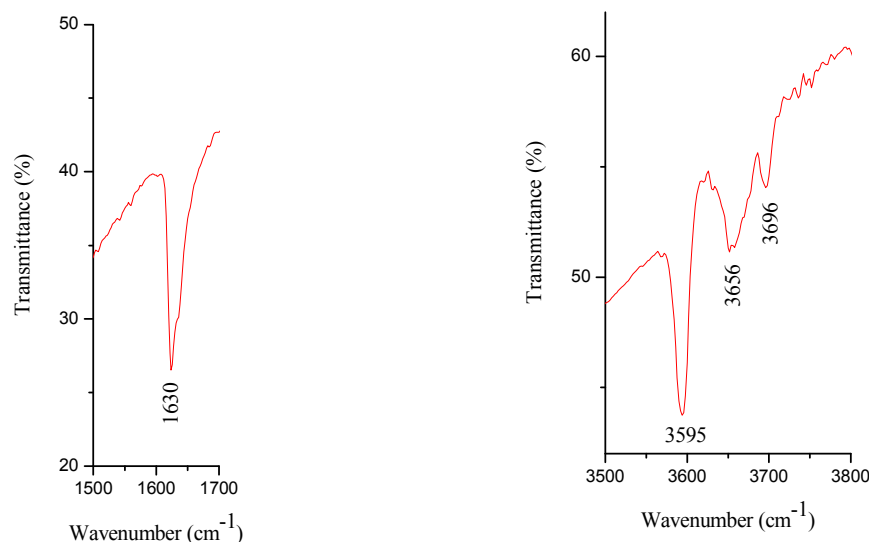
Figure 92: Two ranges of water absorption bands in IR spectrum of one emerald from Socoto, Brazil (sample So889).

Vibrations of water in the channel of beryl can be seen in two ranges, 1500-1700 cm^{-1} and 3500-3800 cm^{-1}. As expected, flux synthetic samples do not show any band in these two ranges. For other emeralds, in the lower range, one band is observed at about 1630 cm^{-1} (shifting from 1624 cm^{-1} to 1632 cm^{-1}). In all water-bearing samples this band can be observed with different intensities. In the higher range, one, two or even three bands are observable: 3595 cm^{-1}, 3656 cm^{-1}, 3696 cm^{-1}, and these bands do not show larger shifts (the sample individual shift is about 2 cm^{-1} at maximum). According to the study of Schmetzer and Kiefert (1990), these bands are assigned to different types of water molecules and hydroxyl groups in the channel of the emerald structure. The band at 3694 cm^{-1} (labelled as A) is assigned to type-I water molecules which are not bound to alkali ions. Band B at 3592cm^{-1} is assigned to type-IIa water molecules which are bound to alkali ions in the sequence H_2O-Na-OH_2. The band C at 3655cm^{-1} is assigned to water molecules or hydroxyl groups which are bound to alkali ions in the sequence H_2O-Na- (vacancy) or HO-Na- (type-IIb). However, bond strength calculations favour the presence of water molecules and the absence of hydroxyl in channel sites of the beryl structure (Howthorne and Cerny, 1977).

Basing on the relative ratio features of water bands investigated by this study, six (without any H_2O or OH^--group) different groups of IR spectra of emeralds may be separated as follows:

Group I: Samples containing none of the bands of water (cases of spectra from flux samples: Chatham, Gilson, Lennix).

Group II: Samples where only one strong absorption band A is observed. This is the case in hydrothermally-grown synthetic "emeralds" by Biron and Tairus. The alkali contents of these samples are about 0,003 to 0,02 wt%.

Group III: In the spectra of Nigerian (Gwantu) samples, all three bands are seen but the intensity of band A dominates those of band B and band C. The alkali contents are about 0, 095 wt% to 0,183 wt%.

Group IV: In the spectra of Colombian (Chivor) samples, the intensities of bands A exceed the intensities of bands B and are higher than that of bands C. The alkali contents are between 0,323 wt% and 0,678 wt%.

Group V: The intensity of bands B are higher than that of bands A and the intensity of bands A are higher than that of bands C. These are found in samples from Madagascar (Mananjary), Zambia (Kafubu), Austria (Habachtal) and China (Malipo). Alkali contents are from 0,8 wt% to 1,5 wt%.

Group VI: The intensities of bands B are higher than that of bands C and the intensities of bands C are higher than that of bands A. These are found in samples from many localities in Brazil (Santa Terezinha, Itabira, Socoto, Capoeirana, Carnaiba) and in samples from Russia (Ural), South Africa (Transvaal). The content of alkali ions in these samples is about 1,6 wt% to 1,8 wt%.

The assignments of Schmetzer & Kiefert (1990) are elucidated, since we found the intensity ratios of bands A, B, C are correlated with the alkali contents.
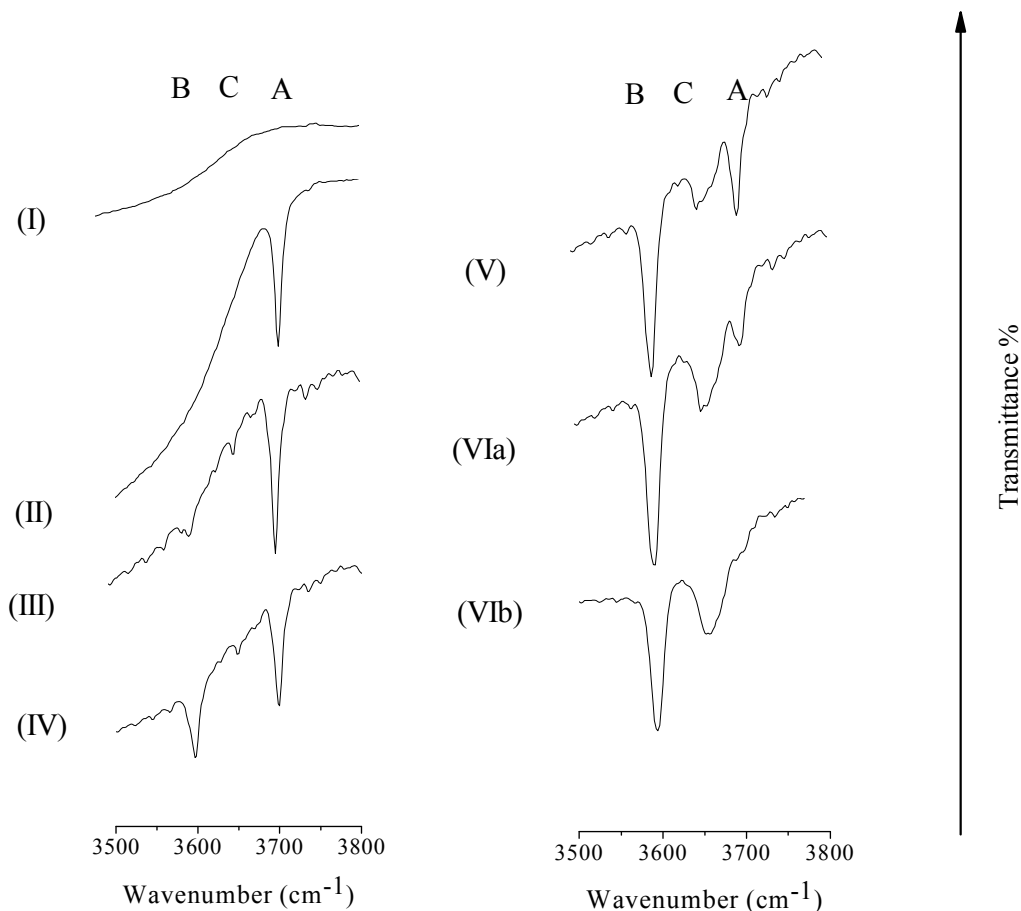
Figure 93: Six groups of IR spectra in the range of 3500-3800 cm^{-1} of water vibration.

The presence of water type I or water type IIa, IIb is as result of the alkali-density in the channels of the beryl structure. Therefore, in the emeralds bearing water (all origins except flux-grown "emeralds"), based on the correlation among water types, the concentration of alkali ions in the emerald structure may be estimated relatively without any chemical analysis. For instance, in the case of emeralds from Nigeria, the fact that the spectrum is dominated by water type I (A), indicates that there is only a small amount of alkalis. Another obvious sample comes with the hydrothermally grown synthetic "emeralds": the absence of water type II indicates the absence of alkali ions in the structure and elucidates also the fact that these "emeralds" were grown in alkali-free environment.

100

Group	Features of bands A = 3694 cm^{-1}, B = 3592 cm^{-1}, C = 3655 cm^{-1}	Localities or manufactures	Features of alkali content
I	No distinct absorption bands	Chatham, Gilson, Lennix	Flux-grown synthetic emeralds.
II	Only A occurs in the spectra	Biron, Tairus	Synthetic "emeralds" grown hydrothermally in alkali-free environment
III	A » B, C	Nigeria – "non-schist-type" emeralds.	Low alkali-bearing eme-ralds, alkali contents ran-ging from 0,095 wt% to 0,183 wt%.
IV	A ≈ B > C	Colombia (Chivor) – "non-schist-type" eme-ralds	Low alkali-bearing eme-ralds, alkali contents ran-ging from 0,323 wt% to 0,678 wt%.
V	B > A > C	Madagascar (Mananjary), Austria (Habachtal), Zambia (Kafubu), China (Malipo).	High alkali-bearing eme-ralds, alkali contents ranging from 0,8 wt% to 1,5 wt%.
VI	B> C > A	Brazil (Santa Terezinha, Itabira, Socoto, Carnaiba, Capoeirana), South Afri-ca (Transvaal), Russia (Ural).	The content of alkalis in these samples is about 1,6 to 1,8 wt%.

Table 10: Classification of natural and synthetic emeralds according to IR spectroscopic features in the range from 3500 cm^{-1} to 3800 cm^{-1} (Schmetzer & Kiefert, 1990; modified).

7. CONCLUSIONS

The presented study is a contribution to the problems concerning microscopic, chemical and spectroscopic research in emeralds – a gem variety of beryl. The differences of microscopic, chemical as well as spectroscopic (here, Raman and IR) features in emeralds between localities can be used to separate synthetic stones from natural ones as well as to determine the provenance of natural stones. Especially, the combination of these methods makes the separation much more precise.

With Raman spectroscopy, it has been found that the bands at about $1067\text{-}1072$ cm^{-1} shifts to longer wavenumbers in emeralds of "schist-type" deposits (about 1069 cm^{-1} to 1072 cm^{-1}), while in synthetic "emeralds" and emeralds of some "non-schist-type" deposits (Gwantu, Chivor) this bands are at around $1067\text{-}1068$ cm^{-1} and $1068\text{-}1070$ cm^{-1}, respectively. Correlating with chemical properties, it is found that the position of these bands depends on the silicon content, that is, in emeralds with less Si content, this band is shifted to lower wavenumbers. This complemented the assignment of other authors who assigned this band to the vibration of Si-O building units.

Types of water can be studied by means of Raman spectroscopy, in which type I water is assigned to the bands at 3608 cm^{-1}, and type II water is assigned to the bands at 3598 cm^{-1}, since the bands at 3608 cm^{-1} occur in alkali-free samples and the intensity ratios of these bands are correlated with the alkalis contents. The features of water bands at room temperature can help to determine "emeralds" produced hydrothermally since this type shows only the bands of water type I at 3608 cm^{-1}, and to determine flux-grown "emeralds" since they show none of those absorption bands in this range. Furthermore, the intensity ratios between bands of type-I and type-II water can be used to separate natural emeralds of between "schist-type" and "non-schist-type" deposits because the intensity of the bands at 3608 cm^{-1} is higher than that of the bands at 3598 cm^{-1} in "non-schist-type" emeralds. In "schist-type" emeralds, this relation is reversed.

With IR-spectroscopy, similar effects have been found and explained. The bands at 1200 cm^{-1} actually positioned at about $1171\text{-}1203$ cm^{-1} in natural emeralds and about

1200-1207 cm^{-1} in synthetic "emeralds" are assigned to Si-O since the band positions are correlated to the actual Si content. The shoulder at about 1140 cm^{-1} is not observed in synthetic "emeralds" and in low-alkali "non-schist-type" emeralds (Nigeria) and therefore can be used as a criterion to separate these emeralds from others. The presence of the shoulder is thought to be concerned with the Si and Na density in the emerald crystal structure. The IR-spectroscopic features of water bands in comparison with alkali contents can separate all investigated emeralds into 6 groups, in which flux and hydrothermally grown "emeralds" can be easily discriminated.

By chemical features, synthetic "emeralds" are differentiated from natural ones by the almost ideal amounts of main elements ($SiO_2 \approx 67$ wt%, $Al_2O_3 \approx 18,9$ wt%, $BeO \approx 14,1$ wt%) and of cause by the limited appearances of trace elements (mainly Mo, Ni, Cu, Fe, Ti, Li). Some localities can be determined basing on the contents of some minor elements; the Chivor (Colombia) and Malipo (China) deposits can be recognised by the extremely low Fe and high V contents, respectively, in comparison with other localities. Moreover, Malipo emeralds are characterised by the low content of Cr^{3+} and so V^{3+} is the main colouring agent in emeralds from this locality. In addition, features of Mg, Na and K content can be used as relative signal to separate emeralds of "schist-type" from "non-schist-type" deposits since these elements are relatively high in the former one and low in later one.

So far, the inclusions observed in synthetic emeralds are fingerprints, veils, and fractures; single occurrences are large two-phase inclusions, nail-head spicule inclusions with gas and liquid phase, phenakite crystals, numerous types of growth features, negative crystals, metals, etc. By means of these inclusions synthetic "emeralds" can be distinguished from natural material. As discussed, also the peculiar inclusions within natural emeralds in some occurrences allow to differentiate one locality from others.

By combination of different studying methods, one can have good strategies to separate some localities. Some proposals for relatively sure, destruction free analyses are suggested as follows indicating the positive effects of the combination of inclusion study with spectroscopic methods at room temperatures:

Inclusion signals   Infrared signals   Locality

Pyrite

$I_{3694} \approx I_{3592} > I_{3655} \longrightarrow$ Chivor

$I_{3592} > I_{3694} > I_{3655} \longrightarrow$ Kafubu

$I_{3592} > I_{3655} > I_{3694} \longrightarrow$ Santa Terezinha

Inclusion signals   Raman signals   Infrared signals   Locality

Tourmaline

$I_{3598} > I_{3608}$

$I_{3592} > I_{3655} > I_{3694} \longrightarrow$ Socoto

$I_{3592} > I_{3694} > I_{3655} \longrightarrow$ { Kafubu / Mananjary }

$I_{3598} < I_{3608}$

$I_{3592} > I_{3694} > I_{3655} \longrightarrow$ Malipo

$I_{3694} \gg I_{3592} , I_{3655} \longrightarrow$ Gwantu
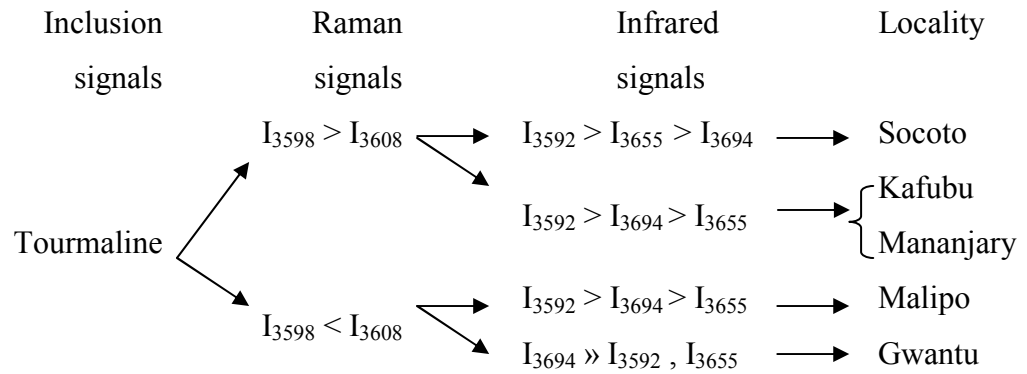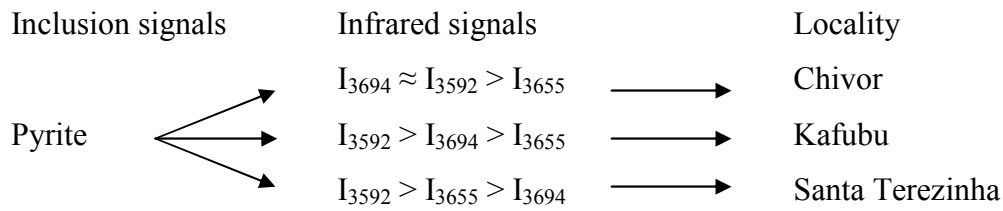
Obviously, there is some reason for the discrimination between "schist-type" and non-schist-type" bound emerald deposits. But this argument must be used very carefully on a completely evaluated and petrologically based investigation. Usually, it is not so easy to find the correct features for discrimination, because the halo of chemical, crystallographic and petrologic influence by the geological setting on a certain beryl crystal is sometimes not clearly determined. Nevertheless, one should try to characterize the geological setting of emerald deposits as clear and definite as possible.

References

Adamo, I., Pavese, A., Prosperi, L., Diella, V., Merlini, M., Gemmi, M., Ajo, D. (2005): Characterization of the new Malossi hydrothermal synthetic emerald. *Gems and Gemmology*, 41, 4, p. 328-338.

Adams, D.M., Gardner, I.R. (1974): Single-crystal vibrational spectra of beryl and dioptase. *Journal of the Chemical Society - Dalton Transactions*, p. 1502-1505.

Aines, R.D. and Rossman, G.R. (1984): The high temperature behaviour of water and carbon dioxide in cordierite and beryl. *American Mineralogist*, 60, p. 319-327.

Andersson L.O. (2006): The positions of H^+, Li^+ and Na^+ impurities in beryl. *Physics and Chemistry of Minerals*, 33, p. 403-416.

Arif, M., Fallick, A.E., Moon, C.J. (1996): The genesis of emeralds and their host rocks from Swat, northwestern Pakistan: a stable-isotope investigation. *Mineralium Deposita*, 31, p. 255-268.

Aurisicchio, C., Grubessi, O., Zecchini, P. (1994): Infrared spectroscopy and crystal chemistry of the beryl group. *The Canadian Mineralogist*, 32, p. 55-68.

Aurisicchio, C., Fioravanti, G., Grubessi, O., Zanazzi, P.F. (1988): Reappraisal of the crystal chemistry of beryl. *American Mineralogist*, 73, p. 826-837.

Barilo, S.N., Byschkov, G.L., Kurnevich, L.A., Leonuk, N.I., Mikhailov, V.P., Shiryaev, S. V., Koyava, V.T., Smirnova, T.V. (1999): Controlled crystallization of emerald from the fluxed melt. *Journal of Crystal Growth*, 198/199, 1, p. 716-722.

Below, N.V., and Matveeva, R.G. (1951): The determination of the structural parameters of beryl by the method of bounded projections. *Doklady Akad. Nauk SSSR*, 6, p. 69-82.

Bershov, L.V. (1970): Methane and atomic hydrogen in some natural minerals. *Geochemistry International*, p. 853-856.

Bowersox, G., Snee, L.W., Foord, E.E., Seal, R.R. (1991): Emeralds of the Panjshir valley, Afghanistan. *Gems & Gemmology*, 27, 1, p. 26-39.

Bowersox, G., and Anwar, J. (1989): The Gujar Kili emeralds deposits, northwest frontier province, Pakistan. *Gems & Gemmology*, 25, 1, p. 16-24.

Bragg, W.L. and West, J. (1926): The structure of beryl, $Be_3Al_2Si_6O_{18}$. *Proceeding of the Royal Society of London* A-111, p. 691-714.

Brown, G.E., and Milis, B. (1986): High-temprature structure and crystal chemistry of hydrous alkali-rich beryl from the Harding pegmatite, Taos County, New Mexico. *American Mineralogist*, 71, p. 547-556.

Cassedanne, J.P. and Sauer, D.A. (1984): The Santa Terezinha de Goias emerald deposit. *Gems & Gemmology*, 20, 1, p. 4-13.

Charoy, B., de Donato, P., Barres, O., Pinto-Coelho, C. (1996): Channel occupancy in an alkali-poor beryl from Serra Branca (Goias, Brazil): Spectroscopic characterization. *American Mineralogist*, 81, p. 395-403.

De Almeida Sampaio Filho, H. and Sighinolfi, G. P. (1973): Contribution to the crystal chemistry of beryl. *Contribution to Mineral and Petrology*, 38, p. 279-290.

Duroc-Danner, J. M. (2006): The identification value of the 2293 cm^{-1} infrared absorption band in natural and hydrothermal synthetic emeralds. *Journal of Gemmology*, 30, ½, p. 75-82.

Duyk, F. (1965): The Gilson synthetic emerald process. *Journal of Gemmology*, IX, 11, p. 369-371.

Eidt, T., and Schwarz, D. (1986): Brazilian emeralds; inclusions and genetic aspects; Socoto and Carnaiba, Brazil. *Fortschritte der Mineralogie*, Beiheft, 64, 1, p. 41.

Eppler, W.F. (1973): *Praktische Gemmologie*. Rühle-Diebener-Verlag, Stuttgart.

Epstein, D.S. (1989): The Capoeirana emerald deposit near Nova Era, Minas Gerais, Brazil. *Gems & Gemmology*, 25, 3, p. 150-158.

Fersmann, A. (1929): Smaragdgruben im Ural. In Geochemische Migration der Elemente und deren wissenschaftliche und wirtschaftliche Bedeutung. Wilhelm Knapp, Halle (Saale), 1, p. 74-116.

Flanigen, E.M., Breck, D.W., Mumbach, N.R., and Taylor, A.M. (1967): Characteristics of synthetic emeralds. American Mineralogist, 52, p. 744-772.

Fumagalli, M., Properi, L., Pavese, A., Bordiga, S. (2003): Natural versus hydrothermal synthetic Russian red beryl: chemical composition and spectroscopic measurements. *Journal of Gemmology*, 28, 5, p. 291-301.

Gervais, F. and Piriou, B. (1972): Étude des spectres de réflexion infrarouge du beryl dans les région 280-1400 cm^{-1}. *Comptes rendus de l'Académie des Sciences Paris*, B274, p. 252-255.

Gibbs, G.V., Breck, D.W., Meagher, E.P. (1968): Structural refinement of hydrous and anhydrous synthetic beryl, $Be_3Al_2Si_6O_{18}$ and emerald $Be_3Al_{1.9}Cr_{0.1}Si_6O_{18}$. *Lithos 1*, p. 275-285.

Ginzburg, A.I. (1955): On the question of the composition of beryl. *Trudy Mineralogischeskogo Muzeya, Akademiya Nauk SSSR*, p. 55-69.

Giuliani, G., Chaussidon, M., Schubnel, H.J., Piat, D.H., Rollion-Bard, C., France-Lanord, C., Giard, D., de Narvaez, D., Rondeau, B. (2000): Oxygen Isotopes and Emerald Trade Routes Since Antiquity. *Science*, 287, 5453, p. 631 – 633.

Giuliani, G., France-Lanord, C., Coget, P., Schwarz, D., Cheilletz, A., Branquet, Y., Giard, D., Martin-Izard, A., Alexandrov, P., Piat, D.H. (1998): Oxygen isotopes systematics of emerald: relevance for its origin and geological significances. *Mineralium Deposita*, 33, p. 513-519.

Golman, D.S., Rossman, G.R., Parkin, K.M. (1978): Channel constituents in beryl. *Physics and Chemistry of Minerals*, 3, p. 225-235.

Graziani, G., Gübelin, E., Lucchessi, S. (1983): The genesis of an emerald from the Kitwe District, Zambia. *Neues Jahrbuch für Mineralogie*, p. 175-186.

Graziani, G., Güblin, E., Martini, M. (1987): The Lennix synthetic emerald. *Gems & Gemmology*, 23, 3, p. 140-146.

Greiff, S., Häger, T. (1992): *Die Synthese von Edelsteinen - Pretiosen aus der Hexenküche*; Artikel in *Faszination Edelstein*. Benteli Verlag Bern, p. 33-40.

Griffith, W.P. (1969): Raman studies on rock-forming minerals. Part 1. Orthosilicates and cyclosilicates. *Journal of the Chemical Society A*, p. 1372-1377.

Grundmann, G. and Morteani, G. (1989): Emerald mineralization during regional metamorphicsm: The Habachtal (Autria) and Leydsdorp (Transvaal, South Africa) deposits. *Economic Geology*, 84, p. 1835-1849.

Gübelin, E.J. (1961): Hydrothermal rubies and emerald-coated beryl. *The Journal of Gemmology*, VIII, 2, p. 49-63.

Gübelin, E.J. (1958): Emeralds from Sandawana. *The Journal of Gemmology*, VI, 8, p. 340-354.

Hagemann, A., Lucken, A., Bill, H., Gysler-Sanz, J., Stalder, H.A. (1990): Polarized Raman spectra of beryl and bazzite. *Physics and Chemistry of Minerals*, 17, p. 395-401.

Hänni, H.A., Schwarz, D., Fischer, M. (1987): The emeralds of the Belmont Mine, Minas Gerais, Brazil. *Journal of Gemmology*, 20, 7/8, p. 446 - 456.

Hänni, H.A. and Schwarz, D. (1986): Brazilian emeralds; inclusions and genetic aspects; Santa Terezinha, Goias; Itabira, Minas Gerais; Tauna, Ceara. *Fortschritte der Mineralogie, Beiheft,* 64, 1, p. 63.

Hänni, H.A. (1982): A contribution to the separability of natural and synthetic emeralds. *Journal of Gemmology*, XVIII, 2, p. 138 - 144.

Hänni, H.A. and Klein, H.H. (1982): Ein Smaragdvorkommen in Madagaskar. *Zeitschrift der Deutschen Gemmologischen Gesellschaft*, 31, ½, p. 71-77.

Howthorne, F.C., and Cerny, P. (1977): The alkali-metal positions in Cs-Li Beryl. *Canadian Mineralogist*, 15, p. 414-421.

Hofmeister, A.M., Hoering, T.C., Virgo, D. (1987): Vibrational spectroscopy of beryllium alumosilicates: Heat capacity calculation from band assignments. *Physics and Chemistry of Minerals*, 14, p. 205-224.

Johnson, P.V. (1961): The Chivor emerald mine. *Journal of Gemmology*, VIII, 4, p. 126-152.

Kane, R.E. and Liddicoat, R.T. (1985): The Biron hydrothermal synthetic emerald. *Gems & Gemmology*, 21, 3, p. 156-170.

Khaibullin, R.I., Lopatin, O.N. Vagizov, F.G., Bazarov, V.V., Bakhtin, A.I., Khaibullin, I.B., and Aktas, B. (2003): Coloration of natural beryl by iron ion implantation. *Nuclear Instrument and Methods in Physics Research Section B*: Beam Interactions with Material and Atoms, 26, p. 277-281.

Kiefert, L. and Schmetzer, K. (1991): The microscopic determination of structural properties fort he characterization of optical uniaxial natural and synthetic gemstones. Part 2: Examples for the applicability of structural features for the distinction of natural emeralds from flux-grown and hydrothermally-grown synthetic emerald. *Journal of Gemmology*, 22, 7, p. 427-438.

Kim, C., Bell, M.I., McKeown, D.A. (1995): Vibrational analysis of beryl ($Be_3Al_2Si_6O_{18}$) and its constituent ring (Si_6O_{18}). *Physica B*, 205, p. 193-208.

Koivula, J.I. (1982): Tourmaline as an inclusion in Zambian emeralds. *Gems & Gemmology*, 18, 4, p. 225-227.

Koivula, J.I., Kammerling, R.C., DeGhionno, D., Reinitz, I., Fritsch, E., Johnson, M.L. (1996): Gemological investigation of a new type of Russian hydrothermal synthetic emerald. *Gems & Gemmology*, 32, 1, p. 32-39.

Kolesov, B.A. and Geiger, C.A. (2000): The orientation and vibrational states of H_2O in synthetic alkali-free beryl. *Physics and Chemistry of Mineral*, 27, p. 557-564.

Lind, T., Schmetzer, K., Bank, H. (1986): Blue and green beryls (aquamarines and emeralds) of gem quality from Nigeria. *Journal of Gemmology*, 20, 1, p. 40-47.

Lind, T., Schmetzer, K., Bank, H. (1984): Schleifwürdige blaue und grüne Berylle (Aquamarine und Smaragde) aus Nigeria. *Zeitschrift der Deutschen Gemmologischen Gesellschaft*, 33, p. 128-138.

Leung, C.S., Merigoux, H., Poirot, J.P., Zecchini, P. (1983): Sur l'identification des pierres fines et de synthèse par spectroscopie infrarouge. *Association francaise de gemmology*, ISSN 0398-9011, 75, p. 14-15.

Manier-Glavinaz, V., Couty, R., Lagache, M. (1989): The removal of alkalis from beryl: Structural adjustments. *Canadian Mineralogist*, 27, p. 663-671.

Mashkovtsev, R.I. and Lebedev A.S. (1993): Infrared spectroscopy of water in beryl. *Journal of Structural Chemistry*, p. 930-933.

Mashkovtsev, R.I., Stoyanov, E.S., and Thomas, V.G. (2004): State of molecules and ions in the structural channels of synthetic beryl with an ammonium impurity. *Journal of Structural Chemistry*, 45, 1, p. 56-63.

Mashkovtsev, R.I. and Solntsev, V.P. (2002): Channel constituents in synthetic beryl: ammonium. *Physics and Chemistry of Minerals*, 29, p. 65-71.

Mashkovtsev, R.I. and Smirnov, S.Z. (2004): The nature of channel constituents in hydrothermal synthetic emerald. *Journal of Gemmology*, 29, 4, p. 215-222.

Miyata, T., Hosaka, M., Chikayama, A. (1987): On the inclusions in emeralds from Santa Teresinha de Goias; Brazil. *Journal of gemmology*, 20, 6, p. 377-379.

Morosin, B. (1972): Structure and thermal expansion of beryl. *Acta Crystallographica*, B28, p. 1899-1903.

Moroz, I., Panczer, G., Roth, M. (1999): Laser-induced luminescence of emeralds from different sources. *Journal of Gemmology*, 26, 5, p. 316-320.

Moroz, I. and Eliezri, I.Z. (1999): Mineral inclusions in emeralds from different sources. *Journal of Gemmology*, 26, 6, p. 357-363.

Moroz, I., Roth, M., Boudeulle, M., Panczer, G. (2000): Raman microspectroscopy and fluorescence of emeralds from various deposits. *Journal of Raman Spectroscopy*, 31, p. 485-490.

Muller-Bastos, F. (1981): Emerald from Itabira, Minas Gerais, Brazil. *Lapidary Journal*, Dec.

Nasssau, K. (1980): *Gems made by man*. Chilton Book Company.

Nassau, K. (1976): Synthetic emerald: the confusing history and the current technology. *Lapidary Journal*, 30, p. 468-488.

Narayanan (1950): The Raman spectrum of beryllium silicate. *Proceedings of the Indian Academy of Sciences, Bangalore*, 31A, p. 354-358.

Pankrath, R., and Langer, K. (2002): Molecular water in beryl, $^{VI}Al_2[Be_3Si_6O_{18}].nH_2O$, as a function of pressure and temperature: An experimental study. *American Mineralogist*, 87, p. 238-244.

Pearce, N.J.G., Perkins, W.T., Westgate, J.A., Gorton, M.P., Jackson, S.E., Neal, C.R., Chenery, S.P. (1997): A compilation of new and published major and trace element data for NIST SRM 610 and NIST SRM 612 glass reference materials. *Geostandards Newsletter*, 21, p. 115-144.

Penfield, S.L. (1884): On the occurrence of alkalies in beryl. *American Journal of Sciences*, 28, p. 25-32.

Polupanova, T.I., Petrov, V.L., kruzhalov, A.V., Laskovenkov, A.F., Nikitin, V.S. (1985): The thermal stability of beryl. *Translated from Geokhimia*, N[o]1, p. 121-23.

Plyusina, I.I., and Surzhanskaya, E.A. (1967): IR spectrum of beryl. *Zhurnal Prikladnoi Spektroskopii*, 7, 6, p. 917-923.

Plyusnina, I.I. (1964): Infrared absorption spectra of beryls. *Geokhimiya*, 1, p. 31-41.

Robb, L.J. and Robb, V.M. (1986): Archean pegmatite deposits in the north-eastern Transvaal, in Anhaeusser, C.R., and Maske, S., eds., Mineral Deposits of South Africa: Johnnesburg, *Geolical Society of South Africa*, v.1 and v.2, p. 437-449.

Schmetzer, K. (1989): Types of water in natural and synthetic emerald. *Neues Jahrbuch für Mineralogie Monatshefte*, p. 15-26.

Schmetzer, K. and Kiefert, L. (1990): Water in beryl – a contribution to the separability of natural andd synthetic emeralds by infrared spectroscopy. *Journal of Gemmology*, 22, 4, p. 215-223.

Schmetzer, K. and Bernhard, H.J. (1994): Isomophic replacement of Al and Si in tetrahedral Be and Si sites of beryl from Torrington, NWS, Australia. *Neues Jahrbuch für Mineralogie Monatshefte*, 3, p. 121-129.

Schmetzer, K., Bernhardt, H.J., Biehler, R. (1997): Emeralds from the Ural Mountain, USSR. *Gems & Gemmology*, 27, 2, p. 86-99.

Schmetzer, K., Schwarz, D., Bernhardt, H.J., and Häger, T. (2006): A new type of Tairus hydrothermally-grown synthetic emerald coloured by vanadium and copper. *Journal of Gemmology*, 30, p. 59-74.

Schrader, H.W. (1987): *Natürliche und synthetische Smaragde*. Dissertation, Institut für Geowissenschaften, Johannes Gutenberg Universität Mainz

Schrader, H.W. (1985): A three-phase inclusion in an emerald from South Africa. *Journal of Gemmology*, XIX, 6, p. 484-485.

Schrader, H.W. (1983): Contribution to the study of the distinction of natural and synthetic emeralds. *Journal of Gemmology*, XVIII, 6, p. 530-543.

Schwarz, D. (1994): Emeralds from the Mananjary region, Madagascar: Internal features. *Gems & Gemmology*, 30, 2, p. 88-101.

Schwarz, D. (1990): Die brasilianischen Smaragde und ihre Vorkommen: Santa Terezinha de Goias/GO. *Zeitschrift der Deutschen Gemmologischen Gesellschaft*, 39, 1, p. 13-44.

Schwarz, D. (1987): Brazilian emerald occurrences and characteristic properties of Brazilian emeralds. International Gemmological Conference, p. 41-42.

Schwarz, D., Bank, H., Henn, U. (1988): Neues Smaragdvorkommen in Brasilien entdeckt: Capoeirana bei Nova Era, Minas Gerais. *Zeitschrift der Deutschen Gemmologischen Gesellschaft*, 37, p. 146-147.

Schwarz, D., Eidt, T., Couto, P.A. (1990): The Brazilian emeralds and their occurences: Socoto, Bahia. *Journal of Gemmology*, 22, 3, p. 147-163.

Schwarz, D. and Eidt, T. (1989): The Brazilian emeralds and their occurrences: Carnaiba, Bahia. *Journal of Gemmology*, 21, 8, p. 474-486.

Schwarz, D., and Henn, U. (1992): Emeralds from Madagascar. *Journal of Gemmology*, 23, 3, p. 140-149.

Schwarz, D., Kanis, J., Kinnaird, J. (1996): Emerald and green beryl from Central Nigeria. *Journal of Gemmology*, 25, 2, p. 117-141.

Sechos, B. (1997): Indentifying characteristics of hydrothermal synthetics. *Australian Gemmologist*, 19, 9, p. 383-388.

Shannon, R.D. (1976): Revised effective ionic radii and systematic studies of interatomic distances in halides and chalcogenides. *Acta Crystallographica,* A32, p. 751-767.

Shatskiy, V.S, Lebedev, A.S., Pavlyuchenko, V.S., Kovaleva, L.T., Kozmenko, O.A., Yudin, A.N., Belov, N.V. (1981): Conditions for entry of alkali cations into beryl. *Translated from Geokhimia*, 3, 351-360.

Sherriff, B.L., Grundy, H.D., Hartman, J.S., Hawthorne, F.C., and Černý, P. (1991): The incorporation of alkalies in beryl: Multi-nuclear MAS NMR and crystal-structure study. *Canadian Mineralogist*, 29, p. 271-285.

Sinkankas, J., and Read, P.G. (1986): *Beryl*. Butterworths Gem Books.

Staatz, M.H., Griffitts, W.R., Barnett, P.R. (1965): Differences in the minor element composition of beryl in various environments. *The American Mineralogist*, 50, p. 1783-1795.

Stockton, C.M. (1984): The chemical distinction of natural from synthetic emeralds. *Gems & Gemmology*, 20, 3, p. 141-145.

Stockton, C.M. (1987): The separation of natural from synthetic emeralds by infrared spectroscopy. *Gems & Gemmology*, 23, 2, p. 96-99.

Souza, J.L., Mendes, J.C., Silveira, R.M., Svisero, D.P., Valarelli, J.V. (1991): Petrographic and microthermometrical studies of emeralds in the Garimpo of Capoeirana, Nova Era, Minas Gerais State, Brazil. *Mineralium Deposita*, 27, 2, p. 161-168.

Tarte, P. (1965): Effet isotopique Li^6-Li^7 dans le spectre infra-rouge de composés inorganiques du lithium. 1. Carbonate, chromoferrite, tungstate, molybdate et nitrate de lithium. *Spectrochimica Acta*, 21, 2, p. 313-319.

Webster, R. (1975): *Gems - their sources, descriptions and identifications*. Butterworth - Heinemann Manchester.

Webster, R. (1964): The French synthetic emerald. *Journal of Gemmology*, IX, 6, p. 191-195.

Webster, R. (1955): The emerald. *Journal of Gemmology*, V, 4, p. 185 – 219.

Wickersheim, K.A. and Buchanan, R.A. (1959): The near infrared spectrum of beryl. *American Mineralogist*, 44, p. 440-445.

Wood, D.L., and Nassau, K. (1967): Infrared spectra of foreign molecules in beryl. *The Journal of Chemical Physics, 47*, 7, p. 2220-2228.

Wood, D.L. and Nassau, K. (1968): The characterization of beryl and emerald by visible and infrared absorption spectroscopy. *American Mineralogist*, 53, p. 777-800.

Zwaan, J.C. (2006): Gemmology, geology and origin of the Sandawana emerald deposits, Zimbabwe. *Scripta Geologica* 131.

Zwaan, J.C. and Burke, E.A.J. (1998): Emeralds from Sandawana, Zimbabwe: the use of Raman microspectroscopy in identification of their solid inclusions. *Journal of Gemmology*, 26, 3, p. 174-187.

Zwaan, J.C., Cheilletz, A., Taylor, B.E. (2004): Tracing the emerald origin by oxygen isotope data: the case of Sandawana, Zimbabwe. *Comptes Rendus Geoscience,* 336, p. 41-48.

Zwaan, J.C., Kanis, J., Petsch, E.J. (1997): Update on emeralds from Sandawana mines, Zimbabwe. *Gems & Gemology*, 33, 2, p. 80-100.

Zwaan, J.C., Seifert, A.V., Vrana, S., Laurs, B.M., Anckar, B., Simmons, W.B., Falster, A.U., Lustenhouwer, W.J., Muhlmeister, S., Koivula, J.I., Guilleminet, H.G. (2005): Emeralds from the Kafubu Area, Zambia. *Gems & Gemology*, 41, 2, p. 116-148.

Web sources:

http://www.snapmania.com
http://www.mineralatlas.com
http://www.coloradogem.com

Programs:

1. Origin 7.5
2. CrystalMaker 2.0

Curriculum Vitae

Name:	LE, Thi-Thu Huong
Date of birth:	14 October 1980
Place of birth:	Thanh-Hoa, Vietnam
Nationality:	Vietnamese
Gender:	Female
Family status:	Married, 1 child
E-mail:	letth80@web.de

Education:

10.2005-present:	Ph.D. Student in Mineralogy-Gemmology, Faculty of Chemistry, Pharmaceutics and Geosciences, Johannes Gutenberg University, Mainz, Germany.
4.2004-10.2005:	German Diploma-Equivalent in Mineralogy, Faculty of Chemistry, Pharmaceutics and Geosciences, Johannes Gutenberg University, Mainz, Germany.
9.2002-9.2003:	German Diploma-Equivalent in Geology, Faculty of Geosciences, the University of Greifswald, Germany.
9.2000-5.2002:	Bachelor in Geology, Faculty of Geology, Hanoi University of Sciences (HUS).
9.1998- 5.2000:	Two years of intermediate diploma, Honour Program, Hanoi University of Sciences (HUS).

Technical skills:

- Laser ablation-inductively coupled plasma-mass spectrometry (LA-ICP-MS): Applications in the Earth sciences.
- Luminescence spectroscopy: Applications in the Earth sciences.
- Raman spectroscopy: Applications in the Earth sciences.
- Infrared spectroscopy: Applications in the Earth sciences.

Special Courses:

Winter term, 2006:	Gem Identification by means of traditional and spectroscopic methods, Institute of Gemstone Research, Mainz - Idar Oberstein, Johannes Gutenberg University.

Languages:	Vietnamese (mother language), English, German, French.